

CLASS GUIDELINE

DNVGL-CG-0041

Edition July 2019

Ice strengthening of propulsion machinery and hull appendages

The content of this service document is the subject of intellectual property rights reserved by DNV GL AS ("DNV GL"). The user accepts that it is prohibited by anyone else but DNV GL and/or its licensees to offer and/or perform classification, certification and/or verification services, including the issuance of certificates and/or declarations of conformity, wholly or partly, on the basis of and/or pursuant to this document whether free of charge or chargeable, without DNV GL's prior written consent. DNV GL is not responsible for the consequences arising from any use of this document by others.

The electronic pdf version of this document, available free of charge
from <http://www.dnvg.com>, is the officially binding version.

FOREWORD

DNV GL class guidelines contain methods, technical requirements, principles and acceptance criteria related to classed objects as referred to from the rules.

© DNV GL AS July 2019

Any comments may be sent by e-mail to *rules@dnvgl.com*

This service document has been prepared based on available knowledge, technology and/or information at the time of issuance of this document. The use of this document by others than DNV GL is at the user's sole risk. Unless otherwise stated in an applicable contract, or following from mandatory law, the liability of DNV GL AS, its parent companies and subsidiaries as well as their officers, directors and employees ("DNV GL") for proved loss or damage arising from or in connection with any act or omission of DNV GL, whether in contract or in tort (including negligence), shall be limited to direct losses and under any circumstance be limited to 300,000 USD.

CHANGES – CURRENT

This document supersedes the March 2016 edition of DNVGL-CG-0041.

Changes in this document are highlighted in red colour. However, if the changes involve a whole chapter, section or subsection, normally only the title will be in red colour.

Changes July 2019

Topic	Reference	Description
Defining class current practice for calculation of ice loads on appendages for vessels with class notation PC .	Front page	Title changed to <i>Ice strengthening of propulsion machinery and hull appendages</i> to include rudders and propeller nozzles, see new Sec.8.
	Sec.8	New section on ice load calculation for ships with class notation PC explaining how loads should be applied for different appendages such as rudder, nozzle and shaft brackets.

Editorial corrections

In addition to the above stated changes, editorial corrections may have been made.

CONTENTS

Changes – current.....	3
Section 1 General.....	6
1 Scope.....	6
2 Application.....	6
3 Symbols, nomenclature and units.....	6
Section 2 Propeller blades.....	9
1 Ice interaction load models.....	9
2 Finite element analysis.....	14
3 Propeller blade strength assessment.....	21
4 Blade failure design loads.....	24
Section 3 Propeller hub and pitch mechanism.....	25
1 Scope and general remarks.....	25
2 Applicable load scenarios.....	27
3 Load transmission.....	28
4 Strength assessment.....	33
5 Stress in components of CP-Mechanism.....	34
6 Material strength.....	47
Section 4 Guidance on simulation calculations.....	56
1 The lumped mass-elastic system.....	56
2 Damping in the mass-elastic system.....	56
3 Excitations.....	61
Section 5 Propulsion shaft design against fatigue.....	62
1 Nomenclature.....	62
2 General.....	62
3 Method for fatigue analysis.....	63
Section 6 Reduction gears.....	69
1 General.....	69
Section 7 Podded propulsors or azimuthing thrusters.....	70
1 Ice loads on pod/thruster body and propeller hub.....	70
Section 8 Ice load on nozzle, rudder, and shaft bracket.....	74
1 Ice load on nozzle, rudder and shaft brackets.....	74

Appendix A General guidance on fatigue analysis of propulsion machinery subject to ice loads.....	80
1 Cumulative Damage by Palmgren-Miner's Rule.....	80
2 Design S-N curve.....	82
3 Long term stress amplitude distribution due to ice loads.....	86
4 Calculation of the Palmgren-Miner's damage sum.....	88
5 Guidance to when detailed fatigue analysis can be omitted.....	91
Changes – historic.....	93

SECTION 1 GENERAL

1 Scope

This class guideline contains procedures and methods necessary for verification of the load carrying capacity (ultimate and fatigue strength) for the following components in the propulsion plant subject to loads due to ice impacts:

- propeller blades, hub and pitch mechanism
- shafts
- reduction gears
- pod/thruster underwater housing.

The assessment of other components together with the general applicability, required safety factors, material requirements and design ice loads for the different ice classes are given in [DNVGL-RU-SHIP Pt.6 Ch.6 Sec.2](#) (Northern Baltic ice classes: **Ice(1A*F)** - **Ice(1C)**) and [DNVGL-RU-SHIP Pt.6 Ch.6 Sec.6](#) (polar ice classes: **PC(1)** to **PC(7)**). Consequently, this document should be read together with the rules referred to above, in order to describe all aspects of the strength assessment.

2 Application

The ice loads described in [DNVGL-RU-SHIP Pt.6 Ch.6 Sec.2](#) and [DNVGL-RU-SHIP Pt.6 Ch.6 Sec.6](#) are meant to be total loads, i.e. in general they include the open water hydrodynamic loads (unless otherwise stated). In cases where the calculations described herein result in smaller scantlings than derived from other class requirements, the latter requirements prevail.

The calculation methods specified herein are to some extent prepared based on empirical considerations and studies of conventional design. This means that they are applicable for "standard" materials and geometrical shapes within a limited range of geometry and size.

Hence, the presented formulae should not be used uncritically for novel designs or be transferred to other applications. In principle, other relevant calculation methods may be applied for this purpose.

3 Symbols, nomenclature and units

Symbols

In addition to the list presented below, the symbols are explained with their first occurrence in the text or an equation.

\bar{a}	= S-N curve parameter, $\log(\bar{a})$ is the intercept of the $\log(N)$ axis
CP	= Controllable pitch
d	= Minimum shaft diameter at considered notch, in mm
D	= Propeller diameter, in m
d_i	= Inner diameter of shaft at considered notch, in mm
F_b	= Maximum backward blade force for the ship's service life, in kN
F_{ex}	= Ultimate blade load resulting from blade loss through plastic bending, in kN
F_f	= Maximum forward blade force for the ship's service life, in kN
h_0	= Depth of the propeller centreline from lower ice waterline, in m
H_{ice}	= Thickness of maximum design ice block entering the propeller, in m
I	= Number of different load magnitudes (load blocks) considered in Palmgren-Miner's usage factor/"damage sum"
k	= Weibull shape parameter

$LIWL$	= Lower ice waterline, in m
m	= Slope parameter for SN curve in log/log scale
M_{bl}	= Blade bending moment, in kNm
MCR	= Maximum continuous rating
MDR	= Miner's accumulated fatigue damage ratio
n	= Propeller rotational speed, in rev./s
$n_i(\tau_{v\ ice})$	= Number of cycles with a constant stress amplitude $\tau_{v\ ice}$
N_{ice}	= Number of load cycles in ice load spectrum
$N_i(\tau_{v\ ice})$	= Number of cycles to failure due to the constant stress amplitude $\tau_{v\ ice}$
q_w	= Weibull scale parameter, in Nm
R	= Propeller radius, in m
S	= Safety factor
T	= Torque, in Nm
T_0	= Torque at maximum continuous power in bollard condition, in Nm
$T_{average}$	= The average torque during an ice milling sequence, in Nm
Th_b	= Maximum backward propeller ice thrust for the ship's service life, in kN
Th_f	= Maximum forward propeller ice thrust for the ship's service life, in kN
Th_r	= Maximum response thrust along the shaft line, in kN
T_{peak}	= The highest response peak torque in the shaft due ice impacts on propeller, in Nm (probability for exceeding = $1/Z \cdot N_{ice}$)
T_A	= The response torque amplitude on the shaft during a sequence of ice impacts on the propeller, in Nm
$T_{A\ max}$	= The highest response torque amplitude on the shaft during a sequence of ice impacts on the propeller, in Nm (probability for exceeding = $1/Z \cdot N_{ice}$)
W_t	= Cross section modulus torsion, in mm^3 = polar moment of inertia divided by distance to the surface
Z	= Number of propeller blades
α_t	= Geometrical stress concentration factor, torsion
$\Delta\sigma_{max}$	= Maximum dynamic stress range, difference in maximum backward bending stress and maximum forward bending stress, in MPa
η	= Palmgren-Miner's usage factor/"damage sum"
σ_{Amax}	= Maximum dynamic stress amplitude, in MPa $\sigma_{Amax} = (\Delta\sigma_{max} / 2)$
σ_{Fat-E7}	= High cycle mean bending fatigue strength - 10^7 load cycles
σ_{mean}	= Mean stress, in MPa
σ_{ref}	= Reference stress, in MPa $\sigma_{ref} = 0.6 \cdot \sigma_{0.2} + 0.4 \cdot \sigma_u$
σ_{ref2}	= Reference stress, in MPa $\sigma_{ref2} = 0.7 \cdot \sigma_u$ or $\sigma_{ref2} = 0.6 \cdot \sigma_{0.2} + 0.4 \cdot \sigma_u$ whichever is less
σ_u	= Ultimate tensile strength of blade material, in MPa
σ_y	= Minimum specified yield strength of shaft material, in MPa

- τ = Nominal mean torsional stress at any load (or r.p.m.), in MPa
 $\tau_{v\text{ice}}$ = Nominal torsional stress on the shaft caused by $\tau_{v\text{ice}}$, in MPa
 $\tau_{v\text{ice max}}$ = Nominal torsional stress on the shaft caused by $\tau_{v\text{ice max}}$, in MPa
 τ_{vHC} = Permissible high cycle ($= 3 \cdot 10^6$ cycles) torsional vibration stress amplitude, in MPa
 τ_{vLC} = Permissible low cycle ($= 10^4$ cycles) torsional vibration stress amplitude, in MPa
 τ_y = Yield strength in shear of shaft material, in MPa ($=$ minimum specified $\sigma_y/\sqrt{3}$).

SECTION 2 PROPELLER BLADES

1 Ice interaction load models

The design loads described in the rules and listed in [Table 1](#) are maximum lifetime forces on a propeller resulting from propeller/ice interaction, including hydrodynamic loads.

The methodology presented here is an approach to be more in accordance with the actual, physical contact between propeller and ice. It covers conventional propeller design not limited to a certain blade skew angle. The background for the ice loads is a combination of ice model tests, full scale measurements and the Society's long service experience with ice classed vessels.

The requirements for concentrated ice loads affecting the blade tips and edges have been removed from these guidelines and will give a unique opportunity for the designers to optimise the blade edges and profiles individually. It is however necessary, during design of blades, to take into consideration the blade edges impact strength to avoid local indentations of the edges. This can be done with either old methods or even better with FEA and local ice pressures on the propeller blade edge and tip. See [\[3\]](#).

Table 1 Ice interaction loads

Load	Definition	Use of the load in design process
Q_{smax}	The maximum lifetime spindle torque on a propeller blade resulting from propeller/ice interaction, including hydrodynamic loads on that blade.	In designing the propeller strength, the spindle torque is automatically taken into account because the propeller load is acting on the blade as distributed pressure on the leading edge or tip area.
Th_b	The maximum lifetime thrust on propeller (all blades) resulting from propeller/ice interaction. The direction of the thrust is the propeller shaft direction and the force is opposite to the hydrodynamic thrust.	Is used for estimation of the response thrust T_{hr} . T_{hb} can be used as an estimate of excitation for axial vibration calculations. However, axial vibration calculations are not required by the rules.
Th_f	The maximum lifetime thrust on propeller (all blades) resulting from propeller/ice interaction. The direction of the thrust is the propeller shaft direction acting in the direction of hydrodynamic thrust.	Is used for estimation of the response thrust T_{hr} . T_{hf} can be used as an estimate of excitation for axial vibration calculations. However, axial vibration calculations are not required by the rules.
T_{max}	The maximum ice-induced torque resulting from propeller/ice interaction on one propeller blade, including hydrodynamic loads on that blade.	Is used for estimation of the response torque ($T_r(t)$) along the propulsion shaft line and as excitation for torsional vibration calculations.
F_{ex}	Ultimate blade load resulting from blade loss through plastic bending. The force that is needed to cause total failure of the blade so that plastic hinge is caused to the root area. The force is acting on $0.8R$. Spindle arm shall be taken as 1/3 of the distance between the axis of blade rotation and leading/trailing edge (whichever is the greater) at the $0.8R$ radius.	Blade failure load is used to dimension the blade bolts, pitch control mechanism, propeller shaft, propeller shaft bearing and trust bearing. The objective is to guarantee that total propeller blade failure should not cause damage to other components.
$T_r(t)$	Maximum response torque along the propeller shaft line, taking into account the dynamic behaviour of the shaft line for ice excitation (torsional vibration) and hydrodynamic mean torque on propeller.	Design torque for propeller shaft line components.

Load	Definition	Use of the load in design process
Th_r	Maximum response thrust along shaft line, taking into account the dynamic behaviour of the shaft line for ice excitation (axial vibration) and hydrodynamic mean thrust on propeller.	Design thrust for propeller shaft line components.

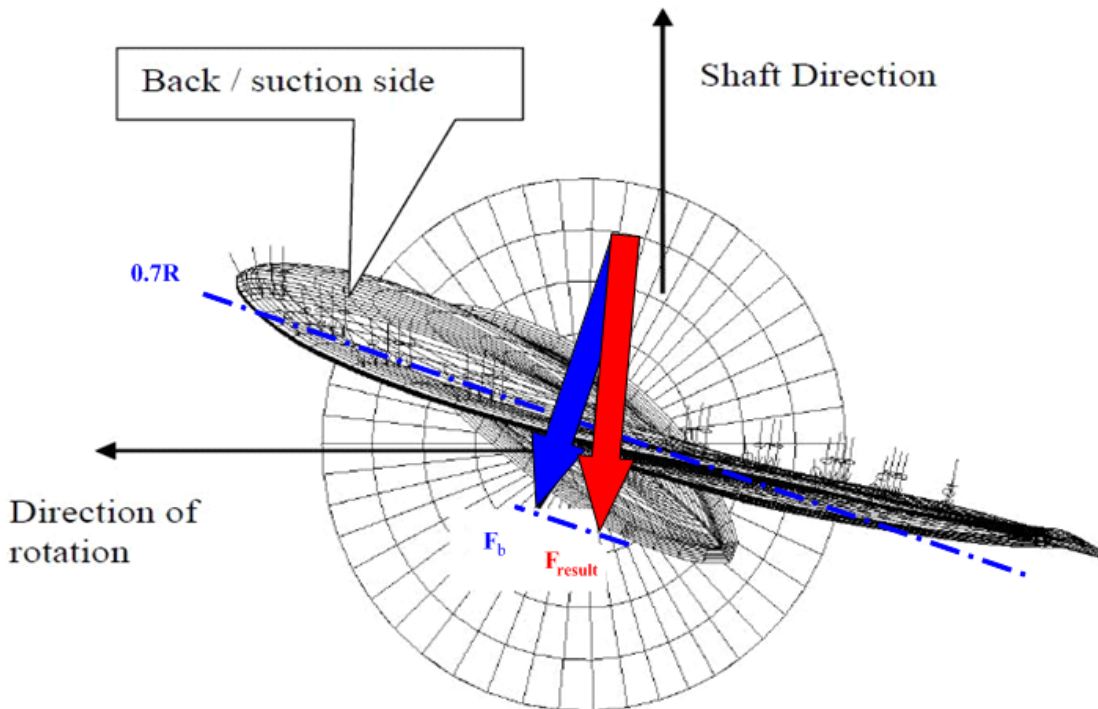


Figure 1 Ice loads acting on propeller

The direction of the forces is perpendicular to the plane defined by the generatrix and the $0.7R$ chord line. Homogenous surface pressure is applied over the part of the blade as specified for the various load cases in [Table 2](#) and [Table 3](#). Because the propeller blade is a curved 3-D shape the force resulting from a homogenous pressure, F_{result} may act in a somewhat different direction than perpendicular to the plane defined by the propeller generatrix and $0.7R$ chord line.

Hence the surface pressure shall be scaled so that the component of the resulting force perpendicular to the plane defined by the generatrix and $0.7R$ chord line equals the design load as derived from formulae in the [DNVGL-RU-SHIP Pt.6 Ch.6 Sec.2 \[15.8\]](#) and [DNVGL-RU-SHIP Pt.6 Ch.6 Sec.6 \[11.3\]](#) and [DNVGL-RU-SHIP Pt.6 Ch.6 Sec.6 \[11.4\]](#). Hence, the resulting force from the ice pressure, F_{result} may be somewhat larger than the design ice load but the difference will normally not be very large.

This is illustrated in the example for F_b in [Figure 1](#).

[Table 2](#), [Table 3](#) and [Table 4](#) give the extreme loads a propeller operating in ice is expected to encounter. The load cases 1-5 are given by the rules and are only reproduced here for convenience.

Table 2 Ice loads on leading edge and tip region – backward bending

	<i>Backward bending force - F_b</i>	<i>Use of the load in the design process</i>
F_b	The maximum lifetime backward force on a propeller blade resulting from propeller/ice interaction, including hydrodynamic loads on that blade. The direction of the force is perpendicular to $0.7R$ chord line. See Figure 1 .	Design force for strength calculation of the propeller blade.
	<i>Load case 1</i>	
Open propeller	Uniform pressure applied on the back of the blade (suction side) to an area from $0.6R$ to the tip and from the leading edge to 0.2 times the chord length. Pressure corresponding to F_b	
Ducted propeller	Uniform pressure applied on the back of the blade (suction side) to an area from $0.6R$ to the tip and from the leading edge to 0.2 times the chord length. Pressure corresponding to F_b	
	<i>Load case 2</i>	
Open propeller	Uniform pressure applied on the back of the blade (suction side) on the propeller tip area outside $0.9R$ radius. Pressure corresponding to 50% of F_b	

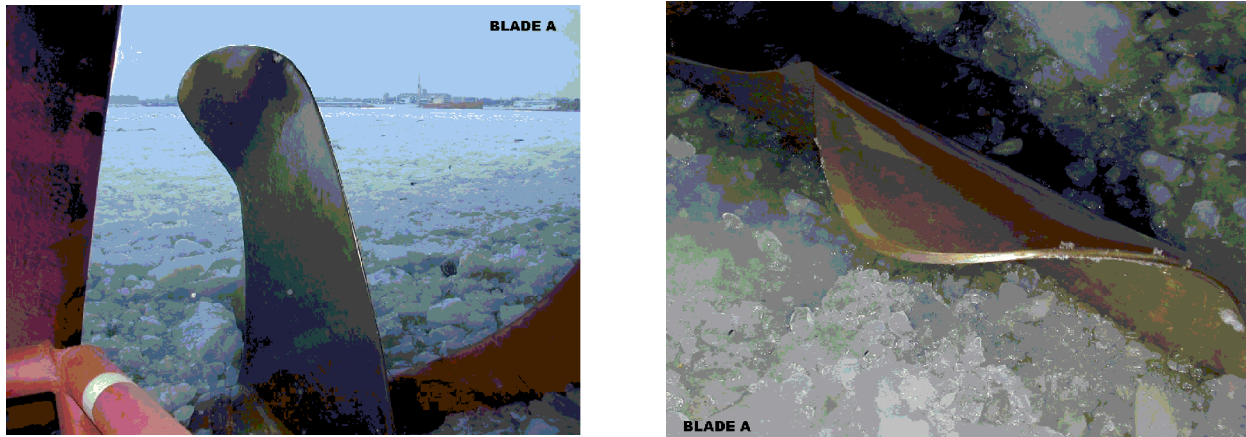


Figure 2 Backward bent blade trailing edge tip resulting in too heavy pitch and loss of propulsion until temporarily repaired

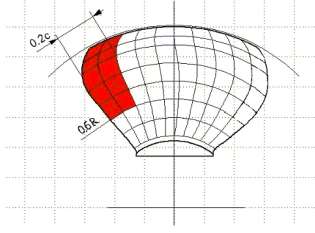
Table 3 Ice loads on leading edge and tip region – forward bending

	<i>Forward bending force - F_f</i>	<i>Use of the load in the design process</i>
F_f	The maximum lifetime forward force on a propeller blade resulting from propeller/ice interaction, including hydrodynamic loads on that blade. The direction of the force is perpendicular to $0.7R$ chord line. See Figure 1 .	Design force for calculation of strength of the propeller blade.
	<i>Load case 3</i>	
Open propeller	Uniform pressure applied on the blade face (pressure side) to an area from $0.6R$ to the tip and from the leading edge to 0.2 times the chord length. Pressure corresponding to F_f	

	<i>Forward bending force - F_f</i>	<i>Use of the load in the design process</i>
Ducted propeller	<p>Uniform pressure applied on the blade face (pressure side) to an area from $0.6R$ to the tip and from the leading edge to 0.5 times the chord length.</p> <p>Pressure corresponding to F_f</p>	
	<i>Load case 4</i>	
Open propeller	<p>Uniform pressure applied on propeller face (pressure side) on the propeller tip area outside $0.9R$ radius.</p> <p>Pressure corresponding to 50% of F_f</p>	

Table 4 Ice loads on trailing edge – forward or backward bending

	<i>Load case 5</i>		
Open propeller	60% of F_f or F_b , whichever is greater	Uniform pressure applied on propeller face (pressure side) to an area from $0.6R$ to the tip and from the trailing edge to 0.2 times the chord length	

Load case 5			
Ducted propeller	60% of F_f or F_b , whichever is greater	Uniform pressure applied on propeller face (pressure side) to an area from $0.6R$ to the tip and from the trailing edge to 0.2 times the chord length.	

2 Finite element analysis

2.1 FE model

The requirement for the finite element model is that it is able to represent the complex curvilinear geometry and the thickness variation of the blade, in order to represent the complex three-dimensional stress state of the structure and to predict the local peak stresses needed to assess the fatigue strength of the structure with acceptable accuracy. The load of the propeller blade is dominated by bending, leading to non-constant stress distribution over the thickness of the blade. Local details such as anti-singing edges etc. are normally excluded.

2.2 FE engineering practice

The use of solid elements is highly recommended for determining the stress distribution of the propeller blades. The use of a very dense parabolic tetrahedron mesh is recommended (see [Figure 4](#)). Parabolic hexahedron solid elements may also be used, but hexahedra require considerable greater modelling effort. Linear elements and, especially linear tetrahedrals should not be used in the stress analysis.

Well shaped elements are a prerequisite for the stress analysis. The element density should capture stress gradients and good element shape is important in the most loaded areas. It is recommended to show that the solution is independent of the mesh density.

Additional geometric details such as root fillet (see [Figure 3](#)) may be modelled however these tend to increase the complexity of the calculation and make it very heavy. This also applies for bolt holes etc. for CP propellers where it is recommended to do such studies separate from the propeller blade analysis but with a check of eventual interaction.

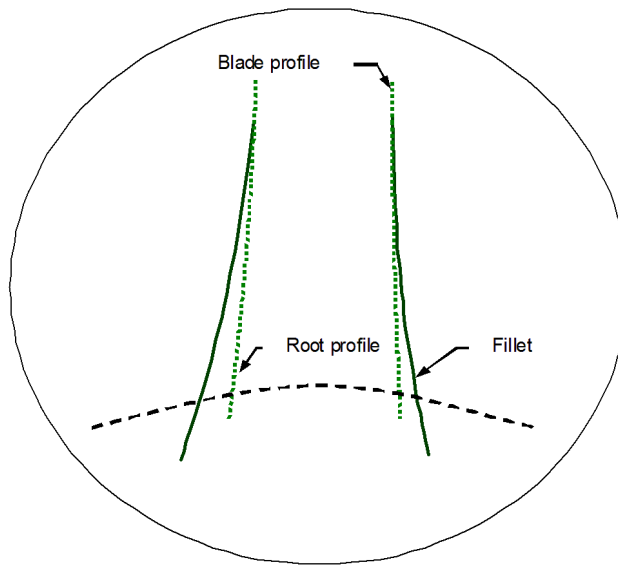


Figure 3 Root fillet of a propeller blade included in the lower blade profiles

A practical workaround would be to model the actual shape of the root fillet included in the sectional geometry of the blade and extend these cylindrical sections inside the propeller hub radius and then neglect the stress concentrations at the boundary connection.

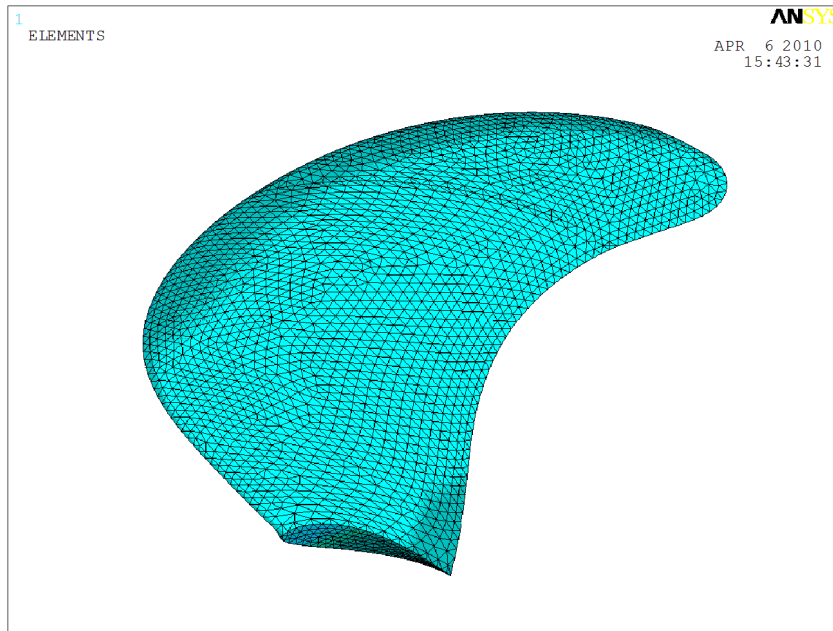


Figure 4 A typical parabolic tetrahedron mesh of a propeller blade

The modelling of the tip region is difficult. Thus, it is allowed, for example, to finish discretisation at the $0.975R$ cylindrical section and to make an artificial chord at the tip. In areas where mesh quality is unimportant is it acceptable to use highly skewed elements as these surfaces are only utilized for application of load/pressure.

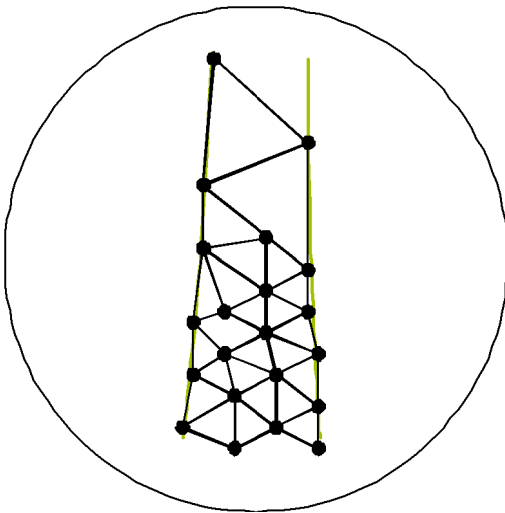


Figure 5 Typical thickness mesh

Where high bending stress occurs is it important to have at least 3-4 elements through the blade thickness as shown in [Figure 5](#).

2.3 Boundary conditions

The boundary conditions of the blade model should be given at an adequate distance from the peak stress location in order to ensure that the boundary condition has no significant effect on the calculated stress in areas of interest.

2.4 Applied pressure loads

The pressure loads applied on the finite element model can be given either in the normal direction of the curved blade surface or alternatively as a directional pressure load. The normal pressure approach leads to a loss of the net applied transversal load as a result of highly curved surface near the edges of the propeller blade. The surface pressure shall be scaled so that the resulting force in the perpendicular (normal) direction of the $0.7R$ chord line equals the design ice load as derived from formulae in the rules. Whichever approach is used, it should be ensured that the total force determined in the particular load case is applied on the model. In the normal pressure case, this can be by scaling the load or, alternatively, by scaling the resulting stresses. See [Figure 6](#) and [Figure 7](#).

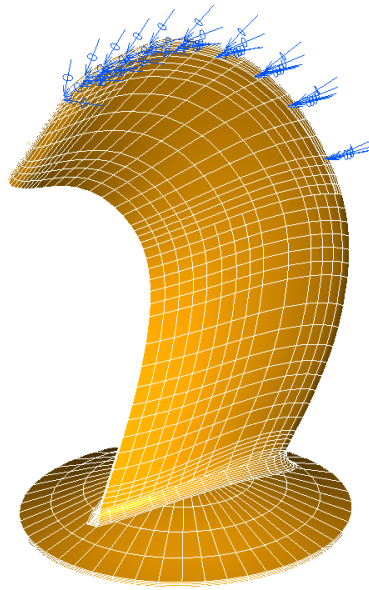


Figure 6 One possible way to apply the pressure load to the propeller blade. If the pressure load is given in the normal direction of the highly curved blade surface, the resulting net applied load will be less than the intended load and should be scaled appropriately

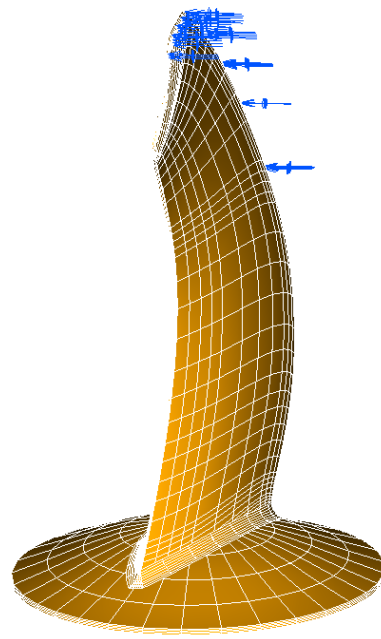


Figure 7 Second alternative: If the pressure load is given in a fixed direction the net applied load is directly the intended load

2.5 Choice of areas for further fatigue analysis

The relevant areas of an FE analysed blade would be where the stress range is largest for the complete lifetime of the propeller i.e. between the backward load, F_b and the forward load, F_f .

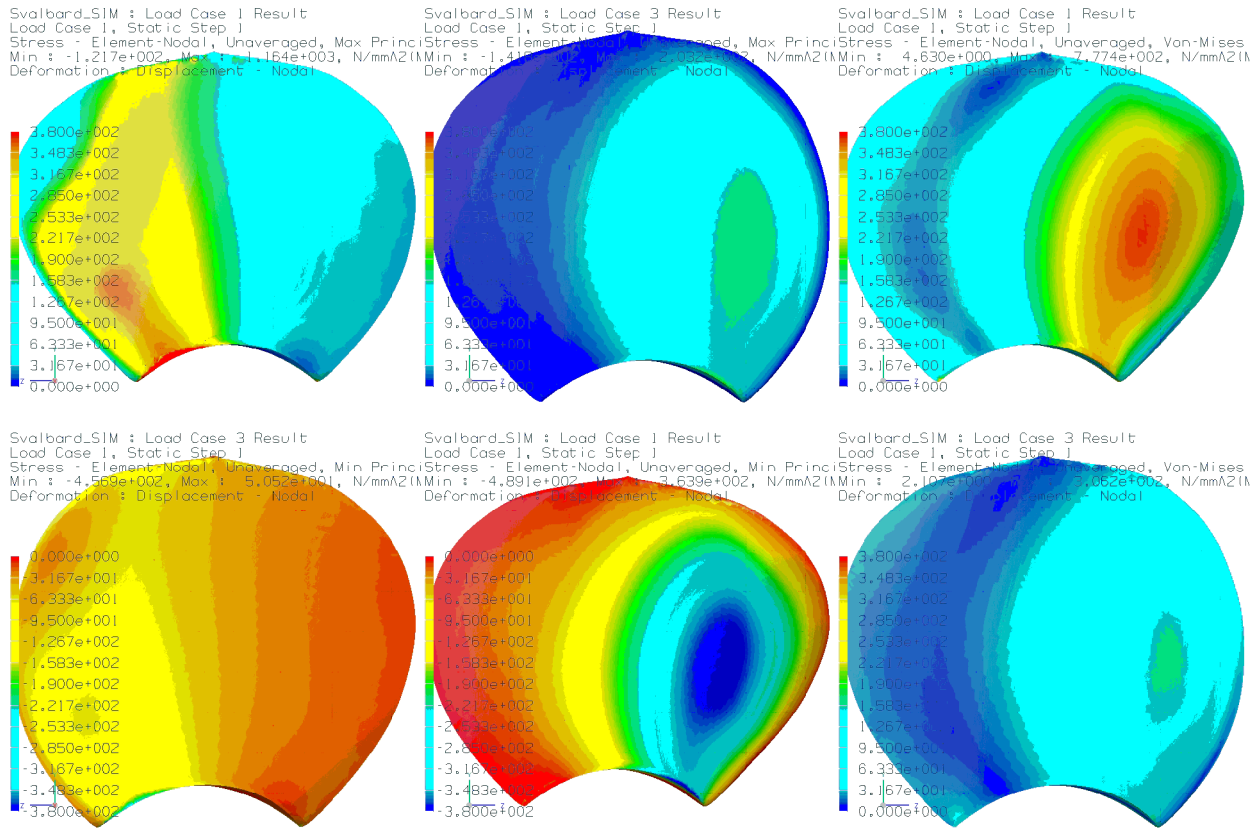


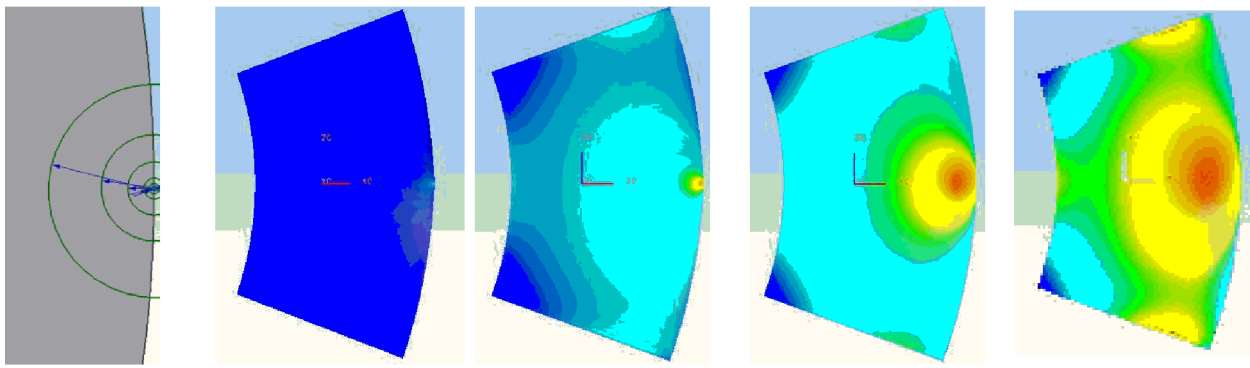
Figure 8 Typical arrangement of compared results: Top left- Max Principal- F_f , Top center -Max Principal- F_f , Bottom left-Min Principal- F_f , Bottom center-Min Principal- F_b Top right-von Mises- F_f , Bottom right – von Mises- F_b

The stresses compared should be Max-Min principal stresses for F_f and F_b respectively. It is important that the main principal stress direction is the same in both load cases. This might not be the case in specific areas of unconventional designs (f. ex. highly skewed propellers) where a lot of torsion occurs. There are in many FE post processors features available that creates stress plots with two load cases and by that shows the actual stress range on the model itself.

2.6 Blade tip and edge strengthening

The requirements for concentrated ice loads affecting the blade tips and edges have been removed from the rules and will give a unique opportunity for the designers to optimize the blade edges and profiles individually. It is however necessary, during design of blades, to take into consideration the blade edges impact strength to avoid local indentations of the edges by making blade edges and tips sufficiently strong to withstand contact with multiyear hard blue ice with pressures that may reach 30...40 MPa very locally.

This can be done with either old methods or even better with FEA and local ice pressures on the propeller blade edges and tips applying local ice loads depending on considered local area on the relevant blade edge and tip regions. Ice force as a function of considered area may be found as for pod/thruster structures, see Sec.7 [1.2].



Series of figures above show how ice load can be applied and corresponding stresses. Pressure on smallest area of 2 mm^2 is 30 MPa and decreases to 9.7 MPa at 3700 mm^2 . Corresponding stresses are from 46 to 340 MPa. The blade section profile is taken from a large propeller where leading edge was found damaged.

Figure 9 Blade tip and edge stress

3 Propeller blade strength assessment

The propeller blade shall be assessed for both fatigue and static loading. The Palmgren-Miner damage theory and the S-N curve will be restricted for stresses exceeding $\sigma_{ref2} / 1.5$.

A cumulative load spectrum is distributed utilizing the Weibull method for the corresponding σ_{Amax} based on the FEA for selected position(s) on the blade where the stress range (F_f vs. $\Delta_{\sigma max} F_b$) is largest.

3.1 Propeller materials fatigue strength, S-N curve

Materials fatigue endurance has mainly been found from literature. However the majority of these tests were conducted several decades ago. The values presented in [Table 5](#) are strictly "mean fatigue strength values" at 10^7 cycles and shall not be directly compared to the values given in [DNVGL-RU-SHIP Pt.4 Ch.5 Sec.1](#) [Table 4](#). The values in [Table 5](#) are not containing any uncertainties which need to be taken into consideration separately.

Table 5 High cycle mean fatigue strengths

<i>Bronze and brass (a=0.10)</i>		<i>Stainless steel (a=0.05)</i>	
Mn-Bronze, CU1 (high tensile brass)	80 MPa	Ferritic (12Cr 1Ni)	120 MPa
Mn-Ni-Bronze, CU2 (high tensile brass)	80 MPa	Martensitic (13Cr 4Ni/13Cr 6Ni)	150 MPa
Ni-Al-Bronze, CU3	120MPa	Martensitic (16Cr 5Ni)	165 MPa
Mn-Al-Bronze, CU4	105 MPa	Austenitic (19Cr 10Ni)	130 MPa

Alternatively, σ_{Fat-E7} can be defined from fatigue test results from approved fatigue tests at 50% survival probability and stress ratio $R = -1$, see [DNVGL-RU-SHIP Pt.4 Ch.5 Sec.1 \[2.1.1\]](#).

Endurance values shall reflect the components actual production methods (casting process, welding, heat treatment etc.), loading patterns (bending vs. tension, shear etc) as well as the materials behaviour of changing over time (corrosion etc.). Due to the effect of variable loading with respect of fatigue (stress memory effects) the S-N curve slope of 4.5 from 10^7 cycles has been extended to 10^8 cycles and thereafter continues with slope 10. Some more details regarding the establishment of S-N curve are given in [DNVGL-RU-SHIP Pt.6 Ch.6 Sec.6](#).

3.2 Blade fatigue assessment

The fatigue assessment can be carried out by means of Palmgren-Miner's theory either utilizing several load blocks (I) as in [Figure 10](#), or by a direct integration method. See [App.A Figure 10](#) showing a two-slope S-N curve combined with σ_{ref2} limitation, extension of slope 4.5 to E8 cycles and the Weibull load function based on $k = 1.0$.

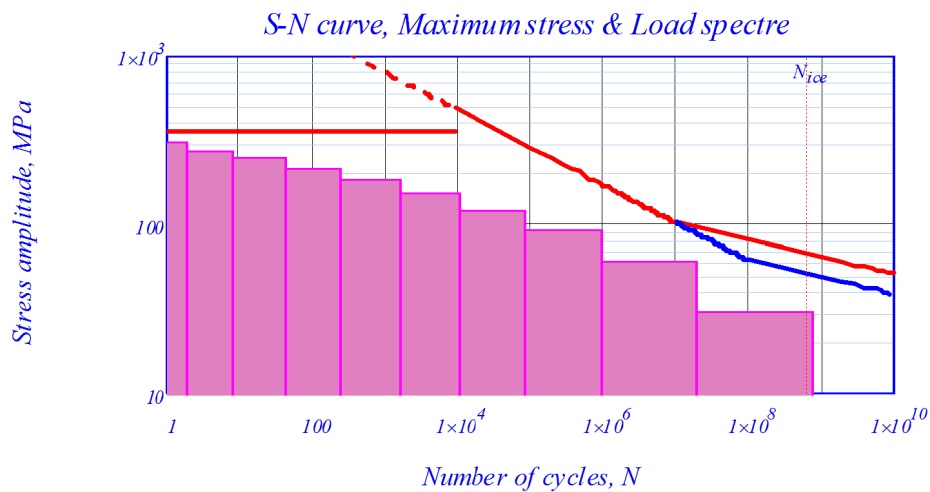


Figure 10 S-N curve, maximum stress and load spectrum

Maximum dynamic stress range; $\Delta\sigma_{max}$ is difference in maximum backward bending stress, $\sigma_{max\ b}$ and maximum forward bending stress, $\sigma_{max\ f}$. The stress amplitude; $\sigma_{A\ max} = \frac{\Delta\sigma_{max}}{2}$

Mean stress; σ_{mean} should be taken as mean stress due to hydrodynamic propeller load in ice condition (bollard condition).

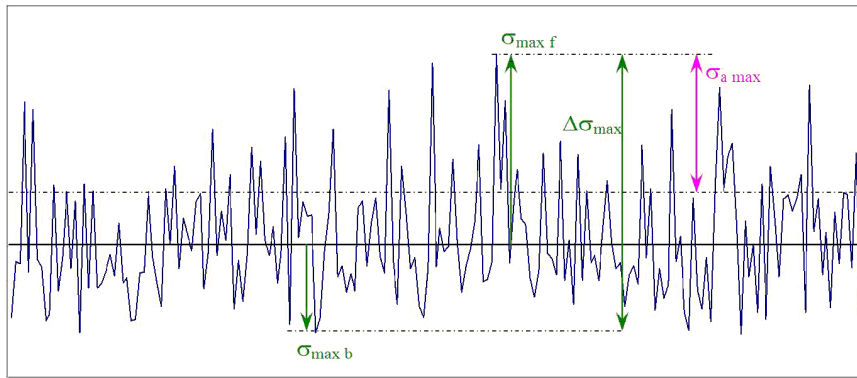


Figure 11 Time series of blade stresses

Investigations have shown that dividing the stress spectrum into minimum $I = 10$ load blocks is necessary to avoid too conservative results.

Stress amplitude for block No. i:

$$\sigma_i = \sigma_{A\ max} \left(1 - \frac{i-1}{I}\right)$$

No. of cycles in block No. i:

$$n_i = N_{ice}^{1 - \left(\frac{1-i}{I}\right)^k} - \sum_{i=1}^{i-1} n_{i-1}$$

Where N_{ice} is the total number of ice impacts.

A Miner sum, $MDR < 1.0$ is sufficient, since safety factors are included in the values for fatigue strength.

The damage rate for a propeller blade can be expressed in the following form:

$$MDR = \sum_{i=1}^I \frac{n_i(\sigma_{Amax})}{N_i(\sigma_{Amax})} = \sum_{i=1}^I \frac{1}{\alpha} n_i(\sigma_{Amax}) \cdot (\sigma_{Amax})^m \leq 1.0$$

where:

- σ_{Amax} = is a constant stress amplitude of the blade due to ice interaction on the propeller
- $n_i(\sigma_{Amax})$ = is the discrete number of cycles with a constant stress amplitude σ_{Amax}
- $N_i(\sigma_{Amax})$ = is the number of cycles to failure of a constant stress amplitude σ_{Amax} based on the relevant part of the design S-N-curve
- $\frac{n_i(\sigma_{Amax})}{N_i(\sigma_{Amax})}$ = degree of cumulative "damage" of a constant stress amplitude σ_{Amax}
- I = number of different load magnitudes (load blocks)
- k = Weibull shape parameter = 0.75 for open propellers and 1.0 for nozzle propellers
- m = negative inverse slope of the relevant part (for σ_{Amax}) of the design S-N curve
- α = intercept with the log(N) axis of the relevant part (for σ_{Amax}) of the design S-N curve.

4 Blade failure design loads

4.1 Blade failure load

Blade failure load has been applied as one of the main design principles since 1971 in design of propulsion plant pyramidal strength. The blade shall be the weak part and bending of one blade shall not lead to successive damages to hub or shaft, or any other relevant part, such as thrust bearing, or azimuth thruster structure or its support.

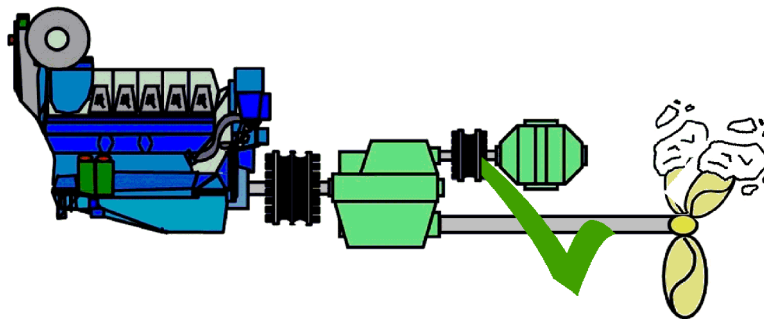


Figure 12 'Pyramide' or selective strength principle = blade failure before shafting failure

4.2 Calculation of the bent blade scenario with FEA analysis

Determination of the blade failure load F_{ex} can either be made by means of a bending beam based equation, or by means of FEA. In both cases the load shall act on genetic axis at 0.8 radius. The load may be given as a point load, or a pressure load on defined area with centriod at defined load acting point. One of assumptions is that blade shall bend near root fillet. This is one reason why load is now defined acting at $0.8R$ rather than 0.85 or $0.9R$, as has been case in the previous ice rules.

It is further assumed that the same load may act on a certain offset of spindle (genetic) axis. Based on a series of FEA the Society has carried out it has been proven that this load may act at a distance of $1/3$ of distance between the spindle axis and leading or trailing edge, which ever is greater. If the distance is made longer a blade starts to deform locally and not as assumed.

4.3 Plastic hinge method

Even if the Society consider plastic bending of the blade over a root section, the Society will accept linear FEA assuming an elastic model. In this respect blade failure load is defined as a force causing von Mises equivalent stresses of 1.5 times σ_{ref} . Because σ_{ref} (which is a function of ultimate tensile strength, UTS and yield strength, YS) has been determined experimentally for stainless steel and bronze materials by means of measuring real force needed to bend rectangular test beam 45° and assuming that plastic section modulus is 1.5 times ditto elastic, the Society consider this sufficiently proven.

σ_{ref} can either be determined based on known mechanical properties of the considered section, or on basis of specified maximum permissible range of the UTS and YS.

SECTION 3 PROPELLER HUB AND PITCH MECHANISM

1 Scope and general remarks

1.1 Scope

In the following it is specified more in detail an acceptable way of assessing the propeller hub and pitch mechanism strength-wise, according to the ice criteria as described in [DNVGL-RU-SHIP Pt.6 Ch.6 Sec.2](#) and [DNVGL-RU-SHIP Pt.6 Ch.6 Sec.6](#).



Figure 1 CP propeller failure resulting in too heavy pitch and thus total loss of propulsion .

Calculation principles and methodologies are specified, and analytical formulae for stress calculations are given as an alternative to more detailed calculations by means of Finite Element Analysis - FEA.

1.2 Considered parts in hub and pitch mechanism

The following calculation method is valid only for crosshead type of pitch mechanism as illustrated in [Figure 2](#) and [Figure 3](#). Other types of pitch mechanisms may be assessed on basis of the equivalency principle.

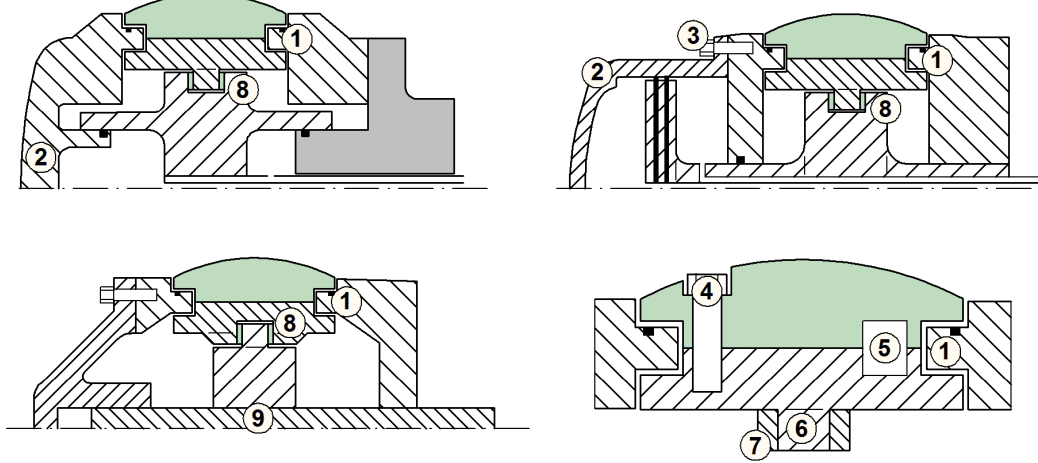


Figure 2 Illustration of considered parts in hub and pitch mechanism for some design types:

- servo cylinder in propeller hub with integrated servo piston and cross head, crank pin on crank disk
- servo cylinder in propeller hub with separate servo piston and cross head, crank pin on crank disk
- servo cylinder in shaft line or reduction gear with crank pin on cross head
- close-up of blade fastening and crank disk of mechanism type a) and b)

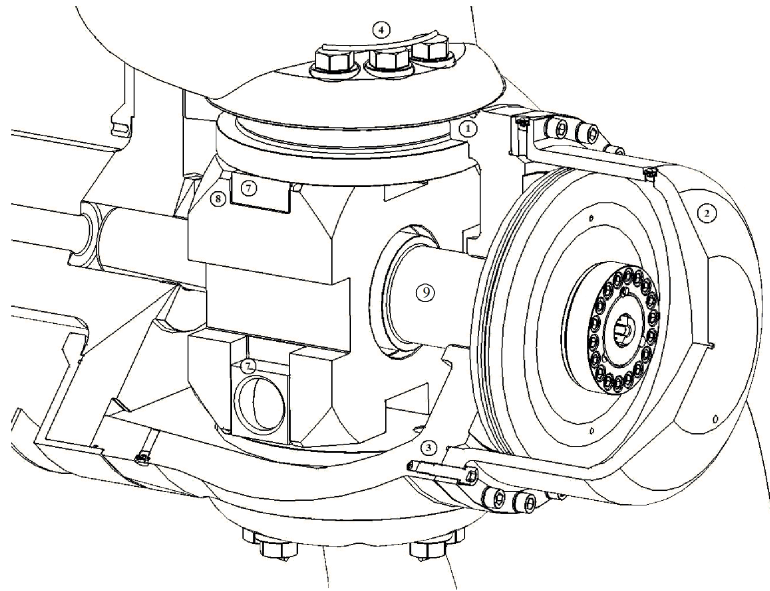


Figure 3 Typical controllable pitch propeller mechanism (courtesy of Berg Propulsion Technology AB)

The following components are considered for mechanical strength:

- propeller hub with blade carrier bearings (1)
- servo cylinder (2), including clamping bolts (3)
- blade bolts (4) and shear pins (5)
- crank pin (6)
- guide block (7)
- retaining wall of slot for guide block (8)
- push-pull rod, including fitting to cross head (9).

2 Applicable load scenarios

2.1 Propeller blade plastic bending (selective strength or “pyramid strength principle”)

A propeller blade exposed to an ice load causing plastic bending of blade shall not lead to significant permanent deformation in the blade fitting arrangement, propeller hub or pitch mechanism. This means that the resulting nominal (excluding local stress concentrations) equivalent (von Mises) tensile stress in each of the components shall not exceed the specified minimum yield strength of respective components material (i.e. safety factor against nominal yielding is 1.0, as given in [DNVGL-RU-SHIP Pt.6 Ch.6 Sec.2](#) and [DNVGL-RU-SHIP Pt.6 Ch.6 Sec.6](#). See also [Sec.2 \[4\]](#))

For blade bolts and hub (blade carriers) the bending moment resulting from the blade failure load, F_{ex} as described in [DNVGL-RU-SHIP Pt.6 Ch.6 Sec.2](#) and [DNVGL-RU-SHIP Pt.6 Ch.6 Sec.6](#) located at the propeller blade spindle axis shall be considered (i.e. no spindle torque is considered).

The torsional capacity of the blade fitting (shear pins and friction capacity in blade bolt connection) and components in pitch mechanism shall be considered on basis of the spindle torque Q_{sex} from the eccentrically located F_{ex} (see [Sec.2 \[4.1\]](#)).

2.2 Propeller blade force due to maximum ice load

When propeller blade is exposed to maximum ice loads (F_b and F_f) as described in [DNVGL-RU-SHIP Pt.6 Ch.6 Sec.2](#) and [DNVGL-RU-SHIP Pt.6 Ch.6 Sec.6](#) the methodology for assessing blade fitting arrangement, propeller hub and pitch mechanism is the same as in the propeller blade plastic bending case (see also [\[2.1\]](#)), i.e. nominal stresses are compared to yield strength.

However, for the maximum ice load case, a safety factor of 1.3 against yielding is required in the [DNVGL-RU-SHIP Pt.6 Ch.6 Sec.2](#) and [DNVGL-RU-SHIP Pt.6 Ch.6 Sec.6](#). Safety factor shall be applied on the acting ice load, unless otherwise is explicitly specified.

2.3 Propeller blade forces due to dynamic ice load amplitudes

When exposed to a spectrum of ice loads derived from the maximum ice loads (F_b and F_f) as described in the ice rules, the safety factor against fatigue for the influenced parts in propeller hub and pitch mechanism shall be at least 1.5, according to Miner's rule, as required in [DNVGL-RU-SHIP Pt.6 Ch.6 Sec.2](#) and [DNVGL-RU-SHIP Pt.6 Ch.6 Sec.6](#). Safety factor shall be applied on the acting dynamic ice load amplitudes.

The application of ice loads on each component is the same as for the two (static) cases above.

3 Load transmission

3.1 Transmission of spindle torque into mechanism

The propeller blade spindle torque caused by ice loads acting eccentrically to the spindle axis will be transmitted into the propeller pitch mechanism.

However, parts of the spindle torque will be taken up as friction loss due to reaction forces set up in the blade carrier bearings. In the radial bearing, there will be reaction forces due to ice load on propeller blade, and forces on the crank pin. The reduction in loads due to these frictional losses may be accounted for as mentioned herein.

3.2 Geometrical relations

The geometrical relations between spindle torque and force on crank pin are given as follows:

In the case crank pin is fixed in crank disk:

$$F_{crp} = \frac{1000Q_{crp}}{R_{crp} \cos \varphi} \quad (\text{kN})$$

In the case crank pin is fixed in cross head:

$$F_{crp} = \frac{1000Q_{crp}}{R_{crp}} \cos \varphi \quad (\text{kN})$$

where Q_{crp} is net spindle torque (kNm) transmitted into the mechanism, see [3.3] next chapter, R_{crp} (mm) is crank pin eccentricity and φ (rad) is considered angular position of crank pin (normally same as pitch angle).

Note that since Q_{crp} includes the frictional losses and the specified safety factors, this also applies for F_{crp} .

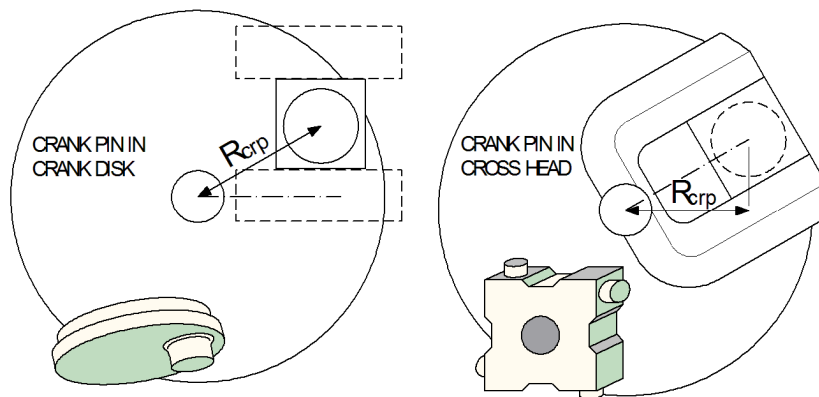


Figure 4 Crank pin in crank disc and in cross head

Further, the force on crank pin is transmitted into a servo, generating a certain increase in servo pressure. In this respect, a direct transformation shall be carried out (i.e. no further internal frictional losses except those mentioned in next chapter shall be accounted for). Servo pressure corresponding to a given force on crank pin is then found as follows:

In case crank pin is fixed in crank disk:

$$p_{\text{servo}} = \frac{10^4 F_{\text{crp}}}{A_{\text{servo}}} \quad (\text{bar})$$

In case crank pin is fixed in cross head:

$$p_{\text{servo}} = \frac{10^4 F_{\text{crp}}}{A_{\text{servo}}} \cos \varphi \quad (\text{bar})$$

Where A_{servo} is effective pressurised area of the servo piston (mm^2).

3.3 Reduction in transmitted spindle torque due to friction

3.3.1 Bending moments taken up by the blade carrier will cause the following friction torque:

$$Q_{\text{frb}} = Mb \left(\frac{D_{\text{blc}}}{D_{\text{bfrc}}} \right) \mu \quad (\text{kNm})$$

Where Mb is bending moment (kNm) *including* relevant safety factor and may be taken in the same way as for the blade bolts (see [5.4]). D_{blc} is effective blade carrier diameter (mm) carrying the load, D_{bfrc} is effective friction diameter (mm) and μ is friction coefficient (-). See also [Figure 5](#).

For lubricated surfaces, the friction coefficient μ shall be taken as 0.10.

Pressure distribution may be assumed to be sinusoidal. Then the relation $D_{\text{blc}}/D_{\text{bfrc}}$ equals $4/\pi$.

Forces taken up radially by the blade carrier will cause the following friction torque, Q_{frf} :

$$Q_{\text{frf}} = \frac{2 F D_{\text{ffric}} \mu}{\pi} 10^{-3} \quad (\text{kNm})$$

Where F is considered radial force (kN) in bearing, *including* relevant safety factor and D_{ffric} is effective friction diameter (mm).

Pressure distribution may be assumed to be sinusoidal. Then D_{ffric} is $4 \times D_{\text{iblc}}/\pi$, where D_{iblc} is inner diameter (mm) of blade carrier (blade thrust) bearing. See also [Figure 5](#).

Compared to the frictional forces generated by the ice loads, the contribution from centrifugal forces is normally relatively small and shall be neglected for safety and simplicity. This will contribute to predicted crank pin forces somewhat more to the safe side, in particular for the high cycle loads.

Note that the ice loads specified in the rules include contribution from hydrodynamic propeller load, when applicable, and hence no separate friction loss shall be calculated for the hydrodynamic propeller load.

3.3.2 Spindle torque transferred into crank pin

Net spindle torque transferred into the pitch mechanism (crank pin), Q_{crp} shall be taken as $Q_{crp} = Q_{sp} - Q_{fr1}$ (kNm) where Q_{sp} is the considered blade spindle torque (kNm), *including* the specified safety factor, Q_{fr1} (kNm) is the sum of relevant friction torque reductions due to blade carrier loads, i.e. $Q_{fr1} = Q_{frb} + Q_{frf}$ (kNm).

3.3.3 Spindle torque for evaluation of blade flange/crank disk connection

When considering the transfer of spindle torque between the blade flange and the crank disk, the following net spindle torque shall be used: $Q_{crp} = Q_{sp} - Q_{fr1} - Q_{fr2}$ (kNm) where Q_{fr2} is the friction torque reduction between the blade flange and crank disk due to bolt pretension forces, to be taken as:

$$Q_{fr2} = \mu \sigma_{bpre} \frac{\pi}{4} D_{bblt}^2 N_{bblt} \frac{PCD}{2} 10^{-6} \quad (\text{kNm})$$

Where σ_{bpre} is bolt pre-stress (N/mm²) in section with minimum diameter, D_{bblt} (mm), N_{bblt} is number of bolts, and PCD is bolt pitch circle diameter (mm). For non-lubricated surfaces the friction coefficient μ shall be taken as 0.15 unless otherwise substantiated.

The relevant friction torque reduction, Q_{fr1} should in this respect only include the friction contribution on the blade flange (not the crank disk). I.e. the following applies:

$$Q_{fr1} = 0.5 Q_{frb} - k_{hcr} Q_{frf} \quad (\text{kNm})$$

Where k_{hcr} is describing the height ratio between blade flange part of radial bearing and total radial bearing height. I.e. if only blade flange has a radial bearing surface, k_{hcr} is 1.0, if only crank disk has a radial bearing surface, k_{hcr} is 0.0. For designs as illustrated in [Figure 2](#), k_{hcr} would be some 0.5.

3.4 Transmission of blade bending moment into blade carrier

Assuming that the peripheral pressure distribution due to a bending moment M_{bl} follows a sinusoidal relationship, the maximum pressure at the blade carrier is found from:

$$p_{bbclmax} = \frac{M_{bl}}{\frac{\pi}{4} B_{blc} D_{blc}^2} 10^6 \quad (\text{N/mm}^2)$$

Where B_{blc} is breadth of blade carrier bearing (mm). See also [Figure 5](#).

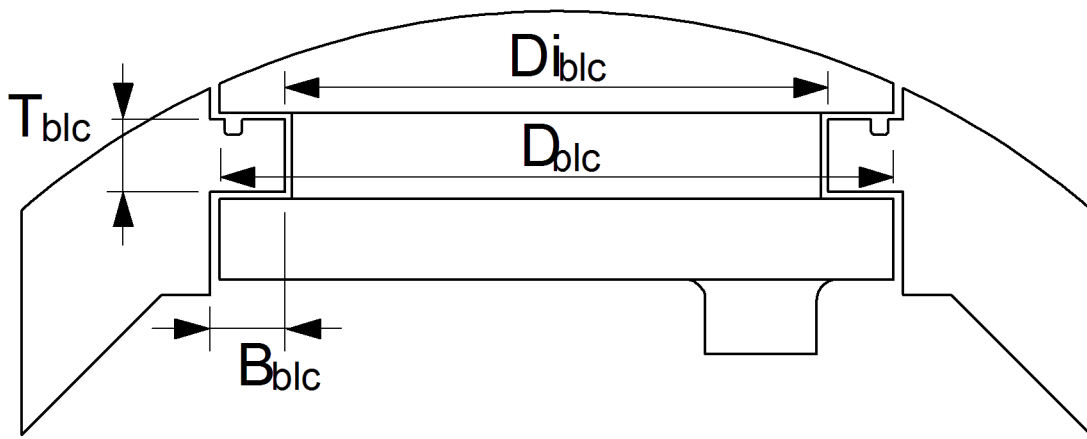


Figure 5 Illustration of blade carrier and blade bearing.

3.5 Transmission of force into blade carrier

Assuming that the peripherical pressure distribution due to a force also follows a sinusoidal relationship, the maximum radial pressure at the blade carrier is found from:

$$p_{fblc \max} = \frac{F}{\frac{\pi}{4} T_{blc} D_{iblc}} 10^6 \text{ (N/mm}^2\text{)}$$

Where T_{blc} is thickness of blade carrier bearing (mm). See also Figure 5.

3.6 Transmission of load between crank pin and retaining wall for guide block

The ice loads from the blade are transferred by means of pressure from the crank disk to the crosshead, via the guide block. These components deflect when loaded. This influences on the pressure distribution and hence, the pressure distribution at the contact surfaces deviates from the nominal pressure. This applies in particular when the loading is high. The skewed pressure distribution changes the effective point of reaction for the transmitted force, as well as introduces local strains and stresses.

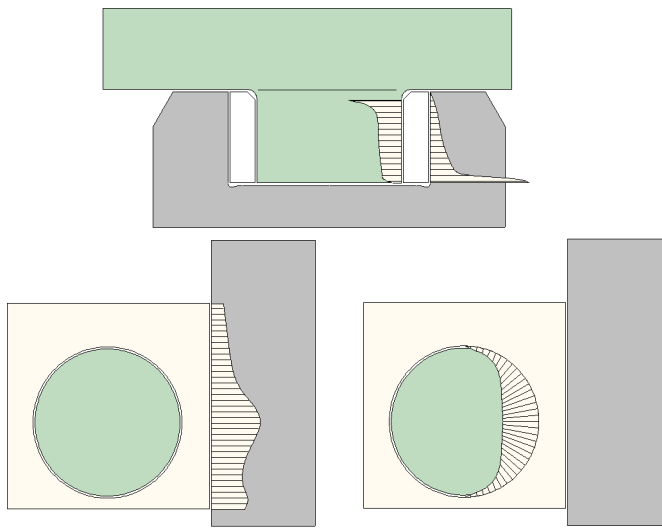


Figure 6 Illustration of possible pressure distribution between crack components

In general, the “footprint” of crank pin cylindrical shape is reflected in the pressure distribution on the retaining wall and vice versa.

Further, a distinct increase in local pressure near the root sections (close to the fillet) of crank pin and retaining wall is normally seen.

Apart from the local high pressure near the root sections, the height-wise pressure distribution on the crank pin is normally quite homogenous. For the retaining wall, the height-wise pressure distribution normally shows more of a triangular shape.

Both for the crank pin and the retaining wall, local maximum stresses in fillets are also influenced by the contact pressure occurring at the surface close to the fillets.

These effects lead to shortcomings when predicting stresses according to classical cantilever beam theory and shall be accounted for. In particular for local stresses (relevant for fatigue calculations) this influence is significant. The above is included in the strength assessment, see [4].

During the transmission of loads via contact surfaces, there will also be some internal friction. However, for safety and simplicity the internal friction losses in the crank mechanism shall not be accounted for.

3.7 Transmission of loads into cross head, push-pull rod and servo

In general ice loads act at one blade at the time. This introduces a bending moment on the cross head, which together with the radial forces is transmitted into the crosshead bearings. Such bearings may be integrated in the crosshead arrangement itself or the push-pull rod bearing support may also act as radial journal bearing for the cross head.

The axial component of the crank pin force is transmitted via the crosshead and push-pull rod (if applicable) and into the servo. To some extent, part of the axial load may also be transmitted back into the crank pins connected to blades which are not exposed to the ice load (and will be taken up as mass forces and friction forces in the respective blade carriers). Such a reduction in servo loading is quite uncertain and shall not be accounted for.

There will also be some internal friction in crosshead / push-pull rod bearings. For safety and simplicity these friction losses shall not be accounted for.

4 Strength assessment

4.1 Static strength

The load conditions referred to in [2.1] (blade failure load) and [2.2] (maximum ice loads) shall be considered as static load cases. That means that the strength assessment is carried out directly against the loads, including the safety factors specified in DNVGL-RU-SHIP Pt.6 Ch.6 Sec.2 and DNVGL-RU-SHIP Pt.6 Ch.6 Sec.6.

For these load cases, the “worst condition” assumption applies, since the loads in principle may apply in any operating condition. For the static strength assessment this means that propeller pitch angle shall be chosen as the one giving highest loads in the components.

In case crank pin is located in cross head this means that pitch angle shall correspond to crank pin in zero angle position (normally, this equals the geometrical zero pitch position).

With the crank pin located in the crank disk, maximum operational pitch angle for ice operation shall be chosen. If not otherwise is substantiated, a pitch angle corresponding to 70% of pitch at ahead free running, *MCR* shall be used.

In case the design pressure is lower than the pressure corresponding to blade failure load, the mechanism shall additionally be checked in a pitch condition corresponding to mechanical stop. The same applies if relief valve arrangement is only provided on the pump side of the directional valves.

4.2 Dynamic strength

The load conditions referred to in [2.3] (dynamic loads) shall be assessed according to fatigue criteria as described in the following sub-sections. In general, such loads will accumulate under all possible ice operating conditions, and hence under varying pitch angles.

However, in order to simplify the calculations, the complete fatigue assessment shall be carried out for one reference pitch setting:

- in case crank pin is located in crank disk a pitch angle corresponding to 60% of pitch at ahead free running, *MCR* shall be used
- in case crank pin is located in cross head a pitch angle corresponding to 40% of pitch at ahead free running, *MCR* shall be used.

4.3 Cumulative fatigue calculation

The hub and pitch mechanism shall be designed to prevent accumulated fatigue when considering loads as described in DNVGL-RU-SHIP Pt.6 Ch.6 Sec.2 and DNVGL-RU-SHIP Pt.6 Ch.6 Sec.6.

There are locations at the components in the hub and pitch mechanism where dynamic stresses due to ice loads are significantly higher than in the surrounding material. These stress risers, such as notches or fillets forming the transition between different shapes, are critical w.r.t. fatigue strength.

The same may apply to welded parts, where fatigue strength is reduced due to the welding.

In case local stresses at maximum load exceeds yield strength (σ_y or $\sigma_{0,2}$) or 70% of the ultimate tensile strength (σ_u) sufficient margin against accumulated fatigue shall be documented using the linear elastic Miner's rule.

The stress spectrum should be divided into minimum $I = 10$ blocks. A lower number of blocks is too conservative, whereas increasing the number of blocks beyond $I = 20$ blocks will not reduce the calculated fatigue damage significantly.

Miner's rule sum up damage fractions, n_i / N_i , where n_i and N_i are respective occurring and allowable number of cycles for the load level (stress block) in question (according to the material SN diagram – see also [6.2]). Hence the total fatigue damage is given by the Miner sum, MDR (-):

$$MDR = \sum_{i=1}^I \frac{n_i}{N_i} \quad (-)$$

A Miner sum, $MDR < 1.0$ is sufficient, since safety factors are included in the ice loads and load level for each block is chosen conservatively.

No. of cycles in block No. i:

$$n_i = (Z_{ice} N_{ice})^{1 - \left(\frac{1-i}{I}\right)^k} - \sum_{i=1}^{i-1} n_{i-1} \quad (-)$$

Where Z_{ice} equals number of propeller blades in case the considered component accumulates ice loads from all blades (for instance push-pull rod). Otherwise $Z_{ice} = 1$. Further, k is the Weibull shape parameter = 0.75 for open propellers and 1.0 for nozzle propellers, and N_{ice} is the number of ice impacts (-) experienced by the propeller blade during its life time, as defined in [DNVGL-RU-SHIP Pt.6 Ch.6 Sec.2](#) and [DNVGL-RU-SHIP Pt.6 Ch.6 Sec.6](#). The formulation is conservative, because each block refers to the nearest load level above.

4.4 Fatigue stress amplitude

The propeller blade ice spindle torque variation spectrum follows a Weibull distribution. However, the relation between load and corresponding stress in parts of the pitch mechanism components is not necessarily strictly linear. This is due to deflections in the mechanism and frictional effects. In the calculation model described herein, this is neglected, and the calculation models are chosen in order to be representative for typical load situations contributing to fatigue damage.

Hence, a Weibull distribution for acting stress is assumed as a simplification, and fatigue stress amplitude for block No. i shall be taken as:

$$\sigma_i = \sigma_{A\max} \left(1 - \frac{i-1}{I} \right) \quad (\text{N/mm}^2)$$

Stress concentration factors, K_t are discussed in subsequent sub-sections for each component.

5 Stress in components of CP-Mechanism

5.1 Stress calculation in general

5.1.1 Static stress

Formulae for nominal equivalent static stresses are given for each of the components in the sub-sections below.

5.1.2 Dynamic stress amplitude/mean stress

Maximum dynamic stress range, $\Delta\sigma_{max}$ (N/mm²) is defined as the difference in component stress when blade is exposed to maximum backward load (F_b) and maximum forward load (F_f) for components that will be influenced by load in both directions.

For components influenced by load in only one direction (retaining wall) maximum backward load or maximum forward load is taken as zero (whichever is less critical).

The maximum stress amplitude $\sigma_{Amax} = \Delta\sigma_{max}/2$ (N/mm²) corresponds to the "once in a life time" ice load situation. For stress range/amplitude distribution, see [4].

Mean stress, σ_{mean} (for determination of reduction in fatigue strength due influence of mean stress, K_{mean} - see [6.2]) shall be taken as a constant = stress due to hydrodynamic propeller load in ice condition (without reduction for friction loss in blade bearings), except for components influenced by load in only one direction (retaining wall) where mean stress shall be taken equivalent to the stress amplitude plus stress from hydrodynamic propeller load in ice condition.

The above is a simplification, since the number of cycles related to backward and forward blade load is not necessarily the same. However due to the conservatism built into the calculation method in total, results will be somewhat on the safe side.

For some components (mainly the retaining wall), the maximum stresses will occur at somewhat different locations, depending on pitch angle. However, as the fatigue calculation is carried out for one reference pitch setting this shall not be accounted for, unless it is substantiated that it will have significant influence on the predicted Miner sum.

Formulae for principal dynamic stresses, including geometrical stress concentration factors, are given for each of the components in the following sub-sections.

Stress concentration factors for short beams have in general been derived from the book *Stress concentration factors* by R.E. Peterson (1973). Corrections to these formulations have been done on basis of finite element calculations and empirical studies.

5.2 Propeller hub / blade carrier bearing

5.2.1 For the propeller hub, only the blade carrier bearings need to be documented for sufficient strength due to ice loads. However, this does not discharge the designer to ensure that the complete propeller hub is designed with sufficient strength and rigidity to withstand the ice loads.

The blade carrier bearing is exposed to bending and shear due to the bearing pressure when the bearing is carrying the blade bending moment from the ice loads.

A sector strip of the bearing in way of the highest pressure shall be considered. For prediction of bending stresses, the reaction point of the resulting force acting on the bearing may be assumed to be in the centre of the considered surface.

5.2.2 Static stress (yielding)

In order to comply with yielding requirements, a prediction of nominal equivalent static stress, σ_{eblc} shall be carried out. The combined effect of bending, compression and shear on the bearing shall be considered:

$$\sigma_{eblc} = \sqrt{(\beta_{cblc}\sigma_{bblc})^2 + 3\tau_{bblc}^2} \quad (\text{N/mm}^2)$$

Where pressure distribution correction factor, β_{cblc} , bending stress, σ_{bblc} , and shear stress, τ_{bblc} , are taken from the following formulae:

$$\beta_{cblc} = 1.2 \quad (-)$$

$$\tau_{\text{blk}} = \frac{p_{\text{bblcmax}} B_{\text{blk}}}{T_{\text{blk}}} \text{ (N/mm}^2\text{)}$$

$$\sigma_{\text{bblc}} = \frac{p_{\text{bblcmax}} B_{\text{blk}}^2}{\frac{1}{3} T_{\text{blk}}^2} \text{ (N/mm}^2\text{)}$$

Where p_{bblcmax} , B_{blk} and T_{blk} are as defined in [3].

5.2.3 Dynamic stress

In order to predict the maximum principal stress for fatigue calculation, σ_{pbpc} , it is relevant to consider the influence of (short beam) bending. Hence, σ_{pbpc} should be taken as for σ_{bblc} above.

Influence from stress concentration and local compression should be represented in fatigue calculations by the total geometrical stress concentration factor $K_t = \beta_{\text{cblc}} \cdot \alpha_{\text{bblc}}$ as described in [6.2]. In this respect, β_{cblc} shall be taken as for the static stress case and α_{bblc} is geometrical (short beam) stress concentration in bending in the bearing notch.

The following empirical formulae applies, unless otherwise substantiated:

U shaped notch for O-ring:

$$\alpha_{\text{bblc}} = \left(1 + 0.22 \left(\frac{rf_{\text{blk}}}{t_{\text{blk}}} \right)^{-0.7} \right) \cdot \left(1 + \left(0.07 \left(\frac{B_{\text{blk}}}{t_{\text{blk}}} \right)^{-1.85} \right) \left(\frac{rf_{\text{blk}}}{t_{\text{blk}}} \right)^{-\left(0.12 + 0.38 \frac{B_{\text{blk}}}{t_{\text{blk}}} \right)} \right) \quad (-)$$

Shoulder Fillet:

$$\alpha_{\text{bblc}} = \left(1 + 0.23 \left(\frac{rf_{\text{blk}}}{t_{\text{blk}}} \right)^{-0.5} \right) \cdot \left(1 + \left(0.07 \left(\frac{B_{\text{blk}}}{t_{\text{blk}}} \right)^{-1.85} \right) \left(\frac{rf_{\text{blk}}}{t_{\text{blk}}} \right)^{-\left(0.12 + 0.38 \frac{B_{\text{blk}}}{t_{\text{blk}}} \right)} \right) \quad (-)$$

Where rf_{blk} is radius of bearing fillet.

The first part in the stress concentration formulae above represents the stress concentration factor in pure bending for flat bar with U-notch / shoulder fillet, respectively, whereas the second part includes the short beam correction.

5.3 Servo cylinder including clamping bolts

5.3.1 The servo cylinder with clamping bolts need normally be assessed only according to static strength criteria.

5.3.2 Static stress servo cylinder/design pressure

In order to comply with yielding requirements, a prediction based on nominal equivalent static stress not exceeding yield stress shall be carried out. I.e. the cylinder minimum thickness, t_{cyl} shall comply with:

$$t_{cyl} = \frac{p_{servo} D_{cyl}}{20\sigma_{y cyl}} K_{shape} \quad (\text{mm})$$

Where p_{servo} is servo pressure (bar) as defined in [3.2] or design pressure, whichever is higher, D_{cyl} is servo cylinder outer diameter (mm) and K_{shape} is factor for increased stress due to shape of dished end.

Unless otherwise is substantiated, K_{shape} shall be taken according to the following empirical formulae for the curved part of the cylinder:

$$K_{shape} = 0.2 \left(\frac{H_{cyl}}{D_{cyl}} \right)^{-\left(1.13 + \frac{D_{cyl}}{1000 t_{cyl}} \right)} \quad (-)$$

Where H_{cyl} is height of curved part of servo cylinder (see Figure 7). H_{cyl} needs not to be taken less than $0.1D_{cyl}$.

K_{shape} shall not be taken less than 1.0.

For the cylindrical part of servo cylinder, K_{shape} is 1.0.

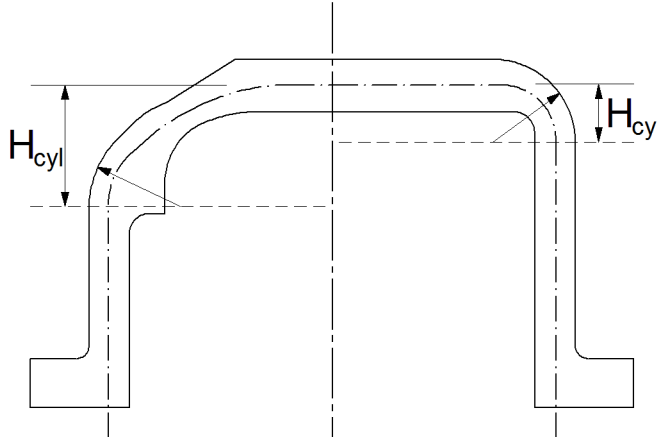


Figure 7 Illustration of curved height of cylinder – two examples

Design pressure of the pitch mechanism system shall be taken as given in DNVGL-RU-SHIP Pt.6 Ch.6 Sec.6 [12.4.6]

5.3.3 Static stress cylinder clamping bolts

In order to comply with yielding requirements, a prediction based on bolt pretension stress plus additional nominal bolt stress due to pressure in servo cylinder shall be carried out in case servo cylinder is clamped to the propeller hub.

Assuming that the complete force on crank pin is transmitted to the servo, the total clamping bolt stress is found from:

$$\sigma_{cblt} = \sigma_{cpre} + k_{cblt} \frac{F_{crp}}{n_{cblt} \frac{\pi}{4} D_{cblt}^2} 10^3 \quad (\text{N/mm}^2)$$

Where σ_{cpre} is pre-tension stress in minimum section of bolt (N/mm^2), D_{cblt} is minimum section diameter of bolt (mm), n_{cblt} is No. of clamping bolts and k_{cblt} is bolt factor describing part of additional load carried by the clamping bolts. Unless otherwise is substantiated, k_{cblt} shall be taken as 0.25 / 0.33 in case of steel / bronze material in hub and servo cylinder, respectively.

5.3.4 Separation between hub and cylinder

The bolt pre-stress shall be sufficient to prevent separation between the mating surfaces between hub and cylinder when servo pressure corresponds to maximum forward, F_f and backward load F_b . This corresponds to a situation where the compression load in the flanges becomes zero. Hence, bolt pre-tension stress shall as a minimum be:

$$\sigma_{cpre} = (1 - k_{cblt}) \frac{F_{crp}}{n_{cblt} \frac{\pi}{4} D_{cblt}^2} 10^3 \quad (\text{N/mm}^2)$$

5.4 Blade bolts and shear pins

5.4.1 The blade bolts and shear pins need normally be assessed only according to static strength criteria.

5.4.2 Static stress of blade bolts

The blade bolt connection shall withstand the blade failure bending moment described in the rules without yielding. Stresses in the bolts, σ_{bblt} shall be calculated according to the following:

$$\sigma_{bblt} = \sigma_{bpre} + k_{bblt} \frac{M_{exbbt}}{W_{bblt}} 10^6 \quad (\text{N/mm}^2)$$

Where σ_{bpre} is pre-tension stress in minimum section of bolt (N/mm^2), k_{bblt} is bolt factor (-) describing part of additional load carried by the blade bolts. Unless otherwise is substantiated, k_{bblt} shall be taken as follows:

Table 1 Blade bolt factors

Blade flange material	Crank disk material	k_{bblt}
Bronze	Steel	0.30
Bronze	Bronze	0.35
Stainless steel	Steel	0.25
Stainless steel	Bronze	0.30

In the case that $\frac{\sigma_{bpre}}{\sigma_{ybbt}} + k_{bbt} < 1.0$ separation between mating surfaces will occur before yielding of bolt

(σ_{ybbt} is yield strength of bolt material in N/mm²). This is acceptable for the blade failure load, but then k_{bbt} may be taken as 1.0 and σ_{bpre} may be taken as 0.0 in the above formula for bolt stress, σ_{bbt} , irrespective of actual values.

M_{exbbt} is bending moment in way of blade bolts due to blade failure load, taken from:

$$M_{exbbt} = S F_{ex} k_{sup} \left(0.8 \frac{D}{2} - r_{bbt} \right) \text{ (kNm)}$$

Where D is propeller diameter (m) and r_{bbt} is radius (m) from shaft centre line to the bolt plane. Safety factor, $S = 1.0$ (as required in [DNVGL-RU-SHIP Pt.6 Ch.6 Sec.2](#) and [DNVGL-RU-SHIP Pt.6 Ch.6 Sec.6](#)) and k_{sup} is support factor, correcting the bending moment due to reaction forces in blade carrier bearing and bolts. When blade flange is resting on a blade carrier, k_{sup} shall be taken as:

$$k_{sup} = 0.5 + \frac{\max(A_{bbt\ i})}{2D_{blc}} \quad (-)$$

Where $\max(A_{bbt\ i})$ is taken as distance (mm) from tilting line to bolt located farthest away (for $A_{bbt\ i}$, see also [Figure 8](#) below), and may normally be taken as equal to the pitch circle diameter, PCD (mm).

W_{bbt} is section modulus (mm³) of bolt connection about the tilting line based on minimum section diameter of bolt.

Tilting line is tangent to the pitch circle diameter (or other relevant axis for non circular joints), parallel to the considered root section. Tilting line is located on "pressurized" side of the flange, i.e. bolt section modulus may depend on whether the considered force is acting in forward or backward direction.

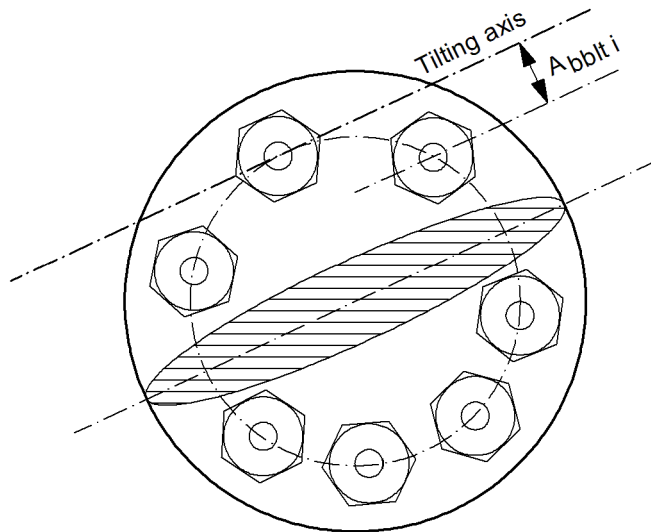


Figure 8 Illustration of tilting line and distance to tilting line ($A_{bbt\ i}$) for bolt No. i

Bolt section modulus for circular location of bolts shall be taken from the following expression:

$$W_{bblt} = \frac{N_{bblt} \frac{\pi}{64} D_{bblt}^4 + \frac{\pi}{4} D_{bblt}^2 \sum_{i=1}^{N_{bblt}} A_{bblt i}^2}{\max(A_{bblt i})} \quad (\text{mm}^3)$$

Where N_{bblt} is number of blade bolts and D_{bblt} is minimum section diameter of bolt (mm).

5.4.3 Separation between mating surfaces

The bolt pre-tension stress shall be sufficient to prevent separation between the mating surfaces with maximum forward, F_f and backward load F_b . This corresponds to a situation where compression load in the flanges becomes zero. Hence, bolt pre-tension stress shall as a minimum be:

$$\sigma_{bpre} = (1 - k_{bblt}) \frac{M_{icebblt}}{W_{bblt}} 10^6 \quad (\text{N/mm}^2)$$

Where $M_{icebblt}$ is maximum bending moment due to ice load, taken from:

$$M_{icebblt} = S F k_{\text{sup}} (r_{ice} - r_{bblt}) \quad (\text{kNm})$$

Where F is maximum forward ice load (kN), F_f or maximum backward ice load, F_b , respectively, r_{ice} is radius from shaft centre to acting ice load (m). Safety factor, S is 1.3, as required in [DNVGL-RU-SHIP Pt.6 Ch.6 Sec.2](#) and [DNVGL-RU-SHIP Pt.6 Ch.6 Sec.6](#).

5.4.4 Static stress of shear (dowel) pins

[DNVGL-RU-SHIP Pt.6 Ch.6 Sec.6](#) specify the minimum required diameter for the shear (dowel) pins, in order to avoid shear yield when blade is exposed to maximum ice load and blade failure load.

Formulations for friction torque reductions (Q_{fr1} and Q_{fr2}) are given in [\[3.3\]](#).

Note that the pitch circle diameter referred to in the ice rules (PCD) describes the diametrical location of the shear pins (which may be different from the PCD for the blade bolts).

5.5 Crank pin

5.5.1 Crank pin is exposed to bending and shear, as well as local compression due to pressure from guide block acting close to the point of maximum bending stress. For prediction of bending stresses, the reaction point of the resulting force acting on crank pin may be assumed to be half way up the crank pin.

Hence, stress in crank pin shall be taken as described in the following.

5.5.2 Static stress (yielding)

In order to comply with yielding requirements, a prediction of nominal equivalent static stress, σ_{ecr} shall be carried out. The combined effect of bending, compression and shear on the crank pin shall be considered:

$$\sigma_{ecr} = \sqrt{(\beta_{ccr} \sigma_{bccr})^2 + 3\tau_{bccr}^2} \quad (\text{N/mm}^2)$$

Where pressure distribution correction factor, β_{ccr} , bending stress σ_{bcr} and shear stress, τ_{cr} , are taken from the following formulae:

$$\beta_{ccr} = 0.7 + \frac{0.4}{\frac{H_{cr}}{D_{cr}}} \quad (1)$$

$$\tau_{cr} = \frac{1000F_{crp} \cdot}{\frac{\pi}{4} D_{cr}^2} \quad (\text{N/mm}^2)$$

$$\sigma_{bcr} = \frac{1000F_{crp} \cdot 0.5H_{cr}}{\frac{\pi}{32} D_{cr}^3} \quad (\text{N/mm}^2)$$

Where F_{crp} is force acting on crank pin (kN), D_{cr} is crank pin diameter (mm) and H_{cr} is height of crank pin (mm).

Additionally, it shall be verified that surface pressure from guide block on crank pin does not exceed yield strength. The following formula for surface pressure on crank pin, p_{cr} shall be used.

$$p_{cr} = \frac{1000F_{crp}}{H_{cr} D_{cr}} \beta_{cr} \quad (\text{N/mm}^2)$$

Where β_{cr} is the peripherical pressure concentration factor (local increase in pressure near the edges of the guide block are not considered). Assuming that the surface pressure has a sinusoidal peripherical distribution over the crank pin, β_{cr} shall be taken as 2.0.

In case effective height of guide block is significantly less than height of crank pin (H_{cr}) due to chamfers or similar, a corresponding change in H_{cr} for calculation purposes shall be done.

5.5.3 Dynamic stress and mean stress (fatigue)

In order to predict the maximum principal stress for fatigue calculation, σ_{pcr} , it is relevant to consider the influence of (short beam) bending. Hence, σ_{pcr} should be taken as for σ_{bcr} above.

The above reflects the assumption that when considering local stresses, it is relevant to distribute the load over an area corresponding to the crank pin profile.

Influence from stress concentration and local compression should be represented in fatigue calculations with the total geometrical stress concentration $K_t = \beta_{ccr} \cdot \alpha_{bcr}$, as described in [6.2].

Influence of local compression β_{ccr} is found as for the static case above, and geometrical (short beam) stress concentration factor α_{bcr} shall be found from the following empirical expression, unless otherwise is substantiated:

$$\alpha_{bcr} = \left(1 + 0.17 \left(\frac{rf_{cr}}{D_{cr}} \right)^{-0.7} \right) \cdot \left(1 + \left(0.07 \left(\frac{H_{cr}}{D_{cr}} \right)^{-1.85} \right) \left(\frac{rf_{cr}}{D_{cr}} \right)^{-\left(0.12 + 0.38 \frac{H_{cr}}{D_{cr}} \right)} \right) \quad (-)$$

Where rf_{cr} is crank pin fillet radius (mm).

The first part in the stress concentration formula above represents the stress concentration factor in pure bending for round bar with shoulder fillet, whereas the second part includes the short beam correction.

5.6 Guide block

5.6.1 The guide block is exposed to compression loads and is normally designed without dominant stress risers. Hence a static consideration of the surface pressure inside guide block is sufficient.

5.6.2 Static surface pressure (yielding)

In order to verify that the surface pressure inside the guide block does not exceed yield strength of material, it is sufficient to calculate nominal surface pressure. This is because some minor compressive deformations in the guide block are not considered critical for the function of the pitch mechanism.

The following formula shall be used for static nominal surface pressure p_{gb} of guide block:

$$p_{gb} = \frac{1000F_{crp}}{H_{cr}D_{cr}} \quad (\text{N/mm}^2)$$

In case effective height of guide block is significantly less than height of crank pin (H_{crp}) due to chamfers or similar, a corresponding reduction in H_{crp} for calculation purposes shall be done.

5.7 Retaining wall

5.7.1 The retaining wall is exposed to bending and shear, as well as local compression due to pressure from guide block acting close to the point of maximum bending stress. For prediction of bending stresses, the reaction point of the resulting force acting on retaining wall may be assumed to be at a height 35% up the wall.

Hence, stress in retaining wall shall be taken as described in the following.

5.7.2 Static stress (yielding)

In order to comply with yielding requirements, a prediction of nominal equivalent static stress, σ_{erw} shall be carried out. The combined effect of bending, compression and shear on the retaining wall shall be considered:

$$\sigma_{erw} = \sqrt{(\beta_{crw}\sigma_{brw})^2 + 3\tau_{rw}^2} \quad (\text{N/mm}^2)$$

Where pressure distribution correction factor, β_{crw} , bending stress σ_{brw} and shear stress, τ_{rw} , are taken from the following formulae:

$$\beta_{crw} = 0.6 + \frac{0.6}{\frac{H_{cr}}{t_{rw}}} \quad (-)$$

$$\tau_{rw} = \frac{1000F_{crp}}{t_{rw}B_{gb}} \quad (\text{N/mm}^2)$$

$$\sigma_{brw} = \frac{1000F_{crp} \cdot 0.35H_{cr}}{\frac{1}{6}t_{rw}^2B_{gb}} \quad (\text{N/mm}^2)$$

Where t_{rw} is thickness of retaining wall (mm) and B_{gb} is breadth of guide block (mm)

The above reflects the assumption that when considering nominal stresses, it is relevant to distribute the load over an area corresponding to the guide block profile.

Additionally, it shall be verified that surface pressure from guide block on retaining wall does not exceed yield strength. The following formula for surface pressure on retaining wall, p_{rw} shall be used.

$$p_{rw} = \frac{1000F_{crp}}{H_{cr}B_{gb}} \beta_{rw} \quad (\text{N/mm}^2)$$

Where β_{rw} is the height wise pressure concentration factor (local increase in pressure near the edges of the guide block are not considered). Assuming that the surface pressure has a triangular height wise distribution over the crank pin, β_{rw} shall be taken as 2.0.

In case effective height of retaining wall is significantly less than height of crank pin (H_{cr}) due to chamfers or similar, a corresponding change in H_{cr} for calculation purposes shall be done.

5.7.3 Dynamic stress and mean stress (fatigue)

In order to predict the maximum principal stress for fatigue calculation, σ_{prw} , it is relevant to consider the influence of (short beam) bending. Hence, σ_{prw} should be taken as follows:

$$\sigma_{prw} = \frac{1000F_{crp} \cdot 0.35H_{cr}}{\frac{1}{6}t_{rw}^2D_{cr}} \quad (\text{N/mm}^2)$$

The above reflects the assumption that when considering local stresses, it is relevant to distribute the load over an area corresponding to the crank pin profile.

Influence from stress concentration and local compression should be represented in fatigue calculations by the total geometrical stress concentration $K_t = \beta_{crw} \cdot \alpha_{brw}$, as described in [6.2].

Influence factor for local compression, β_{crw} shall be taken as for the static case above, whereas the (short beam) stress concentration factor, α_{brw} shall be found from the following empirical expression, unless otherwise substantiated:

$$\alpha_{brw} = \left(1 + 0.23 \left(\frac{rf_{rw}}{t_{rw}} \right)^{-0.5} \right) \cdot \left(1 + \left(0.07 \left(\frac{H_{cr}}{t_{rw}} \right)^{-1.85} \right) \left(\frac{rf_{rw}}{t_{rw}} \right)^{\left(0.12 + 0.38 \frac{H_{cr}}{t_{rw}} \right)} \right) \quad (-)$$

Where rf_{rw} is retaining wall fillet radius (mm).

The first part in the stress concentration formula above represents the stress concentration factor in pure bending for flat bar with shoulder fillet, whereas the second part includes the short beam correction.

5.8 Push-pull rod

5.8.1 The push-pull rod may include many design features which need to be assessed for the axial load. Depending on the direction of the load and the crank pin arrangement, the push-pull rod may be exposed to both compression and tension loads.

5.8.2 Static stress

The push-pull rod needs to be checked for yielding at static peak loads. This may be critical for the following parts:

- minimum section diameter
- threaded connections
- bolted connections.

Further, under the same condition the push-pull rod shall not be exposed to buckling, and if the crosshead is shrink-fitted onto the push-pull rod, the connection shall be able to take the crank pin force without slipping.

Stresses in the minimum section diameter, σ_{ppmin} are calculated according to:

$$\sigma_{ppmin} = \frac{1000 F_{crp}}{\frac{\pi}{4} (D_{ppmin}^2 - D_{ppo}^2)} \quad (\text{N/mm}^2)$$

Where D_{ppmin} is minimum section diameter of push-pull rod (mm) and D_{ppo} is inner diameter of push pull rod (mm). In case parts of the push-pull rod are connected by sleeves, stresses in sleeves are calculated correspondingly, using outer and inner diameter of sleeves instead.

For threaded connections, the same approach is used to find stress in threaded section, σ_{ppthr} (N/mm²) as for the minimum section diameter, replacing D_{ppmin} with the thread diameter D_{ppthr} (mm). In case of a sleeve, the relevant diameters for sleeve and sleeve threads shall be used.

When considering shear yielding of all threads, the following formulation shall be used for *allowable* stress:

$$\sigma_{ppthr} \leq \rho_{ppthr} \frac{\sigma_{ppy}}{\sqrt{3}} \frac{L_{ppthr}}{\frac{\pi}{4} D_{ppthr}} \quad (\text{N/mm}^2)$$

Where σ_{ppy} (N/mm²) is yield strength of push-pull rod (or sleeve as relevant), L_{ppthr} is length of threaded part (mm) and ρ_{ppthr} is part of thread carrying load, found from the following empirical relation:

$$\rho_{ppthr} = 1 - 0.37D_{ppthr}^{-0.15}$$

Stresses in push-pull rod bolts, σ_{ppblt} are calculated according to:

$$\sigma_{ppblt} = \sigma_{pppre} + K_{ppblt} \frac{1000F_{crp}}{N_{ppblt} \frac{\pi}{4} D_{ppmin}^2} \text{ (N/mm}^2\text{)}$$

Where σ_{pppre} is bolt pre-tension stress (N/mm²) in minimum section diameter, D_{ppmin} (mm), K_{ppblt} is bolt factor for part of external load taken up as tension in bolts – to be taken as 0.25, unless otherwise is substantiated and N_{ppblt} is number of clamping bolts.

In order to avoid buckling of the push-pull rod, the distance between radial support points, $L_{ppsupport}$ (mm) shall not be less than derived from the following formula:

$$L_{ppsup\ port} = \sqrt{\frac{\pi^3 E_{pp} (D_{pp}^4 - D_{ppo}^4)}{64000 F_{crp}}} \text{ (mm)}$$

Where E_{pp} is E-modulus of push pull rod (= 2.05×10^5 N/mm² for steel) and D_{pp} is representative diameter of push-pull rod.

If the connection between the cross head and push-pull rod is by means if shrinkage only, the minimum shrinkage pressure shall be:

$$p_{min} = S_{sf} \frac{1000 F_{crp}}{\mu \pi D_{pp} t_{crh}} \text{ (N/mm}^2\text{)}$$

Where S_{sf} is additional safety factor for shrink fit = 1.25, μ is friction coefficient, to be taken as 0.15 for dry connections, D_{pp} is push-pull rod diameter in way of shrink fit (mm) and t_{crh} is effective cross head thickness (mm).

The reason for including the additional factor of 1.25 is because slippage will happen immediately upon an overload, and the general safety factors (if any) applied on the crank pin force as described in the rules refer to yielding criteria, and are considered too small for shrink fit connections.

General formulations for cylindrical shrink-fitted connections shall be used as follows:

- Diameter of outer member, D_{hub} (cross head) shall for simplicity and safety be taken as the width of the cross head, not including retaining walls for guide block or crank pin (as relevant)
- For maximum allowable interference / shrinkage pressure between push-pull rod and cross head, the membrane stresses due to the shrinkage pressure shall not exceed 70% of cross head material yield strength.

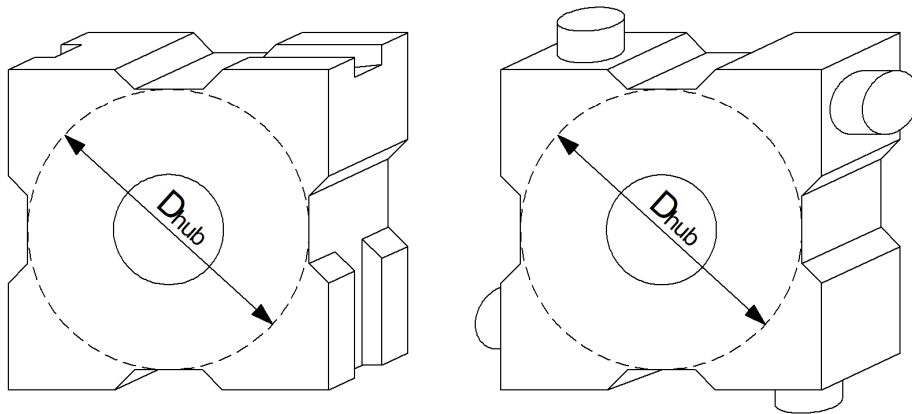


Figure 9 Illustration of diameter of outer member for push-pull rod shrink fit

5.8.3 Dynamic stress and mean stress (fatigue)

The push-pull rod needs to be checked for fatigue in way of significant stress risers. This is typically critical for the following parts:

- fillets
- radial borings.

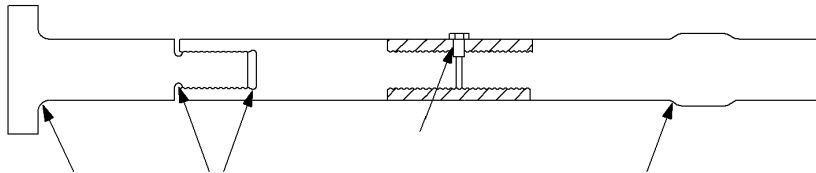


Figure 10 Typical stress raisers in push-pull rod

Principal stresses in way of the stress riser, σ_{app} are calculated as for the static case with minimum section diameter, using relevant diameters.

Influence from local stress concentration should be represented in the fatigue calculations with geometrical stress concentration, $K_t = \alpha_{app}$, as described in [6.2].

Unless otherwise substantiated α_{app} shall be taken as 3.0 for radial borings and according to the following empirical formulation (relevant for axial loading) for shoulder fillets:

$$\alpha_{app} = \left(1.23 - \frac{0.12}{\sqrt{\frac{D_{pps}}{D_{pp}} - 1}} \right) \left(\frac{rf_{pp}}{D_{pp}} \right)^{-0.25} \quad (-)$$

Where rf_{pp} is shoulder fillet radius (mm) and D_{pps} is diameter of shoulder/flange (mm).

Also for welded connections of various types, the push-pull rod needs to be checked for fatigue. Principal stresses may be calculated as above, excluding the influence of stress risers (influence of increased stress in weld is included in the fatigue strength, see [3.2]).

6 Material strength

6.1 Static strength

6.1.1 Static strength vs. yielding (maximum ice load) criterion

With reference to [2.2], the yielding criterion for maximum ice load is complied with when the predicted nominal equivalent stress for the considered component is less than yield strength, σ_y . A safety factor of 1.3 (as specified in DNVGL-RU-SHIP Pt.6 Ch.6 Sec.2 and DNVGL-RU-SHIP Pt.6 Ch.6 Sec.6) is included in the maximum ice load.

6.1.2 Static strength vs. permanent deflection (blade bending) criterion

With reference to chapter [2.1], the yielding criterion for blade failure load is complied with when the predicted nominal equivalent stress for the considered component is less than yield strength, σ_y .

6.2 Fatigue (dynamic) strength

6.2.1 Fatigue strength basic formulation

With reference to [2.3], the fatigue strength criterion is complied with when the Miner sum is less than 1.0. The safety factor of 1.5 (as specified in DNVGL-RU-SHIP Pt.6 Ch.6 Sec.2 and DNVGL-RU-SHIP Pt.6 Ch.6 Sec.6) is then applied on the acting dynamic ice load amplitudes.

Fatigue strength for components in pitch mechanism is influenced by a number of effects. In general, the following applies for fatigue strength in non-corrosive environment at Ei number of cycles:

$$\sigma_{Ei} = \frac{\sigma_{fatEi}}{1 + f_{rough} + q(K_t - 1)} K_{mean} K_{size} K_{var} K_{load} \text{ (N/mm}^2\text{)}$$

Where σ_{fatEi} is fatigue strength in rotating bending in air for un-notched test piece, f_{rough} is influence factor for influence of surface roughness (-), q equals the notch sensitivity factor (-), K_t is the *geometrical* stress concentration factor (-) as found in previous sections, K_{mean} is correction factor for influence of mean stress, K_{size} is correction factor for influence of size, K_{var} is correction factor for influence of variable loading and K_{load} is correction factor for other type of loading than bending. These factors are addressed in the following. For welded connections (push-pull rod), none of the above influence factors shall be included.

6.2.2 Fatigue strength at given No. of cycles

The initial fatigue strength, σ_{fatEi} for common materials applied in components for hub and pitch mechanism not exposed to sea water is derived from SN-curves as described below, unless otherwise substantiated.

The initial SN-curves are limited to / described by linear curves in a log-log diagram as described in the following:

$$\sigma_{fatEi} \leq \sigma_u$$

Where σ_u is ultimate tensile strength of material.

The SN curve is determined with two slopes, which may be different above and below a defined knuckle point, N_{HC} .

$$N_i = N_{HC} \text{ cycles : } \sigma_{Fat\ NHC} = \sigma_{Fat\ E7} \left(\frac{10^7}{N_{HC}} \right)^{1/m_{LC}} \text{ (N/mm}^2\text{)}$$

$$N_i < N_{HC} \text{ cycles : } \sigma_{Fat\ Ei} = \sigma_{Fat\ E7} \left(\frac{10^7}{N_i} \right)^{1/m_{LC}} \text{ (N/mm}^2\text{)}$$

$$N_i > N_{HC} \text{ cycles : } \sigma_{Fat\ Ei} = \sigma_{Fat\ NHC} \left(\frac{N_{HC}}{N_i} \right)^{1/m_{HC}} \text{ (N/mm}^2\text{)}$$

Where N_i is considered number of cycles, $\sigma_{Fat\ E7}$ is material fatigue strength in rotating bending at 10^7 cycles for un-notched test piece, $\sigma_{Fat\ NHC}$ is corresponding fatigue strength at knuckle point and $\sigma_{Fat\ Ei}$ is corresponding fatigue strength at 10^i cycles. Slopes of SN curve, m_{LC} (low cycle) and m_{LH} (high cycle) are material dependent (see [Table 2](#) below).

For parts exposed to sea water, such as propeller hub and blade carrier bearing in way of- or outside of sealing, fatigue properties shall be taken as for propeller blades (see [Sec.2 \[3.1\]](#)).

For welded connections (push-pull rod) made of steel the fatigue strength for N_i No. of cycles shall be taken as follows:

$$\sigma_{Fat\ Ei} = A_{wld} N_i^{B_{wld}} \text{ (N/mm}^2\text{)}$$

Where the welding parameters A_{wld} and B_{wld} are tabulated in [Table 3](#).

$\sigma_{Fat\ Ei} \leq \sigma_u$ of the base material.

6.2.3 Material parameters for calculation of S-N curve

Fatigue parameters for some materials commonly applied in propellers and pitch mechanisms are tabulated in [Table 2](#). These parameters correspond to mean fatigue strength in rotating bending ($R = -1$) for un-notched, polished specimen with a diameter of 25 mm or less.

Table 2 Material fatigue parameters for some common materials

Material	$\sigma_{Fat\ E7}$	N_{HC}
Bronze alloy	$0.30 \sigma_u$	10^8
Cast steel	$0.40 \sigma_u$	10^8
Forged and rolled steel	$0.50 \sigma_u$	10^7
Nodular cast iron	$0.35 \sigma_u$	∞

Fatigue values for other materials may be agreed upon special consideration.

Slope of SN curve in the low cycle part, m_{LC} is calculated from the following:

$$m_{LC} = \frac{4}{\log\left(\frac{\sigma_u}{\sigma_{Fat\ E7}}\right)} \quad (-)$$

Slope of the S-N curve in the high cycle part, m_{HC} shall be taken as 50 for all materials.

Note that for nodular cast iron, no knuckle point is defined. Hence the low cycle slope applies for the whole cycle range. Also note that DNVGL-RU-SHIP Pt.6 Ch.6 Sec.2 and DNVGL-RU-SHIP Pt.6 Ch.6 Sec.6 call for a Charpy V impact strength of minimum 20J at -10°C for propeller materials. Nodular cast iron will normally not comply with this requirement, but is included in Table 2 for the sake of good order. The above formulations include the effect of variable loading by moving the knuckle point from 10^7 to 10^8 cycles for bronze and cast steel materials. For forged steel, the influence of variable loading is small and hence knuckle point is taken at 10^7 cycles.

Hence K_{var} is taken as 1.0 for all materials.

For typical material parameters, an example of initial S-N curves is given in the figure below:

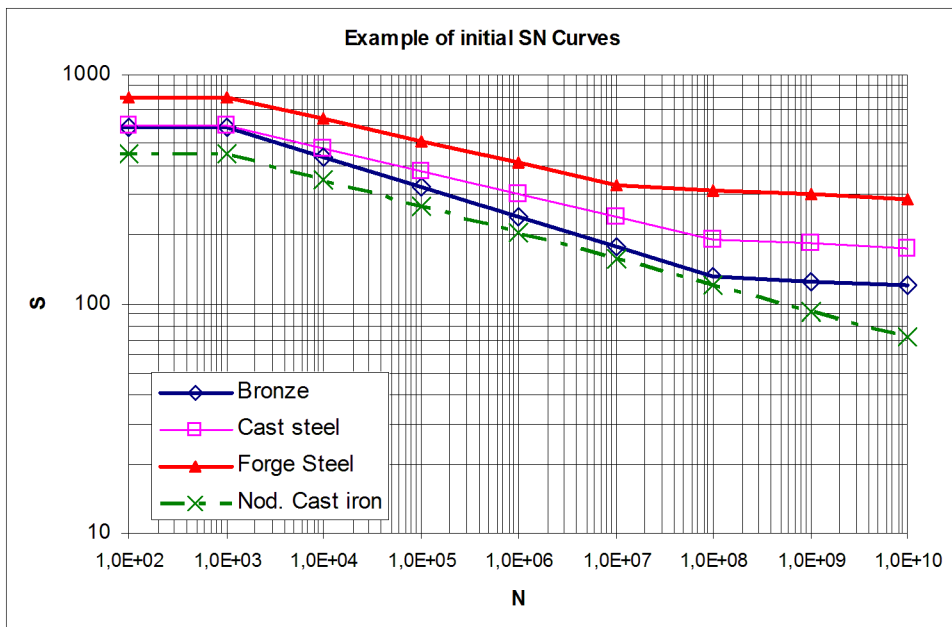
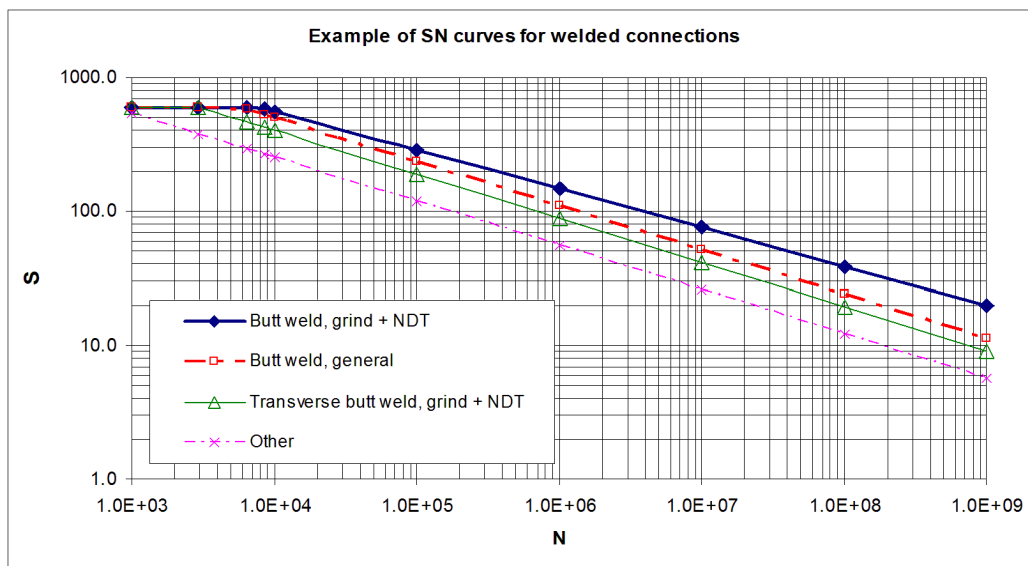


Figure 11 Example of typical initial S-N curve for some materials

For welded connections, the S-N curve is generated (depending on welding type) from the following welding parameters, unless otherwise substantiated:

Table 3 Fatigue parameters for common types of welded connections

Weld type	A_{wld}	B_{wld}
Butt weld, grinding + NDT	8100	-0.29
Butt weld, general	10500	-0.33
Transverse butt weld grinding + NDT	8500	-0.33
Other / unspecified weld	5300	-0.33

**Figure 12 S-N curve for welded connections (tensile strength taken as 600 N/mm²)**

6.2.4 Influence factor for surface roughness

The influence factor for surface roughness shall be taken from the following empirical formula, unless otherwise substantiated:

$$f_{\text{rough}} = \log\left(\frac{N_i}{1000}\right)(\sigma_u - 200)(0.8 + \log R_a) \cdot 10^{-4} \quad (-)$$

Where R_a is average surface roughness (mm) and σ_u is ultimate tensile strength of material (N/mm²). For prediction of roughness influence, number of load cycles, N_i shall not be taken lower than 10^3 or higher than 10^7 .

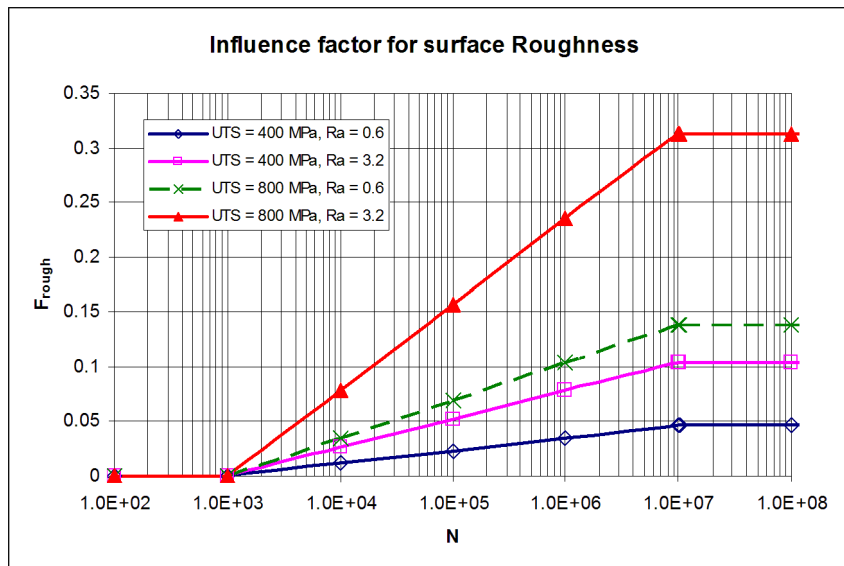


Figure 13 Illustration of influence factor for surface roughness

6.2.5 Influence factor for notch sensitivity

Basis for the prediction of notch sensitivity, q is the Neuber-equation for high cycle axial/bending fatigue. This is used for all materials relevant for propeller hub and pitch mechanism.

The Neuber-equation is modified to include an empirical dependency of number of cycles, N_i , taking into account that high tensile materials show some notch sensitivity even at very low number of cycles:

$$q = \frac{\log\left(\frac{N_i}{N_q}\right)}{\left(1 + \frac{\sqrt{a}}{\sqrt{r}}\right)(7 - \log(N_q))} \quad (-)$$

Where N_q is Number of cycles below which material is assumed to have zero notch sensitivity, taken as:

$$N_q = 2.2 \cdot 10^4 e^{-\frac{\sigma_y}{130}} \quad (-)$$

For prediction of notch sensitivity, N_i shall not be taken lower than N_q or higher than 10^7 . In the same way, yield strength σ_y shall not be taken less than 400 N/mm².

Further, r is notch radius (mm) and \sqrt{a} is material parameter, empirically depending on material yield strength, σ_y (N/mm²).

Unless otherwise substantiated, the values of \sqrt{a} shall as a simplification be based on reported values for steel according to the following empirical formulation:

$$\sqrt{a} = 0.82 - \frac{\sigma_y}{1500} \quad (\sqrt{\text{mm}})$$

The formulations for notch sensitivity may be somewhat on the safe side for some materials such as copper alloys and nodular cast iron, in particular when notches are very sharp.

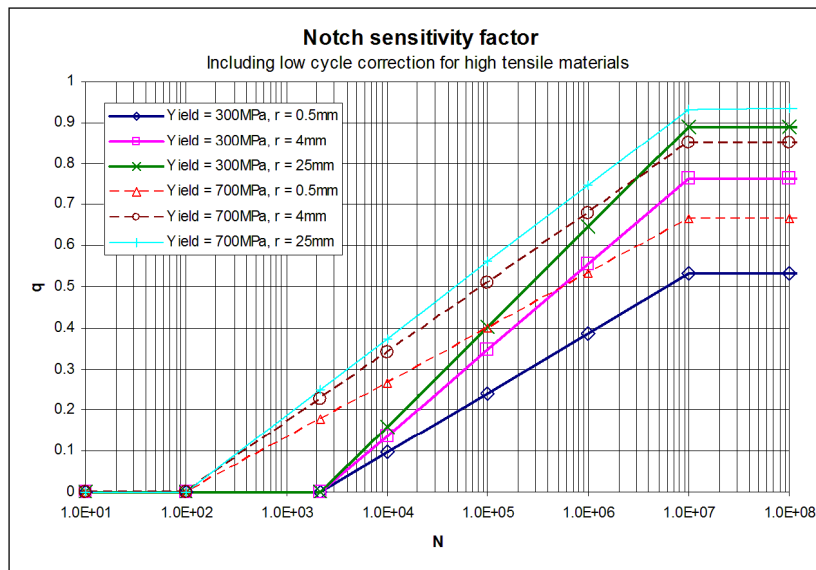


Figure 14 Illustration of Notch sensitivity factor

6.2.6 Influence of mean stress

Influence factor for mean stress, K_{mean} shall be found according to one of the following formulas:

For components in a non-corrosive environment:

$$K_{mean} = 1 - \frac{\sigma_{mean}}{\sigma_u} \quad (-)$$

For components in a corrosive environment:

$$K_{mean} = 1.0 - \left(\frac{1.4 \cdot \sigma_{mean}}{\sigma_u} \right)^{0.75}$$

Where σ_{mean} is nominal mean stress (N/mm^2), i.e. not including geometrical stress concentration, K_t and σ_u is ultimate tensile strength (N/mm^2). Note that for prediction of mean stress, safety factor needs not to be added on the acting load.

6.2.7 Influence of component size

Unless otherwise substantiated, the following empirical formulation shall be used for size influence, K_{size} for bronze, cast steel and nodular cast iron:

$$K_{size} = 1 - 0.03 \log\left(\frac{N_i}{1000}\right) \ln\left(\frac{t}{25}\right) \quad (-)$$

Where the component thickness, t shall refer to a representative thickness or diameter of the loaded part of the component (thickness of bearing/retaining wall, diameter of crank pin/ push-pull rod diameter, etc), not to be taken less than 25mm.

For prediction of size influence, number of load cycles, N_i shall not be taken lower than 10^3 or higher than 10^7 .

The influence of component size on fatigue strength for cast materials is illustrated as follows:

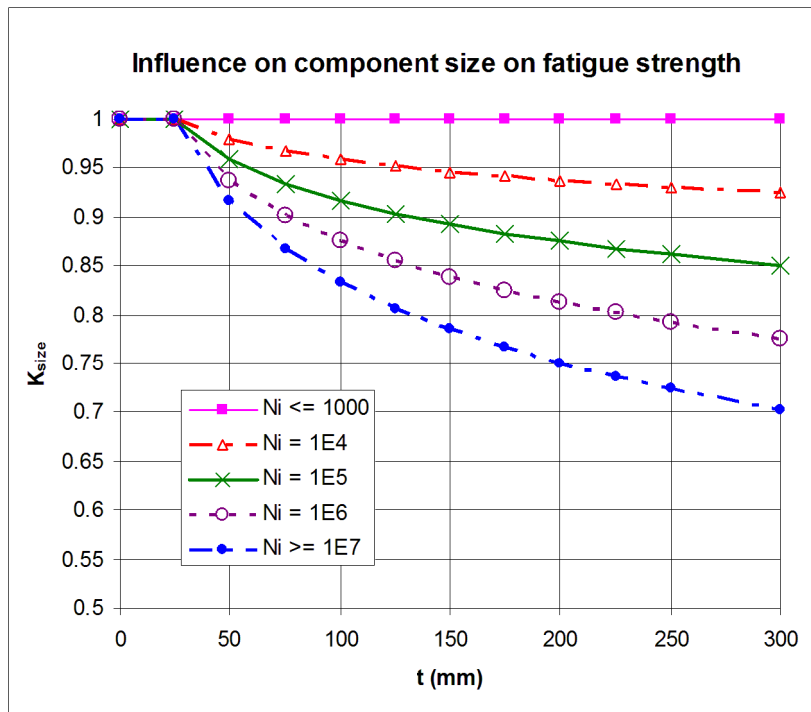


Figure 15 Influence of component size for cast materials

For forged steel, K_{size} is closely connected to mechanical properties and shall therefore be taken as 1.0.

6.2.8 Influence of variable loading

The effect of variable loading on fatigue strength is included by extending fatigue curve with low cycle slope (m_{LC}) from 10^7 cycles to 10^8 cycles for materials influenced by variable loading.

Hence K_{var} is taken as 1.0.

6.2.9 Influence of loading type

For components where bending stresses are not dominating, this shall be compensated for.

If axial stresses are dominating:

$$K_{load} = 1 - 0.04 \log\left(\frac{N_i}{1000}\right) \quad (-)$$

For prediction of load type influence, number of load cycles, N_i shall not be taken lower than 10^3 nor higher than 10^7 .

This is illustrated in the following figure:

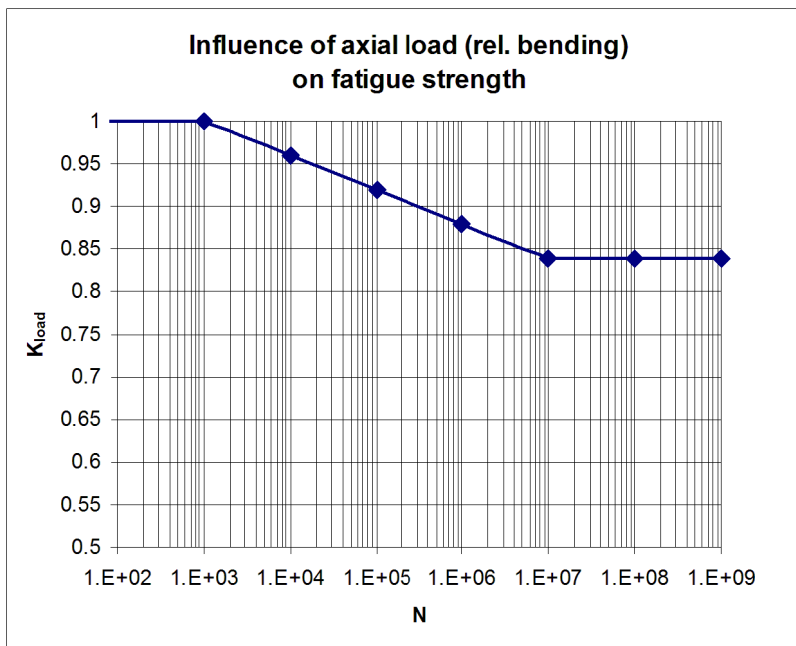


Figure 16 Influence of load type (axial load)

If shear stresses (τ) are dominating:

$$K_{load} = \frac{1}{\sqrt{3}} \quad (-)$$

over the whole cycle range. Then shear stresses may be compared directly against the criteria described in this section.

Note that type of loading also influences on other factors, mainly geometrical stress concentration factor, which is dealt with separately.

SECTION 4 GUIDANCE ON SIMULATION CALCULATIONS

1 The lumped mass-elastic system

Simulation of responses in a propulsion shafting system, which are caused by ice impacts on the propeller blades, shall be made by solving differential state-equations in the time domain. The basis for the mass-elastic system is found in the ordinary torsional vibration calculations (TVC). Since the step time in a numeric time integration should not exceed a few % (< 5%) of the period of the highest natural frequency (of numeric stability reasons), it is strongly advised to simplify the model into a minimum of lumped masses.

This simplification process should aim at the following:

- keeping the total inertia constant (in order to have a representative deceleration of the system during ice impact loads)
- maintain the lowest natural frequencies (the separation margins between the resonance speeds and the real speed are important)
- to minimise total computer calculation time and to avoid numeric challenges introduced by local high frequent vibrations.

This would lead to some corrections (normally an increase) of the stiffness between the various new lumped masses. For elements with linear stiffness this is no problem. However, for nonlinear elements care should be taken.

- a progressive stiffness may be slightly increased, but in such a way that the coefficients describing the progressive characteristics also are modified in the same proportion
- an element with a twist limiter such as a buffer in a steel spring coupling or an emergency claw device in a rubber coupling should be described as correctly as possible. Hitting such limiters can cause extra high peak torque in adjacent elements. Thus the torque-twist characteristic should not be altered, unless it is ensured that the highest twist will not reach the limiter.

The simulation of ice impacts starts from a steady state condition, normally at full load. The coupling twist at this full load is determined by the torque and the static coupling stiffness (use of the dynamic stiffness would lead to a faulty initial twist). During the impact vibrations it would be correct to use the dynamic stiffness for the dynamic part and the static stiffness for the static part. This is hardly possible in practice and it is advised to calculate with the static stiffness only. Alternatively the calculation may be performed with the dynamic stiffness, but then the twist angle when reaching the buffer/claw device shall be reduced correspondingly.

All essential branches shall be included, e.g. PTO/PTI. On the other hand, a torsional vibration damper branch in a 4-stroke engine can simply be added to the engine mass because it hardly will have any influence on the low frequent ice shock vibrations.

The propeller inertia in a TVC will include the entrained water relevant for operation in open water or bollard condition. When hitting large ice blocks the effective propeller inertia may be altered, but due to uncertainties it is suggested to keep the inertia as given in the TVC.

2 Damping in the mass-elastic system

2.1 Relative damping - General

Relative damping, i.e. damping between masses (parallel with the springs), is modelled as in ordinary TVC. If any modification of the stiffness is made in order to have the correct natural frequencies, the damping coefficient should be altered proportionally. With this recipe all "linear" elastic couplings are covered ("linear" means a torque-twist characteristic that is reasonably straight. The fact that most rubber couplings become much softer when subjected to high amplitudes can be dealt with by a "memory function" of the last oscillation). If desired, steel shafts can also be modelled with a small damping (e.g. magnifier $M = 180$) but this will have negligible influence on the results.

For non-linear couplings the stiffness is not often described in such a way that it may be used directly in a simulation calculation. It is convenient to model the torque-twist function as a polynomial function with twist

(φ) to the power of 1, 3, 5 etc. (Power of 2, 4, etc. should be avoided as problems would occur with negative twist.):

$$T_{el} = A \cdot \varphi + B \cdot \varphi^3 + C \cdot \varphi^5$$

The stiffness (K) is the derivative of this torque-twist function

$$K = A + 3 \cdot B \cdot \varphi^2 + 5 \cdot C \cdot \varphi^4$$

The damping coefficient (D_{Rel}) can relate to that stiffness:

$$D_{Rel} = K/(M \cdot \omega)$$

where "M" is the magnifier, i.e. $M \approx 2\pi/\psi \approx 1/\kappa \approx 1/\tan\epsilon \approx 1/2\zeta$ etc., and ω is the major excitation frequency (rad/s).

2.2 Absolute damping - General

Absolute damping, i.e. damping on mass, is not directly modelled in a system that has a variable rpm. A damping torque is the product of the damping coefficient and the vibration velocity. This works well in a system with constant speed and a superimposed vibration. However, when the speed is altered the system cannot clearly distinguish between a vibration and a change in speed, see [Figure 1](#).

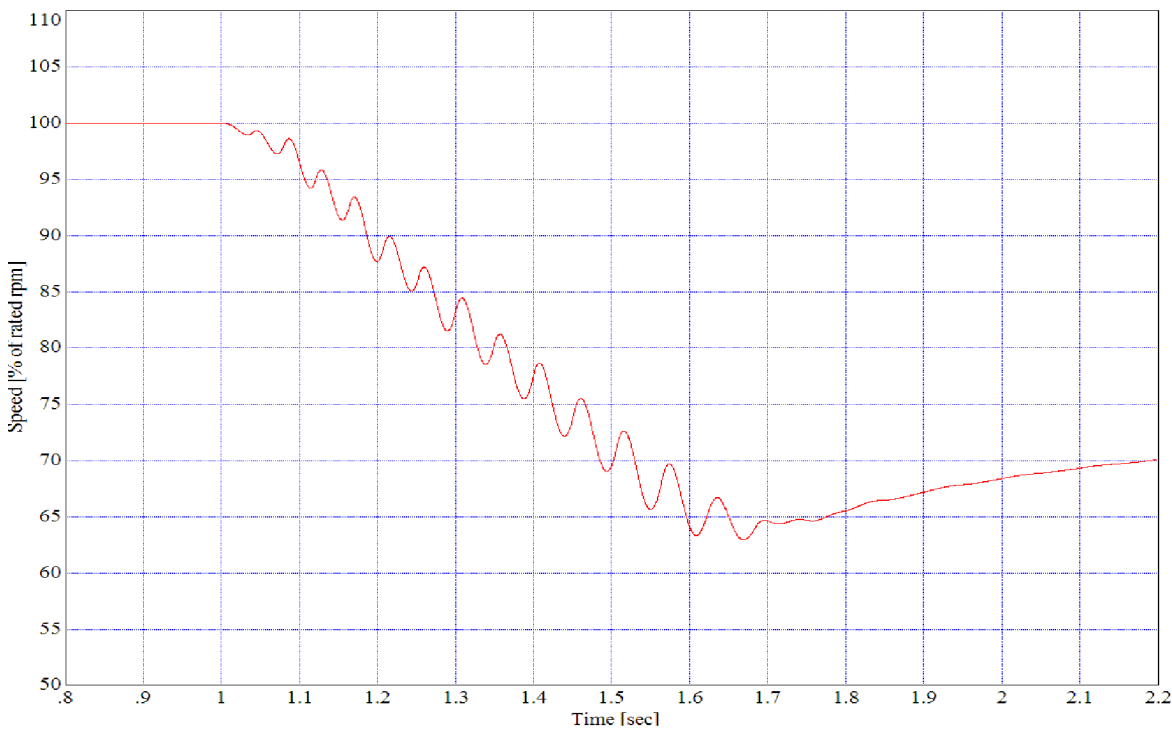


Figure 1 Rotational speed incl. vibrations as function of time

Incorporating absolute damping requires therefore a filtering of the speed signal. [Figure 2](#) shows the same real speed as above, but now the (new) blue curve represents the filtered signal.

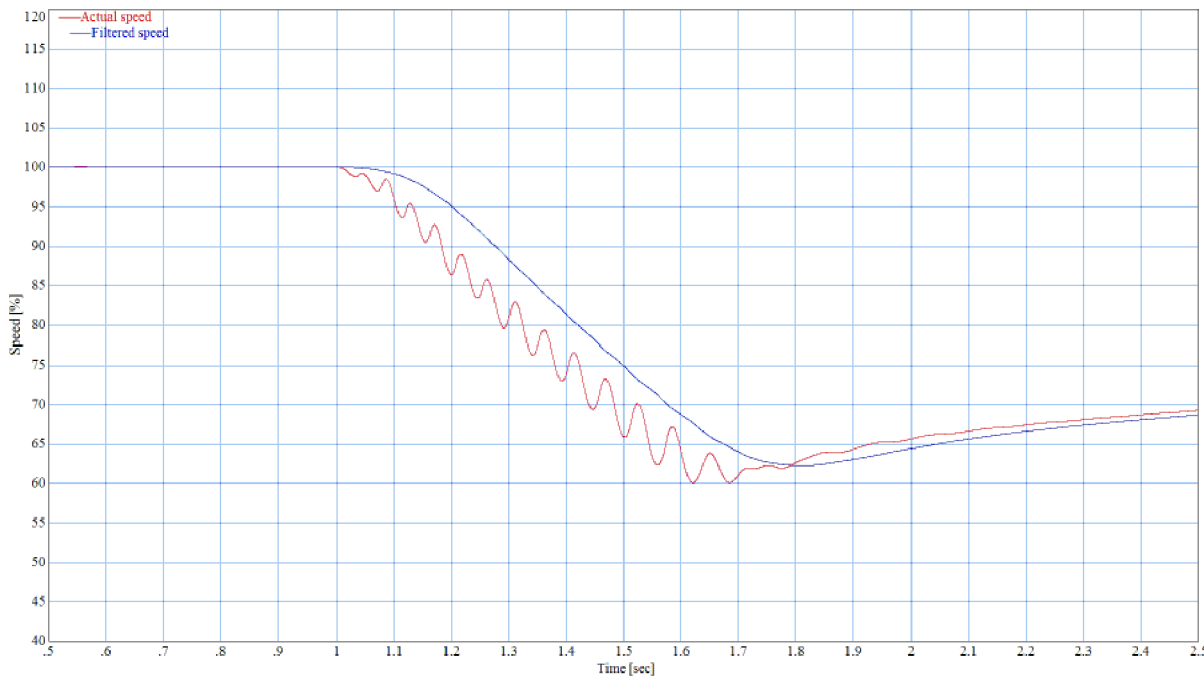


Figure 2 Filtered rotational speed as function of time

A filtered signal has a time lag (as can be seen above). The damping torque is determined as the product of damping coefficient D_{Abs} (kNms/rad) and the difference between unfiltered and filtered speed signal, i.e.:

$$T_D(t) = D_{abs} \cdot [\dot{\phi}(t) - \dot{\phi}_{filtered}(t)]$$

Ideally the filtered signal should have been in the middle of the oscillating speed signal. The difference between the real filtered (blue) signal and this ideal filtered signal (when multiplied with D_{Abs}) will represent a torque. Due to the necessary sign in the above equation, this torque will act as a kind of friction during deceleration of the system. Its magnitude will not be very significant for the final result, but nevertheless the filter characteristics should be chosen so as to minimise this "friction". On the other hand, the filter shall not allow any oscillating output signal as that would falsify the damping action.

2.3 Propeller damping and demand torque characteristics

For a propeller the damping is also a consequence of its torque-speed characteristic. Modelling the propeller demand torque as the square of the rpm or $\dot{\phi}$ (e.g. close to bollard condition would be relevant in ice) will automatically result in a damping action (corresponding to an Archer coefficient of about 20), see [Figure 3](#). (For any driven component the damping coefficient is the tangent to the demand torque versus speed characteristic).

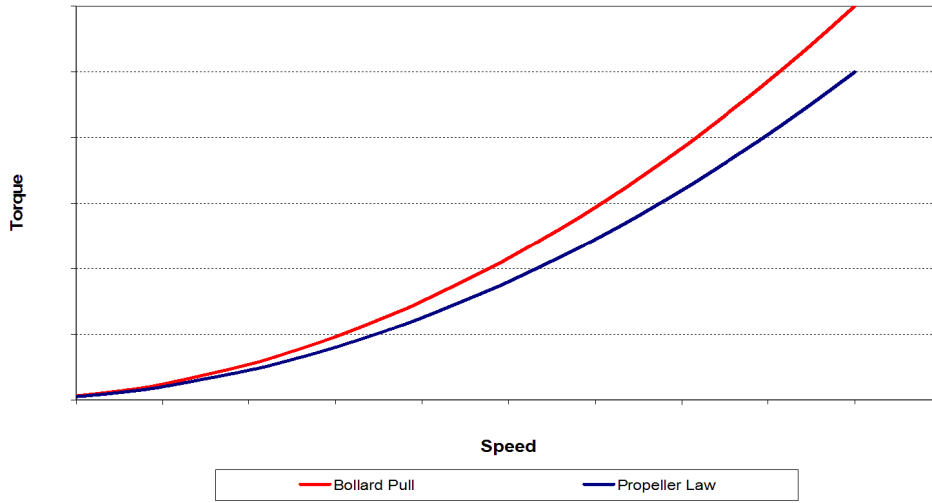


Figure 3 Propeller torque characteristics

In open water the propeller damping coefficient is 20 – 40% higher than the value corresponding to an Archer coefficient of 20. It is uncertain if higher Archer coefficients than 20 are justified in the context of ice interaction, and thus it is advised to keep to 20. However, if it is desired to take a higher coefficient into account, it is necessary to use the trick with filtered speed signal as described in [2.2]. Using this trick for a propeller would also require a continuous updating of D_{Abs} as a function of actual speed.

It is of course important to ensure that the propeller damping is not “doubled” in the way that the demand torque is described together with the damping using the D_{Abs} and the difference between unfiltered and filtered speed. Since the propeller demand torque characteristic is needed anyway, it would be suitable to use the trick of filtering the speed signal for implementation of higher damping than “Archer factor of 20” only.

Last but not least it is unknown how the propeller damping works when in contact with ice blocks.

2.4 Diesel engine damping and torque characteristics

Engine damping is hard to describe correctly. Physically it is neither a relative nor an absolute damping. Damping caused by oil squeezing in journal bearings comes closer to relative than absolute damping. Engine designers sometimes have damping characteristics that are substantiated by measurements, but these are usually applicable for high frequencies such as “crankshaft modes”.

An absolute damping coefficient may be described as in [2.2]. However, using experience values from high frequent (“crankshaft”) vibrations would lead to highly over-estimated engine damping. It is therefore advised to abstain from attempts to describe engine damping as absolute damping.

Since the real engine damping is more a kind of relative damping (even though TVC often wrongly describe the engine damping as absolute damping), this may be modelled. When the engine masses are added together to one mass, this relative damping cannot be modelled. If the engine masses are added to two or more masses with springs in between, it is possible to model relative engine damping. However, the relative engine damping is not a high damping compared to the propeller damping, and disregarding it for the benefit of simplification has a negligible influence on the results.

It is very important that an engine torque characteristic is not made so as to introduce negative damping. If a driver is modelled with a torque that increases with speed, and no special measures are taken to prevent oscillations to influence the driving torque directly, this will function as negative absolute damping, see Figure 4.

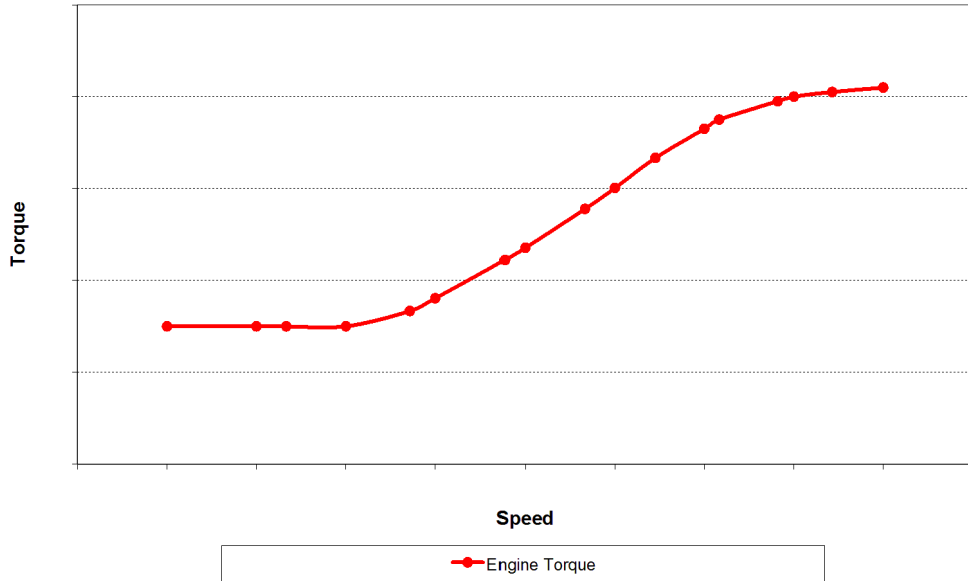


Figure 4 Increasing engine torque capacity with rotational speed

This action is similar to the description of propeller damping above, but now with opposite sign because the element is a driver. It is necessary to model the torque of the driver in order to simulate the drop of speed during ice interaction, but the vibration velocity of the engine inertia shall not be allowed to introduce negative damping. This shall be arranged by filtering that parameter before it is used to update the driving torque. Appropriate filtering also introduces a time delay which to some extent is representative for a diesel engine's firing delays.

The torque characteristic of a diesel engine depends to a large extent on the turbocharger lay out. The "static" characteristic may be available from the engine manufacturer and may have a shape as given on [Figure 4](#). In general the maximum torque is the torque at *MCR* (T_{rated}) which is limited by the blocking of the fuel rack position. At lower speeds the turbocharger cannot feed the engine with sufficient air to prevent excessive exhaust temperatures. Of that reason the maximum fuel rack position is often limited (controlled) by the charge air pressure.

In the context of ice interaction causing sudden overloads with consequential speed drops, the "dynamic" characteristic will be somewhat higher. The engine is assumed to run at full power when the ice shocks occur. The engine speed will be reduced, but due to the kinetic energy of the turbocharger rotor the engine will be fed temporarily with more air than in the "static" case. This can be described as a temporary hump on the characteristic given in [Figure 4](#).

To make an accurate simulation model of this is very complicated, and such extreme efforts are hardly justified by the slightly more accurate result of the simulation process. A rough empirical approach may be justified, and may be laid out as follows:

Engine torque as a function of speed (n) and time (t):

$$T(n; t) = T_{static}(n) + \Delta T_{dyn}(t)$$

Where $T_{static}(n)$ is the torque as shown in [Figure 4](#) and $\Delta T_{dyn}(t)$ is the temporary hump.

$\Delta T_{dyn}(t)$ is assumed to enable the engine to maintain the T_{rated} for a short duration. This can be described as:

$$\Delta T_{dyn}(t) = (T_{rated} - T_{static}) \cdot (1 - t/3) \text{ where } t \text{ starts at 0 when } T_{static} < T_{rated} \text{ and ends after 3 seconds.}$$

2.5 Electric-motor damping and torque characteristics

An Electric-motor damping is associated with its torque characteristic. When viewed in a torque-speed diagram, a characteristic increasing from left to right in the diagram will correspond to a “negative” damping. A characteristic decreasing from left to right will correspond to “positive” damping.

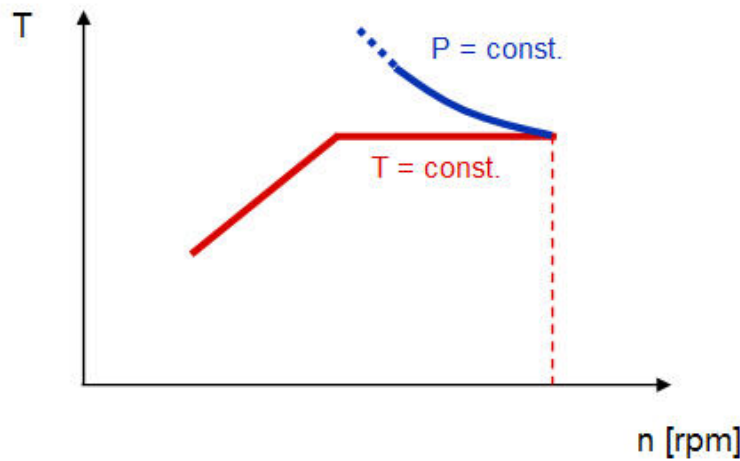


Figure 5 Possible torque characteristics of electric motors (constant power or torque)

The above statements are valid for immediate torque response as a function of the momentary velocity. Any time lag will alter this and introduce a phase angle that may change “negative” to “positive” damping and vice versa. (That is similar to diesel engines where the speed governor and firing system introduce a phase shift of an oscillating fuel rack that can lead to negative, positive or 0 damping.)

Unless the torque response is immediate, it is advised to filter the speed signal and therewith the damping influence.

E-motors may have an overload capacity when the rated speed is suppressed, e.g. having constant power as indicated in [Figure 5](#) with the hyperbolic shape. However, using this overload capacity may lead to motor overheating within short time. The simulation model utilising such overload capacity should also include a time limit function corresponding to the automatic action in the monitoring system.

3 Excitations

The major excitation source is the ice interaction. The ice impacts in the rules are described as sequences of half-sinus waves of blade passing frequency as well as the double frequency.

The start and end of these waves are ramped up respectively down over a given angle of rotation.

A simple way of describing this excitation is to multiply the (constant) sinus waves with a ramp function from 0 to 1 over the specified ramp length. A similar ramp function from 1 to 0 applies at the end.

If the ordinary torsional vibrations cannot be disregarded, e.g. as for direct coupled crosshead engines, it is necessary to have this superimposed to the ice interaction. Such engines usually have a barred speed range or, if not barred, a range where the vibration response is quite significant. These speed ranges are usually below 60% of *MCR* speed and an engine speed drop into these ranges should (or must) be avoided. It is therefore important to model the available driving torque as a function of rpm (see [Figure 5](#)) as correctly as possible. The main engine excitation (normally of the order equal to the number of cylinders) is applied at the lumped engine inertia.

SECTION 5 PROPULSION SHAFT DESIGN AGAINST FATIGUE

1 Nomenclature

Only SI units are used.

2 General

This section describes a recommended method for fatigue analysis of propulsion shafts considering the expected long term ice loads as defined in [DNVGL-RU-SHIP Pt.6 Ch.6 Sec.6](#).

The other design criteria involving ice loads, which also shall be fulfilled like "pyramid bending strength criterion" for the propeller shaft and prevention of shaft bending/yielding due to peak ice torque, are considered to be self explanatory in [DNVGL-RU-SHIP Pt.6 Ch.6 Sec.6](#) and are not elaborated further here. Even though propulsion shafts are exposed to a wide spectrum of other "open water"-loads (torsion and bending loads), just a few of the dominating load cases need to be considered instead of including them all in the Palmgren-Miner cumulative "damage sum". The applicable "open water" load cases and their respective acceptance criteria are described in the Society's document [DNVGL-CG-0038](#). For most of the propulsion shaft designs and applications known in marine applications, only one of these load cases will really form the design condition (i.e. the load case that will be decisive for the dimensions and material properties of the considered shaft). Therefore, it is normally adequate to assess the strength capacity of these load cases separately. However, in cases where two or more of these load cases are close to their acceptable limits, their degree of cumulative "damage" shall be added by using Palmgren-Miner's approach. The fatigue analysis is based on the permissible stress levels as presented in the design S-N-data/curves in the Society's document [DNVGL-CG-0038](#) and the validity of the method is given in the same reference.

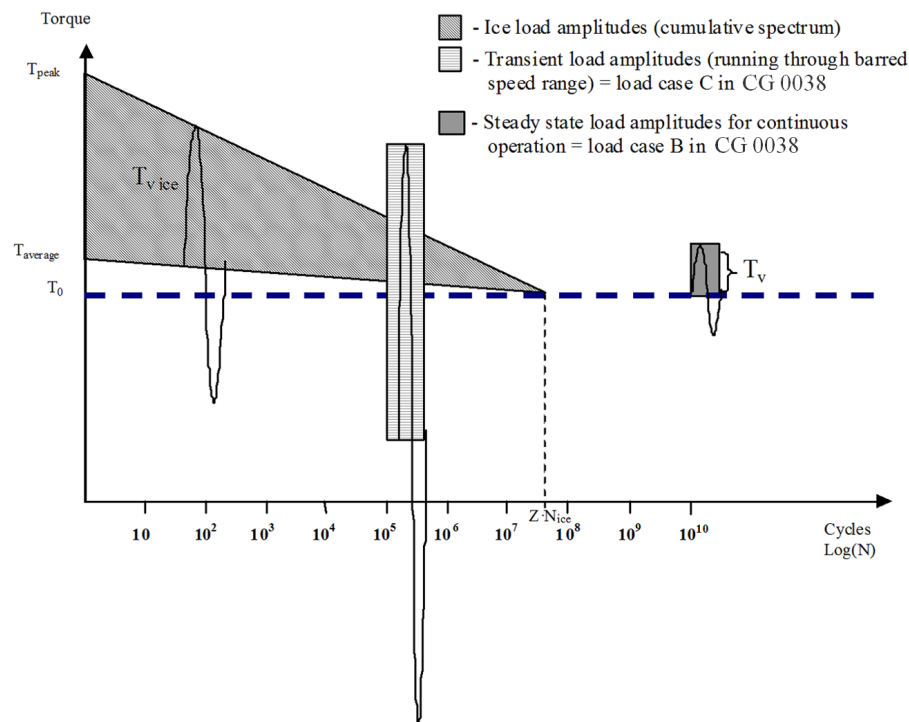


Figure 1 Typical load cases to be assessed for an ice classed vessel with direct coupled 2 stroke plant

3 Method for fatigue analysis

Fatigue design of propulsion shafts subject to variable amplitude stresses due to ice loads are assessed by using the Palmgren-Miner linear damage hypothesis:

$$MDR = \sum_{i=1}^k \frac{n_i(\tau_{\text{vice}})}{N_i(\tau_{\text{vice}})} = \sum_{i=1}^k \frac{1}{a} n_i(\tau_{\text{vice}}) \cdot (\tau_{\text{vice}})^m \leq \eta$$

where:

- τ_{vice} = is a constant stress amplitude in the shaft due to ice interaction on the propeller
- $n_i(\tau_{\text{vice}})$ = is the discrete number of cycles with a constant stress amplitude τ_{vice} .
- $N_i(\tau_{\text{vice}})$ = is the number of cycles to failure due to the constant stress amplitude τ_{vice} based on the relevant part of the design S-N-curve
- $\frac{n_i(\tau_{\text{vice}})}{N_i(\tau_{\text{vice}})}$ = degree of cumulative "damage" of a constant stress amplitude τ_{vice}
- I = number of different load magnitudes (load blocks)
- m = negative inverse slope of the relevant part (for τ_{vice}) of the design S-N curve
- a = intercept with the $\log(N)$ axis of the relevant part (for τ_{vice}) of the design S-N curve
- η = accept usage factor or "damage sum" = 1.

Applying a histogram to express the stress distribution, the number of stress blocks, I, shall be large enough to ensure reasonable numerical accuracy, and should not be less than 10. If integration is used, due consideration should be given to selection of integration method as the position of integration points may have a significant influence on the result.

The stress cycles interaction effect is taken into account by conservative safety factors and continuous slope in the high cycle end of the S-N curve.

3.1 Ice loads

The ice load spectrum (exceedance diagram of ice load history) is by DNVGL-RU-SHIP Pt.6 Ch.6 postulated by a two-parameter Weibull distribution with shape parameter $k = 1$ and scale parameter $q_w = \frac{T_{A_{\max}}}{\ln(Z \cdot N_{\text{ice}})}$, see Figure 2:

$$T_A(N) = T_{A_{\max}} \cdot \left\{ 1 - \frac{\log(N)}{\log(Z \cdot N_{\text{ice}})} \right\}$$

The corresponding Weibull probability density function:

$$f(T_A, T_{A_{\max}}) = \frac{1}{q_w(T_{A_{\max}})} \cdot e^{-\left(\frac{T_A}{q_w(T_{A_{\max}})} \right)} = \frac{\ln(Z \cdot N_{\text{ice}})}{T_{A_{\max}}} \cdot e^{-\left(\frac{T_A \cdot \ln(Z \cdot N_{\text{ice}})}{T_{A_{\max}}} \right)}$$

The highest shaft response torque in the load spectrum, $T_{A\max}$ shall be based on the transient torsional vibration analysis of the propulsion system (simulation calculations) as described in Sec.4.

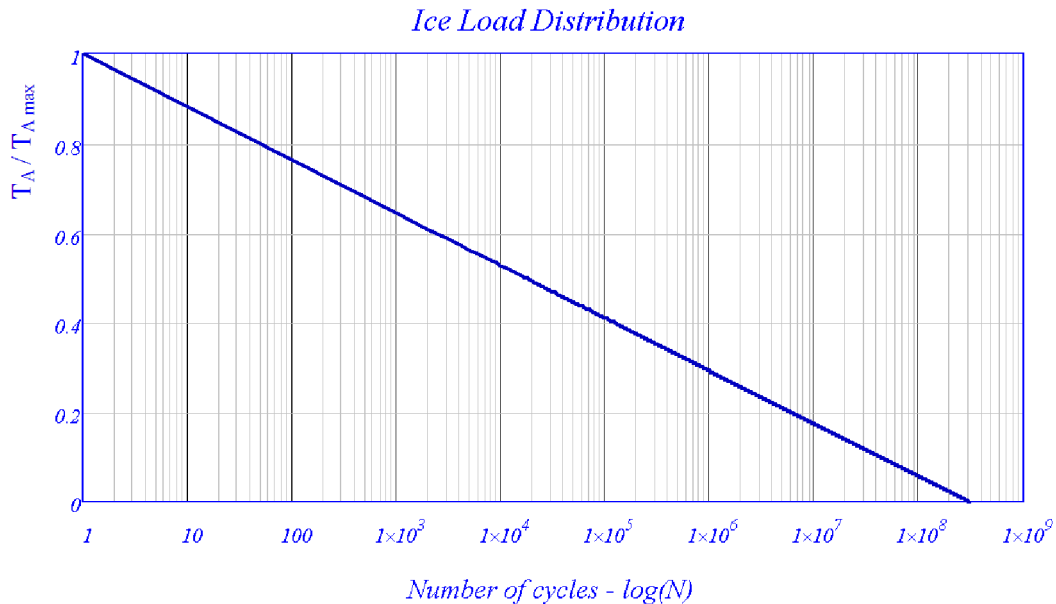


Figure 2 Example of an ice load spectrum (cumulative distribution) with total number of ice loads; $Z \cdot N_{ice} = 3 \cdot 10^8$, presented in a semi-log scale

With $\tau = \frac{T \cdot 10^3}{W_T} = \frac{16 \cdot d \cdot T \cdot 10^3}{\pi \cdot (d^4 - d_i^4)}$, the same can be expressed in terms of stress:

Weibull scale parameter:

$$q_W = \frac{\tau_{v\text{ ice max}}}{\ln(Z \cdot N_{ice})}$$

Stress amplitude distribution:

$$\tau_{v\text{ ice}}(N) = \tau_{v\text{ ice max}} \cdot \left\{ 1 - \frac{\log(N)}{\log(Z \cdot N_{ice})} \right\}$$

Stress amplitude probability function:

$$f(\tau_{v\text{ ice}}, \tau_{v\text{ ice max}}) = \frac{\ln(Z \cdot N_{ice})}{\tau_{v\text{ ice max}}} \cdot e^{-\left(\frac{\tau_{v\text{ ice}} \cdot \ln(Z \cdot N_{ice})}{\tau_{v\text{ ice max}}} \right)}$$

3.2 Design S-N curve

The design S-N curve for the shaft section in question is established according to the Society's document [DNVGL-CG-0038](#), which takes into account the materials fatigue strength including the mean stress influence, geometrical stress concentration (if any), notch influence/sensitivity, size factor and the required safety factors for low and high cycle fatigue respectively. For each shaft section and load case, this leads to a set of 3 points describing the bi-linear design S-N curve, see [Figure 3](#):

- τ_{vLC} = permissible low cycle torsional stress amplitude corresponding to 10^4 cycles (with safety factor 1.25)
- τ_{vHC} = permissible high cycle torsional stress amplitude corresponding to $3 \cdot 10^6$ cycles (with safety factor 1.5)
- τ_f/S = fatigue strength amplitude corresponding to 10^9 cycles (with safety factor 1.5) $\tau_f/S \rightarrow \tau_f$ includes a safety factor of 1.5.

The rest of the S-N- curve is found by linear interpolation/extrapolation in a log(t)-log(N) scale.

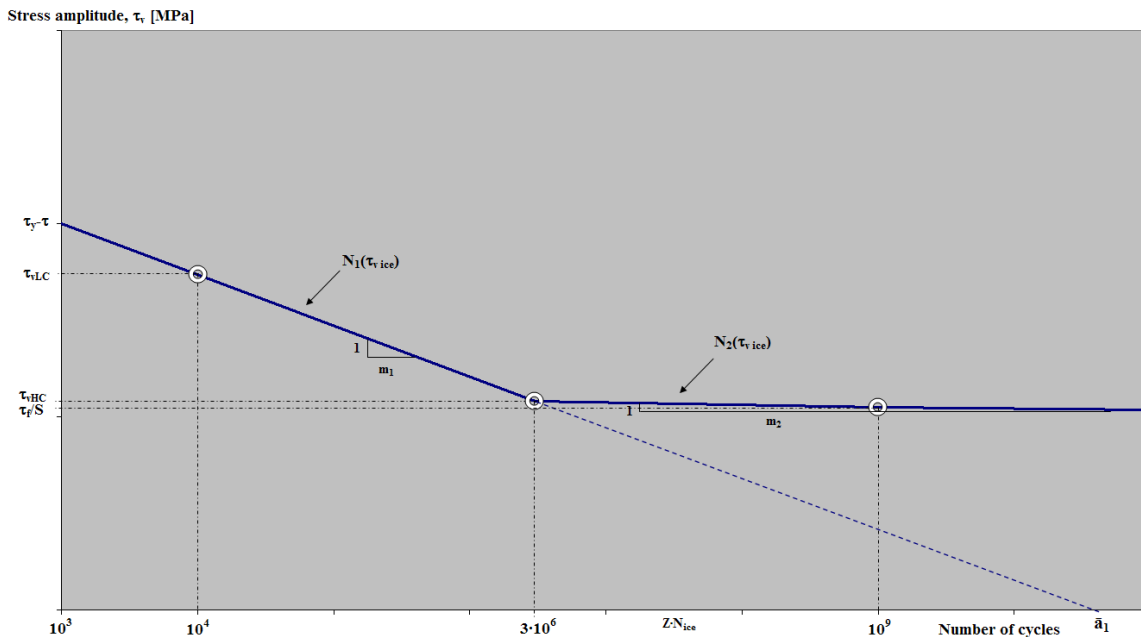


Figure 3 Example of a design S-N curve for steel in air condition

The following bi-linear S-N curve can be used for fatigue assessment:

For $N \leq 3 \cdot 10^6$ cycles:

$$N_1(\tau_{v,ice}) = \bar{a}_1 \cdot \tau_{v,ice}^{-m_1}$$

For $N > 3 \cdot 10^6$ cycles:

$$N_2(\tau_{\text{vice}}) = \overline{a}_2 \cdot \tau_{\text{vice}}^{-m_2}$$

Where

$$m_1 = \frac{\log\left(\frac{10^4}{3 \cdot 10^6}\right)}{\log\left(\frac{\tau_{vHC}}{\tau_{vLC}}\right)} \approx \frac{2.477}{\log\left(\frac{\tau_{vLC}}{\tau_{vHC}}\right)}$$

$$\overline{a}_1 = 3 \cdot 10^6 \cdot \tau_{vHC}^{m_1}$$

$$m_2 = \frac{\log\left(\frac{3 \cdot 10^6}{10^9}\right)}{\log\left(\frac{\tau_f}{1.5 \cdot \tau_{vHC}}\right)} \approx \frac{2.523}{\log\left(\frac{1.5 \cdot \tau_{vHC}}{\tau_f}\right)}$$

$$\overline{a}_2 = 3 \cdot 10^6 \cdot \tau_{vHC}^{m_2}$$

3.3 Fatigue damage due to ice interaction

The degree of damage accumulated from the stress amplitudes due to ice loads may be calculated by a direct integration of each part of the S-N curve:

In terms of torsional stress:

$$\text{MDR} = Z \cdot N_{\text{ice}} \cdot \int_0^{\tau_{vHC}} \frac{f(\tau_{\text{vice}}, \tau_{\text{vice max}})}{N_2(\tau_{\text{vice}})} d\tau_{\text{vice}} + Z \cdot N_{\text{ice}} \cdot \int_{\tau_{vHC}}^{\tau_{\text{vice max}}} \frac{f(\tau_{\text{vice}}, \tau_{\text{vice max}})}{N_1(\tau_{\text{vice}})} d\tau_{\text{vice}}$$

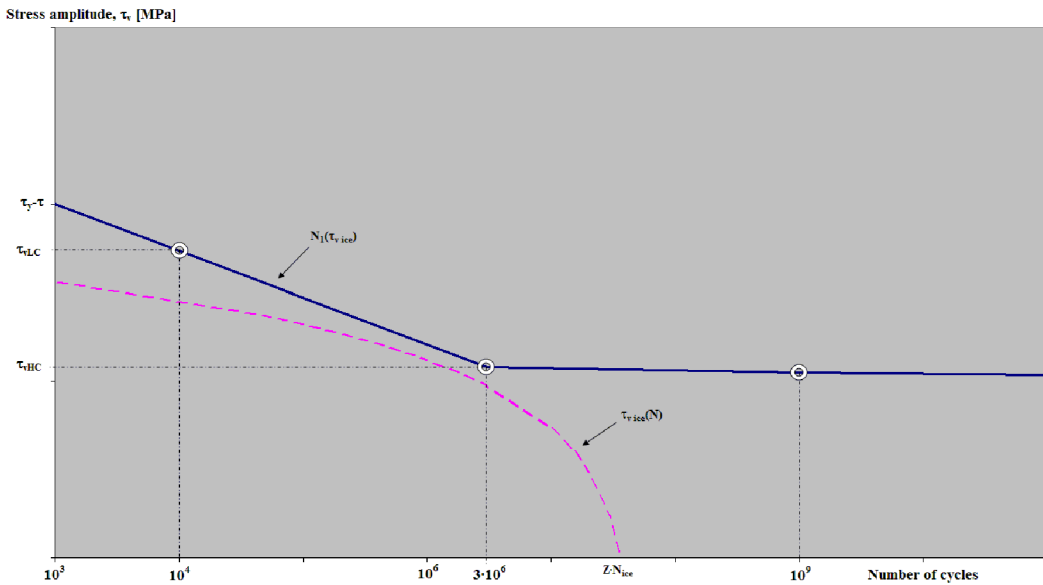


Figure 4 Example of a typical ice stress distribution and design S-N curve for steel in air condition

Since the permissible ice stress amplitude below 1000 cycles is limited by the shaft bending/yielding criterion:

$$MDR \approx Z \cdot N_{ice} \cdot \int_{\tau_{vHC}}^{\tau_{vice max}} \frac{f(\tau_{v ice}, \tau_{v ice max})}{N_1(\tau_{v ice})} d\tau_{v ice}$$

and the shape of the Weibull distribution is as indicated in [Figure 4](#), it can be seen that the fatigue damage due to ice will by far be dominated by the second integral:

$$D_{ice} \approx Z \cdot N_{ice} \cdot \int_{\tau_{vHC}}^{\tau_{vice max}} \frac{f(\tau_{v ice}, \tau_{v ice max})}{N_1(\tau_{v ice})} d\tau_{v ice}$$

If the highest response torque amplitude on the shaft during a sequence of ice impacts on the propeller, $\tau_{v ice max}$, is lower than the design knee point of the design resistance S-N curve, τ_{vHC} , the fatigue life of the shaft due to ice impacts can be assumed as verified and no ice damage calculation is necessary.

It is also possible to calculate an equivalent constant ice stress amplitude, $\tau_{eq ice}$ associated with a certain accumulated number of cycles, which will give the same fatigue damage, D_{ice} as the long term stress distribution calculated above. The equivalent ice stress amplitude associated with 10^6 accumulated stress cycles will be, see [Figure 5](#):

$$\tau_{eq ice} = \left(\frac{10^6}{MDR \cdot a_1} \right)^{\frac{1}{m_1}} = \sqrt[m_1]{\frac{10^6}{MDR \cdot a_1}}$$

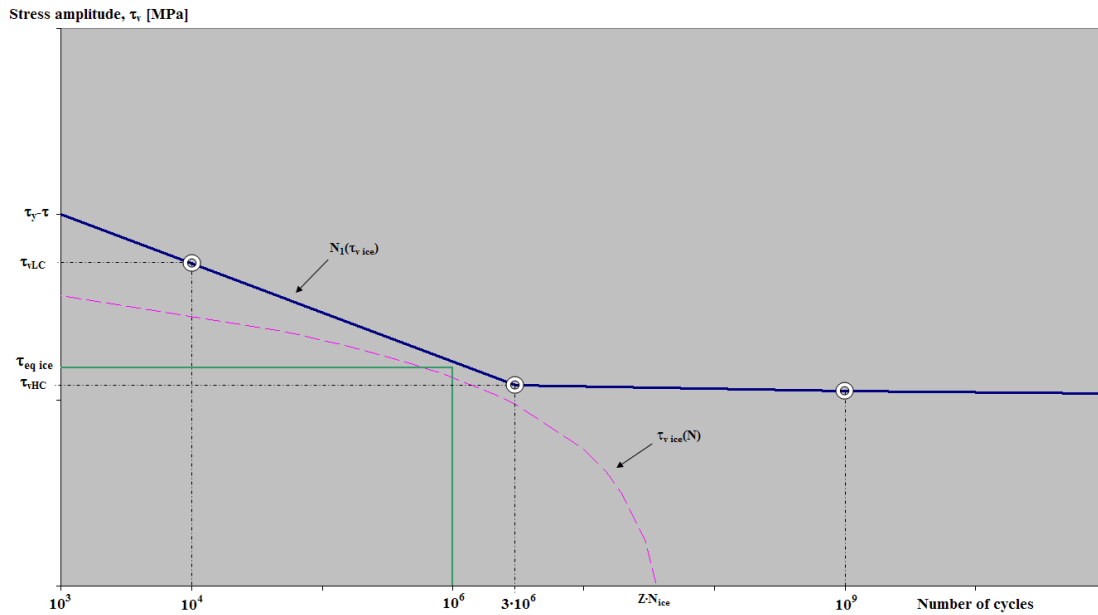


Figure 5 Equivalent ice stress amplitude, $\tau_{eq\ ice}$ associated with 10^6 accumulated stress cycles giving the same fatigue damage as the ice stress distribution $\tau_{v\ ice}(N)$

3.4 Bending stress influence

The influence on the fatigue damage by significant bending stresses due to ice impacts should be considered in the following shafts:

- in propeller shafts aft of the 2nd aftermost bearing caused by maximum propeller blade forces F_b/F_f
- in gear- and thruster shafts due to the coupled torsional-lateral mode through the gear mesh.

SECTION 6 REDUCTION GEARS

1 General

The general procedure in appendix A may be used in combination with the Society's document [DNVGL-CG-0036](#) for tooth root fracture and pitting of flanks. Scuffing calculations may be carried out according to [DNVGL-CG-0036](#) based on the maximum response torque.

Subsurface fatigue safety can be roughly estimated by the following:

- 1) Apply the response torque according to the Weibull distribution at $3 \cdot 10^6$ cycles.
- 2) Calculate high cycle subsurface safety factor according to [DNVGL-CG-0036](#).
- 3) If the calculated safety factor is somewhat higher than required by [DNVGL-RU-SHIP Pt.6 Ch.6](#), further detailed sub-surface calculations can be omitted.

SECTION 7 PODDED PROPULSORS OR AZIMUTHING THRUSTERS

1 Ice loads on pod/thruster body and propeller hub

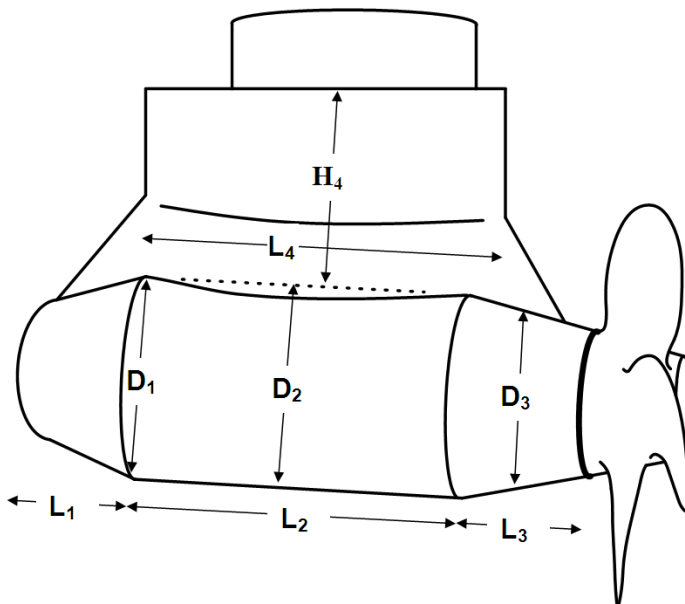


Figure 1 Typical podded propulsor

1.1 Introduction

Ice loads may be calculated for the entire exposed area of pod/thruster, or any other actual partial area separately. The method may also be applied on icebreakers and deeply submerged "under bottom mounted" units.

These ice loads are also applicable for the Baltic ice classes **Ice(1C)...(1A*)**, see [DNVGL-RU-SHIP Pt.6 Ch.6 Sec.2 \[15.17.2\]](#). However due to the initiation of the project at TraFi "Development of technical background for Finnish-Swedish ice class rules for azimuthing main propulsion" it was decided to exclude these from the [Table 1](#) in this edition for elaboration at a later stage.

Both axial and transversal ice load cases shall be covered. Following cases shall normally be calculated:

- 1) transversal force on strut
- 2) transversal force on pod
- 3) axial force on strut
- 4) axial force on pod, or propeller hub for pulling propeller
- 5) transversal force on nozzle if any
- 6) axial force on nozzle if any.

In addition, total transversal and axial forces using the sum of projected areas for pod, strut and nozzle (if applicable), shall be considered.

In calculation of total axial force for pulling propeller case, the projected propeller blade area and ditto hub area shall be used.

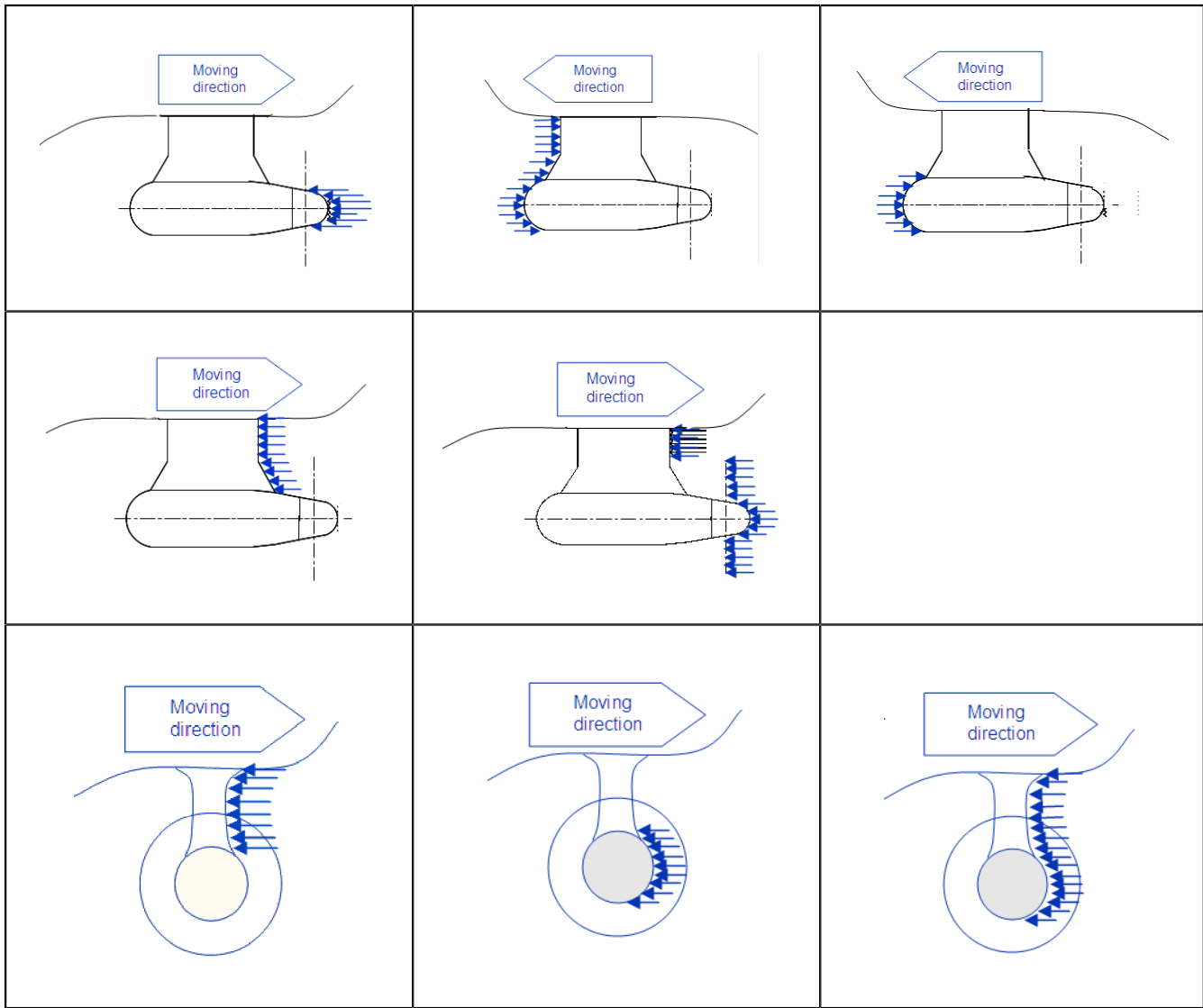


Figure 2 Illustration of actual load cases to be considered

1.2 Ice load definition

1.2.1 Ice load on a defined area may be expressed by:

$$F = p_0^{0.8} (A C^{0.3})^{\text{exp}} C_1 C_2 C_3 C_4 \text{ [MN]}$$

where:

p_0 = ice pressure, in MPa, see **Table 1**

Table 1 Reference ice thickness and –pressure. Ref. technical background note and in accordance with IACS UR I2

<i>Ice Class</i>	H_{ice} (m)	p_0 (MPa)
PC-1	4.0	6
PC-2	3.5	4.2
PC-3	3.0	3.2
PC-4	2.5	2.45
PC-5	2.0	2
PC-6	1.75	1.4
PC-7	1.5	1.25

A = considered projected area exposed to ice pressure in m^2 if less than $2H_{ice}^2$

= $2H_{ice}^2$ otherwise

exp = 0.3 when area is $1\ m^2$ and more

= 0.85 when $A < 1\ m^2$

C = $A / 2H_{ice}^2$, or minimum 1

H_{ice} = reference ice thickness for machinery strength design, see [Table 1](#)

C_1 = location and propeller type factor for hub and strut loads

= 1 in general

= 1.5 for pulling and pushing "front propeller" strut loads and pushing propeller axial pod loads

= 2.2 for pulling propeller axial load ("hub load") calculated based on projected hub area

C_2 = factor that reduces pod ice loads by 1/3 for under bottom mounted units

= 1 in general

= 2/3 for "deeply submerged" under bottom located propellers

C_3 = ship type factor

= 1 in general

= 1.25 for icebreakers and ice management vessels

C_4 = statistical factor for expected maximum load during 20 years lifetime

= 1.2 in general.

1.2.2 Dynamic load

Axial load on the propeller hub exceeding propeller thrust will push the shaft "backwards" and cause dynamic response in the thrust bearing in excess of what is reflected in the factor C_1 above. The magnitude is depending on thrust bearing design and axial clearance. For a spherical roller bearing this factor shall be taken minimum 1.1. This load is normally transmitted from the thrust bearing to its supporting structure and shall be included into the peak load transmitted via thruster support bearing (slewing bearing) to supporting hull structure.

Deep submerged under bottom located propellers – C_2

Maximum ice load on propeller is not depending on submerged depth of propeller, only on total number of ice loads. This is reasonable for propellers, where ice impacts are mainly caused by propeller blades hitting ice blocks and not reversely. Propeller blade rotational speed is much higher than ship speed - normally tip speed is in the range of 20 to 40 m/s. Therefore it will not make any difference for a propeller blade if it hits ice under the bottom, or close to the surface.

The selected 1/3 load reduction reflects to some degree reduction applied to ice loads acting on ship bottom. However, since a thruster penetrating ship hull forms an obstruction for ice moving mutually along the bottom, there will always be crushing of ice against the thruster strut, pod and propeller hub. The given load reduction is not based on measurements, but is selected based on our best knowledge.

A deep submersion must also be seen in relation to ice class. The following may be applied as criterion when a unit may be considered as "deeply submerged":

$$\text{Depth of propeller shaft centreline at LIWL } (h_o) > H_{ice} + D$$

where D is propeller diameter in m.

Propellers located in areas Mb, Sb and Bib (see [DNVGL-RU-SHIP Pt.6 Ch.6 Sec.6 Figure 1](#)) are considered as "under bottom located propellers" for **PC**. Propellers located under bottom, but in area BII, or B shall be specially considered. For such thrusters, pod and strut parts may belong to different location categories.

For Baltic ice classes similar definitions for locations do not exist. A propeller may be considered as located under bottom when it is in flat bottom area, "5 frame spacings" or equivalent distance aft from "fore foot" as defined in [DNVGL-RU-SHIP Pt.6 Ch.6 Sec.2 Figure 1](#).

SECTION 8 ICE LOAD ON NOZZLE, RUDDER, AND SHAFT BRACKET

1 Ice load on nozzle, rudder and shaft brackets

1.1 General

This section gives guidance on how to calculate and apply ice load on appendages for ships with **PC** class notation.

1.2 Ice load - rudder below ice horn

Ice force on rudder shall be calculated for **PC(7)** to **PC(1)** as follow:

$$F_R = 140 \cdot (hl_R)^{0,85} \cdot K \cdot \sigma_{ice} \cdot C_6 [kN] \quad (1)$$

$$K = 1 + \frac{Z}{Z_{BL} - 0,01 \cdot L}$$

h = effective patch height in [m], see [Table 1](#)

σ_{ice} = ice strength in [MPa], see [Table 1](#)

Z = distance from rudder bottom to the centre of the assumed ice load area in [m]

Z_{BL} = distance from rudder bottom to the ballast water line (LIWL) in [m]

l_R = cord length of rudder in [m]

L = rule length in [m]

C = area mode factor, where

= 0,6 in general

= 0,8 for **Icebreaker**.

Table 1 Ice thickness and strength for different PC class notations

Class notation PC	σ_{ice}	h
PC(1)	10	1,2
PC(2)	8,5	0,8
PC(3)	7,3	0,7
PC(4)	7	0,6
PC(5)	5,6	0,4
PC(6)	4,8	0,28
PC(7)	4,2	0,2

In addition to the ice load expressed above, ice load on appendages for **PC(6)** and **PC(7)** shall be also calculated for respectively **Ice(1A*)** and **Ice(1A)**, whichever is greater.

1.3 Ice load - upper part of rudder, ice horn and other appendages

Ice force on appendages such as upper part of rudder, ice horn, nozzle, shaft and shaft bracket shall be calculated for **PC(7)** to **PC(1)** as follows:

$$F = 580 \cdot k \cdot A^{0,85} \cdot \sigma_{ice} \quad [kN] \quad (2)$$

Where:

k = 0,6 in general

= 0,8 for **Icebreaker**

A = patch contact area in [m^2] as defined in [Table 1](#), [Figure 3](#), [Figure 4](#) and [Figure 5](#).

1.4 Nozzles, Pt.6 Ch.6 [7.5]

The nozzle force F shall be considered in the position that maximizes bending moment and shear on nozzle and its connection to the hull structure and shall be calculated as expressed by equation (2) considering ice patch areas listed in [Table 1](#).

The nozzle shall be assessed as follows.

Global check includes:

- the integrity of the whole nozzle
- struts connection to both nozzle and hull structure
- shaft and shaft brackets.

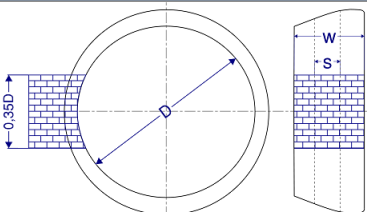
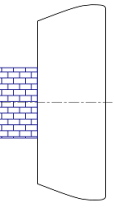
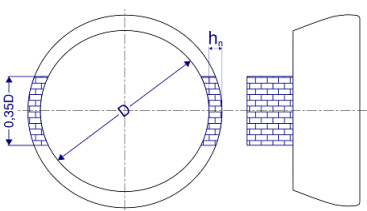
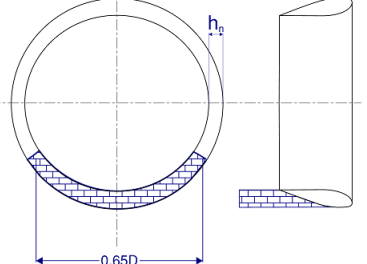
Description	Figure	Load for global check
LC 1 Ice force F applied in transverse direction		$A=0,35 \cdot D \cdot w$
LC 2 Ice force F asymmetrically applied in longitudinal direction		$A=0,35 \cdot D \cdot h_n$
LC 3 Ice force F symmetrically applied in longitudinal direction		$A=0,35 \cdot D \cdot h_n$
LC 4 Ice force F applied in longitudinal direction at the lower edge of the nozzle		$A=0,65 \cdot D \cdot h_n$

Figure 1 Load cases to be considered for ice load on nozzle

1.5 Rudder, Pt.6 Ch.6 [7.2]

1.5.1 Ice horn arrangement

To protect the upper edge of the rudder and to prevent wedging of ice between the ship and rudder top, an ice horn shall be arranged as described by [Figure 2](#).

To avoid extreme dimensions of ice horn in the case of large vessel with high PC class, the extension of the ice horn below the upper edge of the rudder shall not be more than 20% rudder height H.

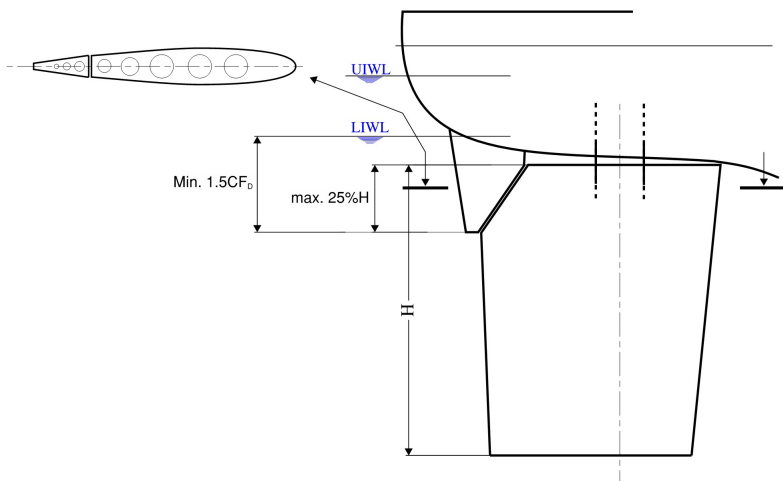


Figure 2 Ice horn arrangement

1.5.2 Ice force on rudder

Rudder force C_R shall be considered in the position that maximize bending moment and shear on rudder stock, rudder blade, rudder horn and ice horn, and shall be calculated as expressed by equation (1).

The scantlings of rudders, rudder stocks and shafts, pintles, rudder horns and rudder actuators shall be calculated considering the formulae given in Pt.3 Ch.14 Sec.1, inserting the torque Q_R , bending moments M and rudder force C_R resulting from the load cases listed in [Figure 3](#).

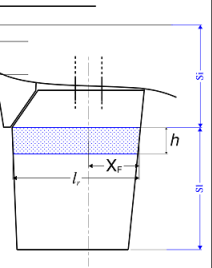
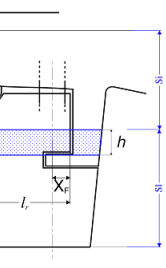
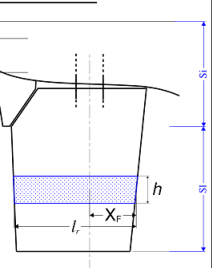
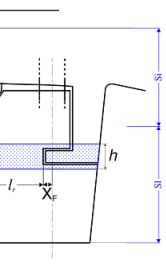
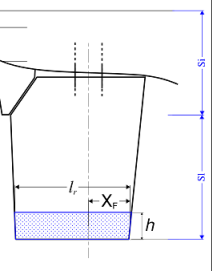
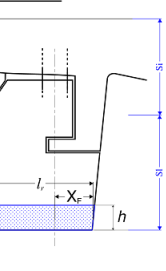
	Description	Spade rudder	Semi-spade rudder
LC2	Ice force Q_R right below the lower edge of the ice horn		
LC3	Ice force Q_R in the middle of the rudder		
LC4	Ice force Q_R at lower edge of the rudder		

Figure 3 Load cases to be considered for ice load on rudder blade

A grillage including girder system supporting the rudder trunk, rudder horn and ice horn may be necessary considering the load cases listed in [Figure 4](#).

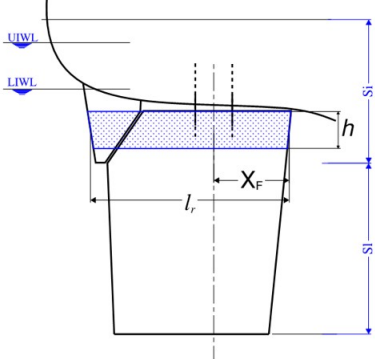
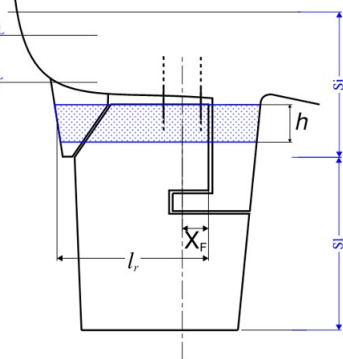
	Description	Spade rudder	Semi-spade rudder	Load area
LC1	Ice patch on the upper part of the rudder including ice knife.			$A = h \cdot l_r$

Figure 4 Load cases to be considered for ice load on upper part of rudder blade, including ice horn

1.6 Shaft and shaft brackets

Ice force on shaft and shaft brackets F shall be considered in the position that maximize bending moment and shear, and shall be calculated as expressed by equation (2) considering the Ice patch areas listed in Figure 5.

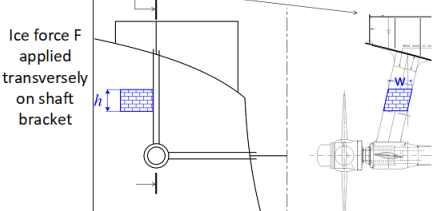
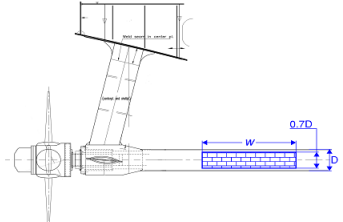
	Description	Figure	Load
LC1	Ice force F applied transversely on shaft bracket		$A = h \cdot w$
LC2	Ice force F applied transversely on shaft		$A = 0.7 \cdot D \cdot w$ $w = 4 \cdot D$

Figure 5 Load cases to be considered for ice load on propeller shaft and brackets

APPENDIX A GENERAL GUIDANCE ON FATIGUE ANALYSIS OF PROPULSION MACHINERY SUBJECT TO ICE LOADS

1 Cumulative Damage by Palmgren-Miner's Rule

In general, fatigue design of machinery components may be carried out by methods based on fatigue tests (S-N data) and estimation of cumulative damage ratio (Linear Damage Rule or Palmgren – Miner's Rule). The theory of the Palmgren – Miner's linear cumulative damage rule is that the total damage of the considered component or more precise the considered section of a component, may be expressed as the accumulated damage from each load cycle at different stress levels, independent of their sequence of occurrence:

$$MDR = \sum_{i=1}^I \frac{n_i}{N_i} \leq 1.0$$

where:

- MDR = Miner Palmgrens accumulated fatigue damage ratio
- n_i = number of cycles in stress block i with constant stress amplitude (component stress history, see [3])
- N_i = number of cycles to failure at constant stress amplitude (design S-N curve, see [2])
- I = total number of stress blocks in the components stress history.

The damage ratio (MDR) also called usage factor, represents the ratio of the consumed life of the component. Theoretically, a $MDR = 0.35$ means that 35% of the component's life is consumed. Ideally, failure due to fatigue occurs when the damage ratio exceeds 1.0.

The general procedure to calculate the damage ratio is as shown in Figure 1:

- 1) establish the relevant S-N curve for the section of the component in question, taking into account the required safety factor, material of the component, mean stress and notch influence, size effect, stress interaction effect, etc., see [2]
- 2) establish the long term stress amplitude distribution (stress amplitude exceeding spectrum) by relevant Weibull parameters, which are calculated based on the ice impact loads prescribed by convention for the applicable ice class notation and their response to the component in question, duly taking care of the dynamic properties of the system where the component is installed, see [3]
- 3) check if detailed fatigue analysis can be omitted, see [5]
- 4) depending on item 3. collate the S-N curve and the Weibull distributed stress amplitudes from step 1 and 2, respectively, by calculating the resulting damage ratio by Palmgren-Miner's rule (MDR), see [4].

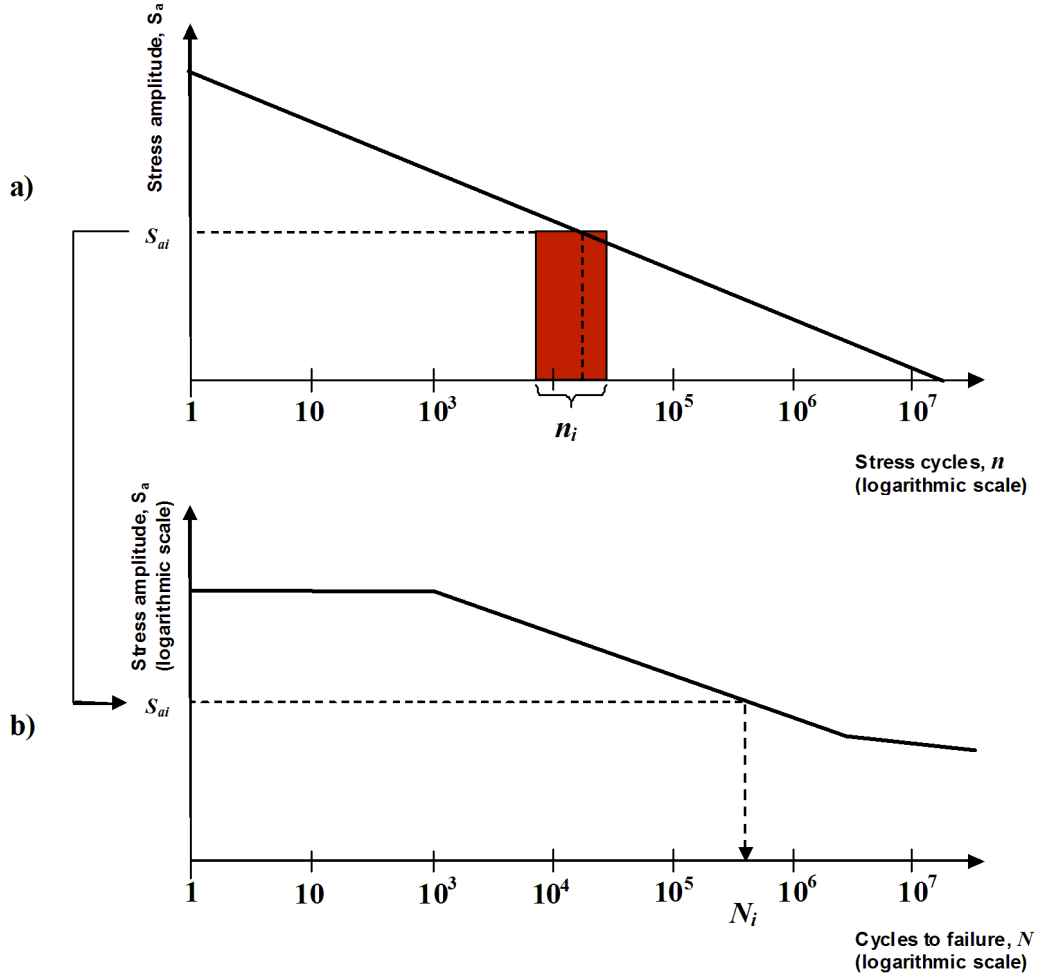


Figure 1 The Palmgren-Miner's rule for one particular stress block i with stress exceedance diagram according a) and design S-N curve b)

Considerable test data has been generated in an attempt to verify Palmgren-Miner's Rule. Most of the "original" test cases for this rule have been using a two step stress history. This involves testing at an initial stress level S_1 for a certain number of cycles and then the stress level is changed to a second level S_2 until failure occurs. If $S_1 > S_2$, often referred to as a "high-low" stress test, and opposite if $S_1 < S_2$, a "low-high" stress test. The observed results of these tests are that the damage ratio - MDR corresponding to failure ranged from 0.61 to 1.45. Other researchers have shown variations as large as 0.18 to 23.0, with most results tending to fall between 0.5 and 2.0. In most cases, the average value is close to Palmgren-Miner's proposed value of 1.0.

One problem with two-level step tests is that they do not accurately represent many service load/stress histories. Most load/stress histories do not follow any step arrangement and instead are made up of a random distribution of loads of various magnitudes. However, tests using random histories with several stress levels show good correlation with Miner's rule.

The Palmgren-Miner's linear damage rule has two main shortcomings when it comes to describing observed material behaviour:

- 1) Load sequence and interaction effects are ignored. The theory predicts that the damage caused by a stress cycle is independent of where it occurs in the load history. Fatigue is a consequence of cycle-by-cycle plastic strains locally at a notch. The state of stress and strain in the damage area is a result of the preceding stress-strain history. Hence, the damage in one cycle is not a function of that stress cycle only, but also of the preceding cycles, leading to interaction or stress memory effect. An example of this discrepancy was discussed above regarding "high-low" and "low-high" tests. It has also been demonstrated by such two step tests that the stress state at the end of the last cycle of first "high" cycles before the second "low" cycles starts has a considerable influence on the total number of cycles to failure, see [Figure 2](#).
- 2) The rate of damage accumulation is independent of the stress level. However, observed behaviour indicates that a crack initiates in a few cycles at high strain amplitudes, whereas almost all the life is spent on initiating a crack at low strain amplitudes (i.e. very little propagation fatigue).

Despite these limitations, the Palmgren-Miner's linear damage rule is still widely used. This is due to its simplicity and the fact that more sophisticated methods do not always result in better predictions.

The proposed value of $MDR = 1.0$ can be used as long as the above limitations are acknowledged by taking them into account with conservative estimates of the design S-N curve for the component. In this respect by extending the slope of the S-N curve, m_1 (i.e. adjusting the fatigue limit at the "knuckle point"), introducing a proper second slope m_2 in the high cycle end (see [Sec.2 Figure 5](#)) and selecting a proper safety factor.

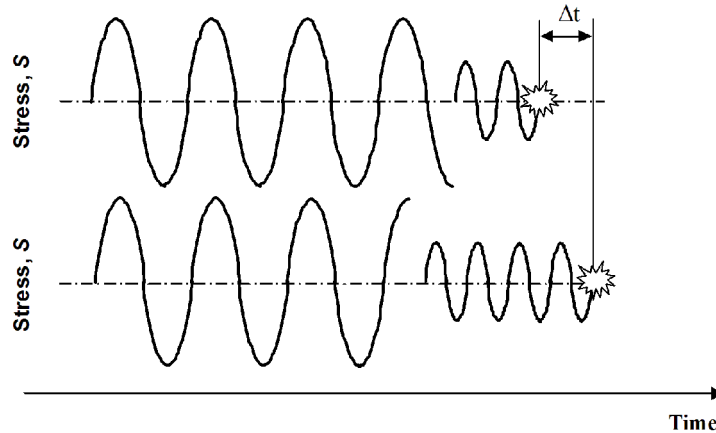


Figure 2 Stress interaction effect

2 Design S-N curve

An illustrative S-N curve is shown in [Figure 3](#). The Y-axis represents the alternating stress amplitude (S_a) and the X-axis represents the number of cycles (N) required to cause failure.

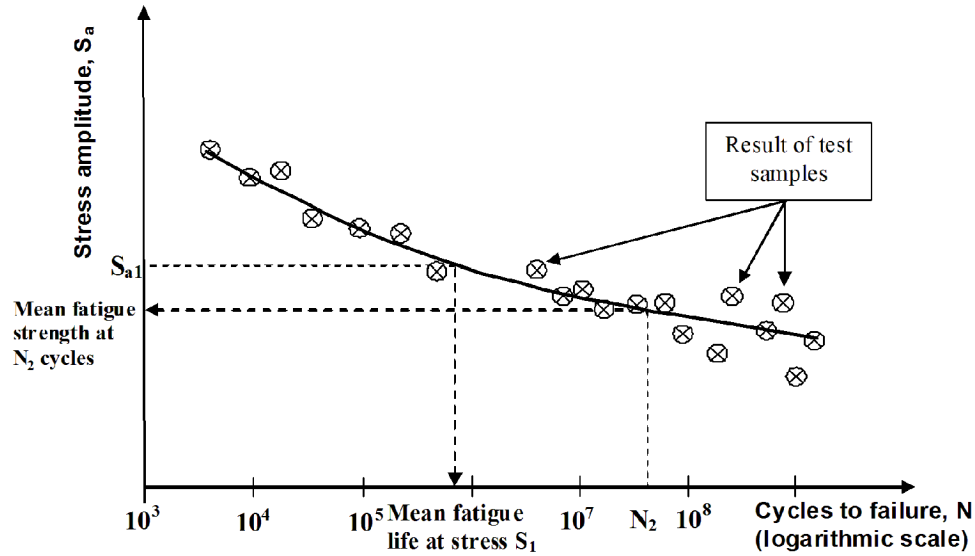


Figure 3 Schematic S-N curve (semi-logarithmic scale)

S-N curves are normally presented for small test specimens as mean fatigue life (50% probability of failure) or for a given probability of failure. Generating an S-N curve for a certain material requires many tests to statistically vary the stress (regular sinusoidal) and count the number of cycles to failure. The type of stress variation has a major effect on the fatigue performance and the S-N curves are normally determined for one specific stress ratio value, which is defined as minimum peak stress divided by the maximum peak stress:

$$R = \frac{S_{min}}{S_{max}}$$

The mean stress, S_m and stress amplitude, S_a is then defined as

$$S_m = (1 + R)/2 \text{ and } S_a = (1 - R)/2, \text{ see Figure 4}$$

It is most common to test at a ratio close to 0, e.g. 0.1 (\approx pulsating load) or -1 (= alternating load, e.g. push-pull). However, it shall be noted that testing with mean stress $S_m = \text{constant}$ and stress ratio $R = \text{constant}$ will in general give different S-N curves. Therefore, it is important that the experimental basis for the reference S-N curve corresponds to the type of alternating stress applicable for the component in question.

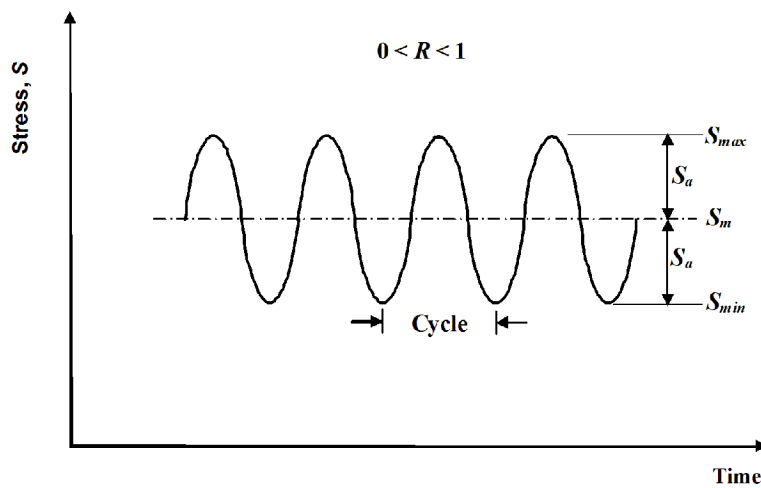


Figure 4 Definition of terms related to fatigue testing

The design S-N curve for the considered section of the component in question is then derived by adjusting the mean S-N curve with the following as found relevant:

- notch influence:
 - a) geometrical stress concentration
 - b) notch sensitivity/stress gradient influence.
- surface condition (roughness)
- surface hardening
- mean stress influence
- size influences:
 - a) metallurgical (if the mechanical properties used for the fatigue limit is not achieved from representative test specimens)
 - b) statistical (if not already accounted for by a reduction of the mean S-N curve for probability of failure $\neq 50\%$, i.e. reduction by one or more standard deviations).
- required safety factor.

The design S-N curve is then linearised into a curve with two slopes in a double logarithmic chart (log-log scale), see [Figure 5](#). The bi-linear S-N curve for $N \geq 10^3$ stress cycles may be expressed as:

$$N_{i1}(S_a) = \bar{a}_1 S_a^{-m_1}$$

$$\text{and } N_{i2}(S_a) = \bar{a}_2 S_a^{-m_2}$$

or:

$$\log[N_{i1}(S_a)] = \log \bar{a}_1 - m_1 \log S_a$$

$$\text{and } \log[N_{i2}(S_a)] = \log \bar{a}_2 - m_2 \log S_a$$

where:

- S_a = stress amplitude
- \bar{a}_1 = the intercept of the logN axis for $N_{i1} < N_x$
- \bar{a}_2 = the intercept of the logN axis for $N_{i2} > N_x$
- m_1 = the inverse negative slope of the S-N curve for $N_{i1} < N_x$ (i.e. actual slope is $-1/m_1$)
- m_2 = the inverse negative slope of the S-N curve for $N_{i2} > N_x$ (i.e. actual slope is $-1/m_2$)
- N_x = the number of cycles to the "knuckle point" of the bi-linearised S-N curve (i.e. where the S-N curve flattens out and changes slope).

In the low cycle end of the S-N curve, a cut-off is introduced for $N < 10^3$ stress cycles by the stress amplitude S_a resulting in a peak stress $S_{max} = S_m + S_a$ equal to the yield strength of the material, see [Figure 5](#). This is introduced in order to prevent permanent deformation of the component.

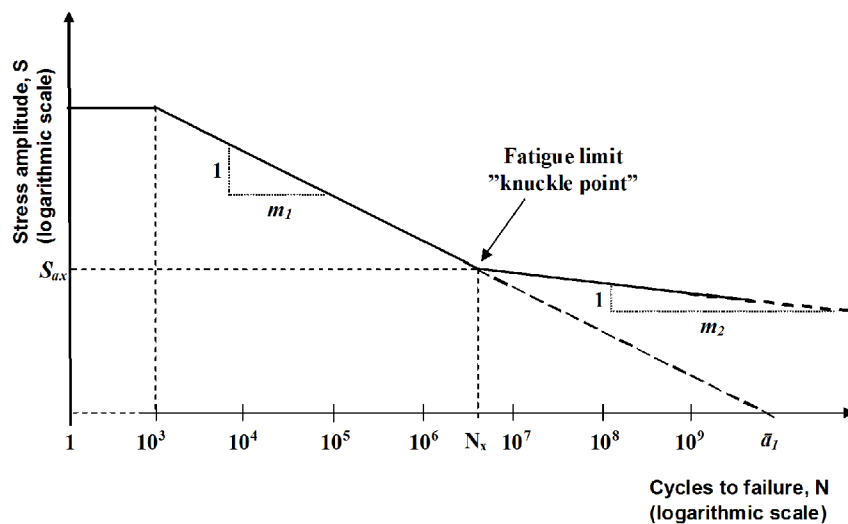


Figure 5 Schematic bi-linear S-N curve (log-log scale)

3 Long term stress amplitude distribution due to ice loads

According to [DNVGL-RU-SHIP Pt.6 Ch.6](#), the ice load spectrum and correspondingly the ice stress amplitude spectrum (exceedance diagram of ice load/stress history) is postulated by a two-parameter Weibull distribution, see [Figure 6](#):

$$S_a(n) = S_{a0} \cdot \left\{ 1 - \frac{\log(n)}{\log(n_0)} \right\}^{1/k}$$

where:

- $S_a(n)$ = load/stress amplitude spectrum as a function of load/stress cycles
- k = Weibull shape parameter as given by [DNVGL-RU-SHIP Pt.6 Ch.6](#)
- n = number of load/stress cycles
- n_0 = total number of load/stress cycles in the Weibull distribution as calculated for the component in question according to [DNVGL-RU-SHIP Pt.6 Ch.6 App.A](#)
- q_w = Weibull scale parameter is defined from the highest stress amplitude, S_{a0} , as:

$$q_w = \frac{S_{a0}}{[\ln(n_0)]^{1/k}}$$

- S_{a0} = the highest stress amplitude out of n_0 cycles, i.e. the highest stress amplitude in the Weibull distribution calculated for the component in question according to [DNVGL-RU-SHIP Pt.6 Ch.6 App.A](#). This load/stress has a probability for being exceeded equal to $1/n_0$, see [Figure 7 b](#)).

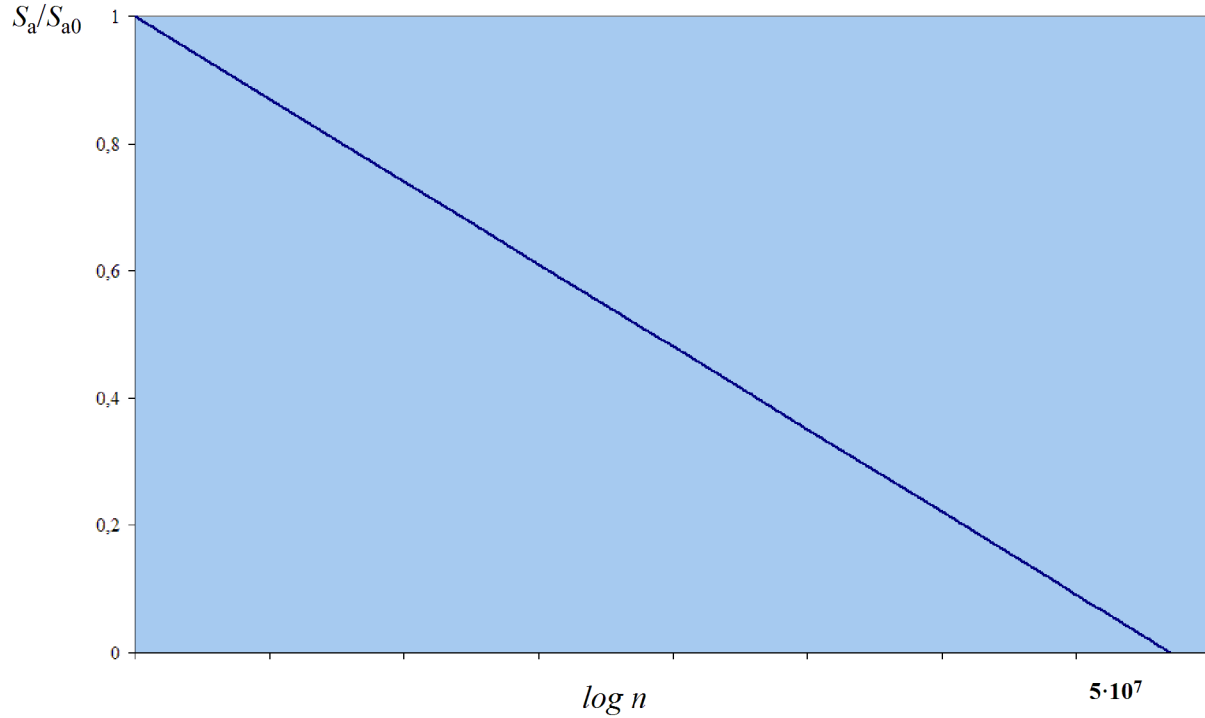


Figure 6 Weibull stress distribution with $k = 1.0$ and $n_0 = 5 \cdot 10^7$ cycles

The corresponding probability density function and probability of exceedance function of the two-parameter Weibull distribution are:

$$f(S_a) = \frac{k}{q_w} \cdot \left(\frac{S_a}{q_w} \right)^{k-1} \cdot e^{-\left(\frac{S_a}{q_w} \right)^k} = k \cdot \frac{S_a^{k-1}}{S_{a0}^k} \cdot \ln(n_0) \cdot e^{-\left[\left(\frac{S_a}{S_{a0}} \right)^k \cdot \ln(n_0) \right]}$$

$$Q(S_a) = 1 - \int_0^{S_a} f(S_a) \cdot dS_a = \frac{n}{n_0} = e^{-\left(\frac{S_a}{S_{a0}} \right)^k} = e^{-\left[\left(\frac{S_a}{S_{a0}} \right)^k \cdot \ln(n_0) \right]}$$

where:

$f(S_a)$ = Probability density function of the stress amplitude S_a , see Figure 7 a)

$Q(S_a)$ = Probability for exceedance of the stress amplitude S_a , see Figure 7 b)

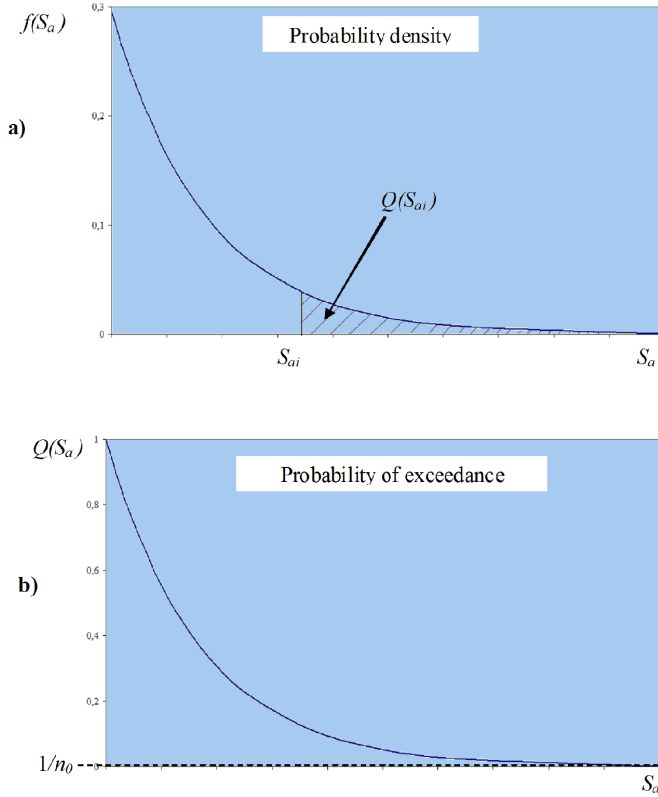


Figure 7 Probability density and Probability functions of Weibull distribution with $k = 1.0$, $n_0 = 5 \cdot 10^7$ cycles and $q_w = 3.38$

4 Calculation of the Palmgren-Miner's damage sum

4.1 By using stress histograms

If the general procedure described in [1] for calculating the damage sum shall be applied, the Weibull stress distribution described in [3] shall be transformed to a representative histogram with I columns (i.e. discrete frequency spectrum). The numerical accuracy of the damage sum depends on the transformation method (distribution of columns) and the total number of columns, I used.

For the method described below, the total number of columns, I , should not be less than 10, see Figure 8.

The ordinate (stress amplitudes) of the Weibull stress distribution is divided into z equidistant stress columns. The stress amplitude in each of the column will then be:

$$S_{ai} = \left(1 - \frac{i-1}{I}\right) \cdot S_{a0} \text{ which for 10 columns become: } S_{ai} = (1.1 - 0.1 \cdot i) \cdot S_{a0}$$

where:

- S_{ai} = the stress amplitude of column i
- I = total number columns in the stress distribution histogram
- S_{a0} = the highest stress amplitude out of n_0 cycles, i.e. the highest stress amplitude in the Weibull distribution calculated for the component in question according to [DNVGL-RU-SHIP Pt.6 Ch.6](#). This load/stress has a probability for being exceeded equal to $1/n_0$, see [Figure 7 b](#)).

Since the Weibull stress distribution is an accumulated continuous spectrum, the individual stress amplitudes of the columns are then calculated by:

$$n_i = n_0^{1 - \left(\frac{1-i}{I}\right)^k} - \sum_{i=1}^{i-1} n_{i-1}$$

where:

- n_i = number of stress cycles in column i
- n_0 = total number of stress cycles in the Weibull distribution as calculated for the component in question according to [DNVGL-RU-SHIP Pt.6 Ch.6](#)
- I = total number columns in the stress distribution histogram
- k = Weibull shape parameter as given by [DNVGL-RU-SHIP Pt.6 Ch.6](#).

The calculation of the damage sum will be on the safe side since the number of cycles in each of the columns in the histogram is higher than given by the Weibull distribution, i.e. the height of the columns exceeds the Weibull distribution, see [Figure 8](#). Consequently, the fewer stress blocks used the more conservative is the calculated damage sum.

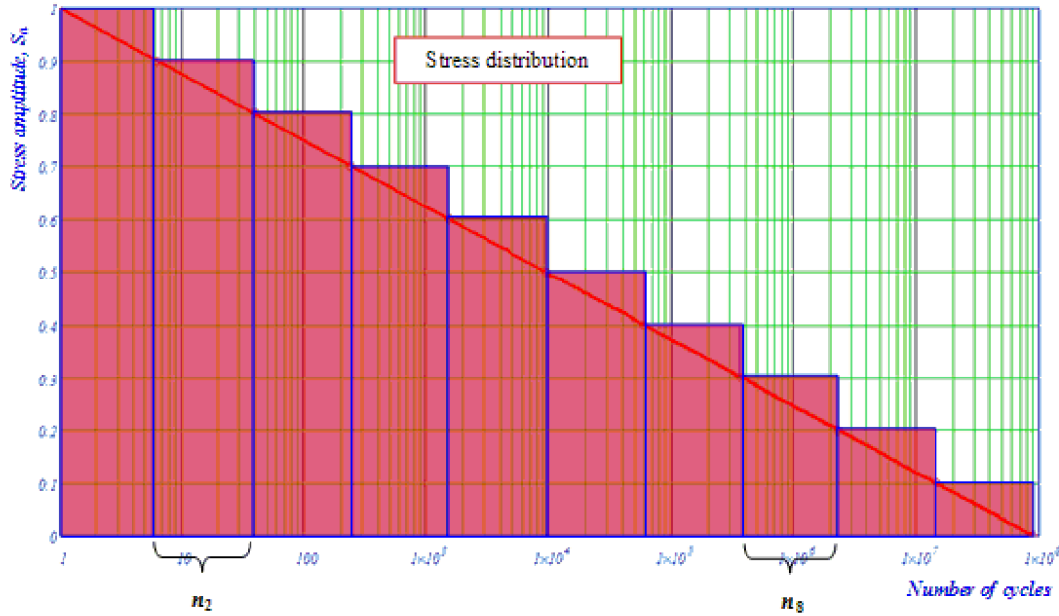


Figure 8 Stress amplitude distribution divided into $I=10$ stress blocks $k = 1.0$ and $n_0 = 8.8 \cdot 10^7$ cycles

4.2 By using closed form solution

If the component is subject to n_0 number of randomly distributed stress cycles in total with a Weibull probability function $f(S_a)$, the number of cycles with stress amplitudes within S_a and $(S_a + dS_a)$ is $n_0 \cdot f(S_a) \cdot dS_a$. Since the mathematical expression for the S-N curve $S(N_i)$ is known, the fatigue damaged ratio MDR can be expressed in a closed form by direct integration of damage below each part of the bi-linear S-N curve, see Figure 9:

$$MDR = \sum_{i=1}^{I=\infty} \frac{n_i(S_a)}{N_i(S_a)} = \int_0^{\infty} \frac{n_0 \cdot f(S_a)}{N_i(S_a)} dS_a = n_0 \cdot \left[\int_0^{S_{ax}} \frac{f(S_a)}{N_{i2}(S_a)} dS_a + \int_{S_{ax}}^{S_{ax}} \frac{f(S_a)}{N_{i1}(S_a)} dS_a \right] = n_0 \cdot \left[\int_0^{S_{ax}} \frac{f(S_a)}{a_2 S_a^{-m_2}} dS_a + \int_{S_{ax}}^{S_{ax}} \frac{f(S_a)}{a_1 S_a^{-m_1}} dS_a \right]$$

where:

- n_0 = total number of load/stress cycles in the Weibull distribution as calculated for the component in question according to DNVGL-RU-SHIP Pt.6 Ch.6 App.A
- S_{ax} = the fatigue limit (stress amplitude) at the change of slope ("knuckle point"), see Figure 5
- S_{ax} = The highest stress amplitude out of n_0 cycles, i.e. the highest stress amplitude in the Weibull distribution calculated for the component in question according to DNVGL-RU-SHIP Pt.6 Ch.6 App.A
- $f(S_a)$ = probability density function of the stress amplitude S_a , see [3]

- $N_{i1}(S_a)$ = S-N curve for $10^3 \leq N \leq N_x$ stress cycles, see [2]
 $N_{i2}(S_a)$ = S-N curve for $N \geq N_x$ stress cycles, see [2]
 N_x = the number of cycles to the "knuckle point" of the bi-linearised S-N curve (i.e. where the S-N curve flattens out and changes slope), see [2].

These definite integrals can be numerically evaluated by various methods, e.g. Recursive Trapezoid rule, Romberg algorithm or Adaptive Simpson's rule.

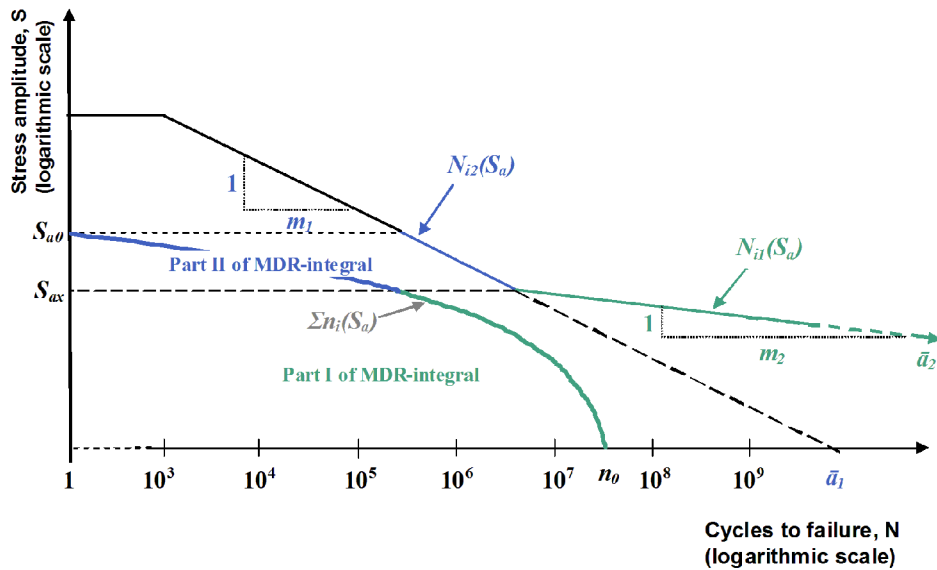


Figure 9 Direct integration of damage below each part of the bi-linear S-N curve

5 Guidance to when detailed fatigue analysis can be omitted

A detailed fatigue analysis can be omitted if the largest stress amplitude in the Weibull distribution for the actual detail (section of the component in question) is less than the fatigue limit at the "knuckle point", see Figure 10 a).

For components where a yield criterion is introduced, it would be meaningless to carry out detailed fatigue analysis when the peak stress = largest stress amplitude in the Weibull distribution + the mean stress is higher than the yield strength of the component (including the effect of any stress concentrations), see Figure 10 b).

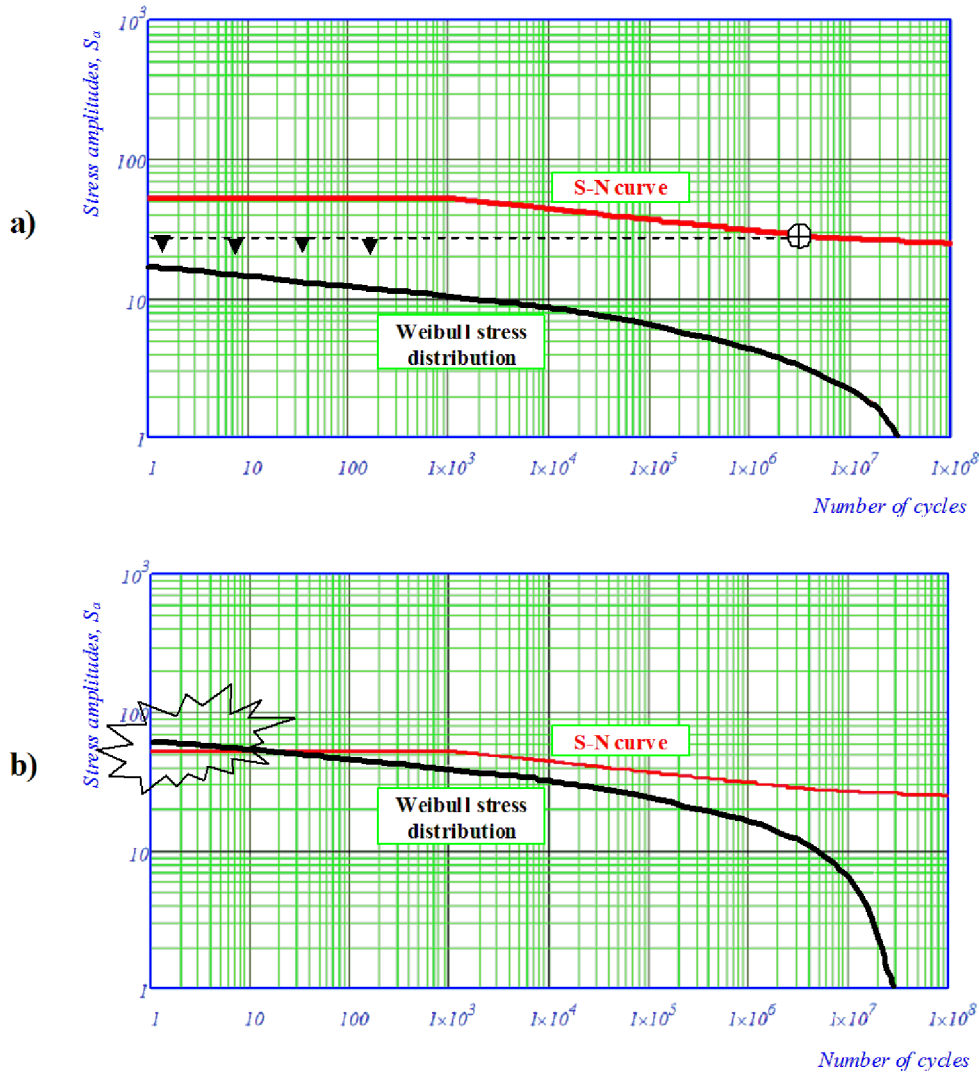


Figure 10 Stress distribution where a detailed fatigue assessment can be omitted

CHANGES – HISTORIC

There are currently no historical changes for this document.

About DNV GL

DNV GL is a global quality assurance and risk management company. Driven by our purpose of safeguarding life, property and the environment, we enable our customers to advance the safety and sustainability of their business. We provide classification, technical assurance, software and independent expert advisory services to the maritime, oil & gas, power and renewables industries. We also provide certification, supply chain and data management services to customers across a wide range of industries. Operating in more than 100 countries, our experts are dedicated to helping customers make the world safer, smarter and greener.